



Bantam Lake

2018 - 2019 Water Quality Monitoring

Prepared for the
Bantam Lake Protective Association
Morris, CT
January 9, 2020

EXECUTIVE SUMMARY

Aquatic Ecosystem Research (AER) conducted monthly water quality monitoring and biweekly cyanobacteria monitoring from April through October in 2018 and 2019 at two sites on Bantam Lake. Two additional sites were visited during each visit where profile data (temperature, oxygen, etc.) and Secchi disk transparency data was collected. Supplemental data was also collected by researchers from the White Memorial Environmental Center and utilized in this assessment.

- Profile data revealed a trend of the water column to regularly mix with intermittent stratification at three of the four sites, all of which were <7m deep. The one site >7m deep stratified over a continuous period of time beginning and ending in May through August of 2018 and June through September of 2019.
 - Where continuous stratification was observed, biochemical reactions near the lake bottom, after oxygen was depleted, resulted in high concentrations of total phosphorus by mid-July of both seasons.
 - Biochemical reactions also resulted in increased ammonia levels, manganese, iron, and alkalinity, as well as phosphorus.
 - The area of lake bottom >7m deep was estimated to be 120 acres or 12% of the bottom.
 - Buildup of phosphorus and other byproducts of anaerobic cellular respiration occurred at the site that was 6m deep but to a lesser degree.
 - Concurrent with the buildup of phosphorus at the lake bottom was the increase over the season of the mass of phosphorus in the water column implicating internal loading of phosphorus as an important source for algal growth.
- The pelagic algal community was largely dominated by the cyanobacteria, aka blue-green algae.
 - Cyanobacteria concentrations modestly increased through mid-July, but decreased in August following a late July copper sulfate treatment both years.
 - By September of both years, concentrations had increased substantially and reached cell concentrations in excess of 100,000 cells/mL and in some cases were closer to 200,000 cells/mL.
 - High nitrogen to phosphorus ratios were clearly characteristic of phosphorus limitation early in both seasons, but after mid-July ratios decreased and neared levels characteristic of nitrogen limitation.
 - Approximately 37% of the bottom of the lake lies between 0 and 4m deep which are the depths where cyanobacteria akinetes germinate and produce future populations.
- Other variables closely corresponded with total and cyanobacteria cell concentrations including chlorophyll-*a* concentrations, fluorometrically measured relative cyanobacteria levels, and Secchi transparencies.
 - The strength of the relationships between those variables may be useful in supplementing biweekly cyanobacteria cell concentrations as a way to aid the public make informed decisions on recreational use of the lake.

- Although not part of the original study plan, cyanotoxin testing was introduced by AER in 2018 and the BLPA continued with analyses in 2019 by Dr. Edwin Wong in the Biological and Environmental Science Department of Western Connecticut State University. Sample collections and deliveries to WCSU were performed by AER.
 - Concentration of the most common cyanotoxin, microcystin, never exceeded the threshold adopted by the State of 4ppb in 2018, which changed to 8ppb in 2019.
- Most levels of dissolved salts and minerals, and specific conductance levels at Bantam Lake were notably higher in 2018 and 2019 than corresponding levels of the early 1990s.
 - This implicates a watershed influence on the lake.
 - Any effort to control internally derived phosphorus should be accompanied by a concerted effort to understand watershed input and plans to control them if necessary.
- Bantam Lake starts the season as a mesotrophic lake but is clearly eutrophic by September.
 - The copper sulfate treatment appears to prolong through August acceptable water quality conditions.
- A set of recommendations have been provided for consideration to help advance water quality management efforts.

TABLE OF CONTENTS

Executive Summary.....	2
Introduction	9
Methods.....	10
Monthly Water Quality Monitoring.....	10
Biweekly Algal Monitoring.....	14
Additional Data Collections	14
Mixing and Stratification	15
Temperature and Oxygen Dynamics.....	15
Biological Assessments.....	22
Secchi Transparencies.....	22
Chlorophyll-a Concentrations.....	24
Secchi Transparency and Chlorophyll-a.....	24
Algal Community Structure.....	25
Cell Concentrations and Biological Surrogates.....	27
Cyanobacteria Profiles.....	29
Cyanotoxins.....	34
Cyanotoxins vs Cyanobacteria Counts and Relative Concentrations.....	35
Nutrient Assessments.....	37
Total Phosphorus.....	37
Phosphorus Mass Balance	38
Nitrogen.....	39
Total Nitrogen to Total Phosphorus Ratios	43
Chemical Assessments.....	45
Specific Conductance	45
pH and Alkalinity	48
Iron and Manganese.....	50
Oxidation-Reduction Potential	52
Base Cations and Chloride	56
General Trends.....	57
Trophic Trends.....	57
Dissolved Salts on the Rise.....	58
Management Considerations.....	59

Copper Sulfate Treatments.....	59
Stratified and Mixed Water Columns.....	59
Internal Loading of Phosphorus and Depth	60
Cyanobacteria at Bantam Lake.....	62
Recommendations.....	67
Plan for an Alum Treatment.....	67
Monthly Water Quality Monitoring.....	67
Biweekly Cyanobacteria Monitoring.....	67
Cyanotoxin Monitoring.....	68
Statistical Analyses of Phycocyanin and Chlorophyll-a Data.....	68
Forward-thinking Measures to Reduce Cyanobacteria Population.....	68
Assess Watershed Management Strategies	69
Cyanobacteria Bloom Watch.....	69
References.....	70
Appendix 1. List of algal genera observed in 2018 and 2019.....	71
Appendix 2. 2018 and 2019 Nutrient and Chemical Data.....	76

LIST OF FIGURES

Figure 1. Locations of the sampling sites on Bantam Lake during the 2018 and 2019 seasons.....	11
Figure 2. Temperature and oxygen isopleth diagrams for the North Bay site in 2018 (top) and 2019 (bottom).....	18
Figure 3. Temperature and oxygen isopleth diagrams for the Center Lake site in 2018 (top) and 2019 (bottom).....	19
Figure 4. Temperature and oxygen isopleth diagrams for the Folly Point site in 2018 (top) and 2019 (bottom).....	20
Figure 5. Temperature and oxygen isopleth diagrams for the South Bay site in 2018 (top) and 2019 (bottom).....	21
Figure 6. Secchi transparency measurements in the 2018 (top) and 2019 (bottom) season at the North Bay (NB), Center Lake (CL), Folly Point (PF), and South Bay (SB) sites.....	23
Figure 7. Chlorophyll- <i>a</i> concentrations at the North Bay (NB) and Center Lake (CL) sites in 2018 (left) and 2019 (right) seasons.....	24

Figure 8. Regression analysis of paired Secchi transparency and chlorophyll-*a* data collected at the North Bay and Center Lake sites during the 2018 and 2019 sampling season..... 25

Figure 9. Relative abundance of algae taxa at the NB (top) and CL (bottom) sites on Bantam Lake in 2018 (left) and 2019 (right)..... 26

Figure 10. The 2018 and 2019 algal community dynamics..... 27

Figure 11. Relative cyanobacteria isopleth diagrams for the North Bay, Center Lake, Folly Point, and South Bay sites in 2018..... 30

Figure 12. Relative cyanobacteria isopleth diagrams for the North Bay, Center Lake, Folly Point, and South Bay sites in 2019. The black lines and dots represent the location of a thermocline in the water column. Lines represent continuous observation of a thermocline over time while dots represent isolated events of stratification separated by mixed conditions..... 31

Figure 13. Changes in relative cyanobacteria concentrations over time in 2018 and 2019 at North Bay (NB), Center Lake (CL), Folly Point (FP) and South Bay (SB)..... 32

Figure 14. Relationships between A) cyanobacteria cell concentration and relative cyanobacteria levels, B) microcystin concentrations and cyanobacteria cell concentrations, C) microcystin concentrations and relative cyanobacteria levels, and D) microcystin concentration and dates the samples were collected..... 36

Figure 15. Total phosphorus concentrations at the North Bay (NB) and Center Lake (CL) sites in the 2018 (top) and 2019 (bottom) seasons..... 37

Figure 16. The top panels display the averaged phosphorus mass in the epilimnion (Epi), metalimnion (Meta), and hypolimnion (Hypo) in 2018 (left) and 2019 (right). The bottom panel displays the total mass of phosphorus in the water column from May 21st to October 22nd of 2018..... 40

Figure 17. Ammonia concentrations in the 2018 (top panels) and 2019 (bottom panels) seasons at the North Bay (NB; right panels) and Center Lake (CL; left panels) in the epilimnion (Epi or 1m from the surface), metalimnion (Meta or mid-level depths when not stratified), and hypolimnion (Hypo or 0.5m from the bottom). 41

Figure 18. Total Kjeldahl nitrogen (TKN) concentrations in the 2018 (top panels) and 2019 (bottom panels) seasons at the North Bay (NB; right panels) and Center Lake (CL; left panels) in the epilimnion (Epi or 1m from the surface), metalimnion (Meta or mid-level depths when not stratified), and hypolimnion (Hypo or 0.5m from the bottom).... 42

Figure 19. Regression of all total Kjeldahl nitrogen (TKN) levels against total nitrogen levels from both sites, all depths, and both seasons..... 43

Figure 20. Redfield ratios (total nitrogen: total phosphorus) at the North Bay (NB) and Center Lake (CL) sites from May to October in 2018 and 2019..... 44

Figure 21. Specific conductance isopleth diagrams for the North Bay, Center Lake, Folly Point, and South Bay sites in 2018	46
Figure 22. Specific conductance isopleth diagrams for the North Bay, Center Lake, Folly Point, and South Bay sites in 2019	47
Figure 23. Alkalinity in the epilimnion at 1m (Epi), metalimnion or mid-depths (Meta), and hypolimnion (Hypo) at the North Bay and Center Lake sites in 2018 and 2019.....	49
Figure 24. Manganese in the epilimnion at 1m (Epi) and hypolimnion (Hypo) at the North Bay and Center Lake sites in 2018 and 2019.	51
Figure 25. Ferrous iron in the epilimnion at 1m (Epi) and hypolimnion (Hypo) at the North Bay and Center Lake sites in 2018 and 2019.	52
Figure 26. Oxidation reduction potential isopleth diagrams for the North Bay, Center Lake, Folly Point, and South Bay sites in 2019.....	54
Figure 27. Regression of the sum total of ion concentration against the corresponding specific conductance in samples collected at the North Bay and Center Lake sites in 2018 and 2019.....	56
Figure 28. Wind directions and speeds on selected sampling dates. Data from the White Memorial Weather Station.....	59
Figure 29. Ratios of ammonia (NH ₄), manganese (Mn), iron (Fe), total phosphorus (TP), and alkalinity measured in the surface and bottom of the North Bay and Center Lake sites in 2018.....	61
Figure 30. Map of Bantam Lake with areas of >7 meters of depth delineated.	63
Figure 31. A filament of <i>Dolichospermum spp.</i> The yellow arrow points to the heterocyst in the filament; the red arrow points to the akinete.....	64
Figure 32. Generalized life cycle of <i>Anabaena</i> (aka <i>Dolichospermum</i>) <i>spp.</i> , <i>Aphanizomenon spp.</i> , and similar Cyanobacteria genera (Kortmann 2015).....	64
Figure 33. Map of Bantam Lake with areas of ≤4 meters of depth delineated.....	65

LIST OF TABLES

Table 1. Summary of data collections for Bantam Lake in 2018 and 2019 used in this report.....	12
Table 2. Relationships between total algae cell concentrations and cyanobacteria cell concentrations with chlorophyll- <i>a</i> concentrations and Secchi transparencies.....	28
Table 3. Microcystin concentrations from samples collected on July 16 th , July 30 th , and August 16 th of 2018.....	33

Table 4. Microcystin concentrations measured in samples collected at the North Bay and Center Lake sites in 2019..... 34

Table 5. Summary statistics for the base cations, chloride, and alkalinity data collected at North Bay (NB) and Center Lake (CL) sites in 2018 and 2019 55

Table 6. Comparisons of the 2018 and 2019 Bantam Lake season averaged water quality variables to averages in an early 1990s and to ranges observed in lakes located in the Connecticut Western Uplands (Canavan and Siver 1995) conducted in the early 1990s. 57

Table 7. Trophic classification criteria used by the Connecticut Experimental Agricultural Station (Frink and Norvell, 1984) and the CT DEP (1991) to assess the trophic status of Connecticut lakes 58

INTRODUCTION

Bantam Lake is located in the Towns of Litchfield and Morris, CT; it is approximately 966 acres and is the largest natural lake in Connecticut. Geologically, it lies in the Western Uplands of Connecticut (Bell 1985, Canavan & Siver 1995) that has a bedrock geology characterized by erosion-resistant crystalline rock including schists, gneiss, granite gneiss, and granofels (Healy & Kulp 1995).

The watershed of Bantam Lake is 20,218 acres resulting in a watershed to lake ratio of approximately 21. In a 1995 survey, land use was characterized as mainly deciduous forest and agriculture lands with smaller areas of medium-density residential land use, wetlands, and coniferous forests (Healy & Kulp 1995). Much of the shoreline is lined with homes, beaches, and several camps. There is also open space along the northern shoreline, which is owned by the White Memorial Foundation.

There is a rich history of lake research and management activities at Bantam Lake. The lake was included in numerous State-wide surveys of Connecticut Lakes as far back as the 1930s (e.g. Deevey 1940, Frink & Norvell 1984, Canavan & Siver 1994, 1995, and Healy & Kulp 1995). Many of the management efforts centered on two issues: 1) invasive aquatic plant control and, 2) algal blooms / eutrophication. Although an important component of a lake ecosystem, aquatic plants and their management are not the subject of this report due to that contract being awarded to Northeast Aquatic Research LLC. However, management of aquatic plants can have an adverse impact on water quality if programs do not include rigorous oversight. Water quality monitoring is an important component of aquatic plant management because significant shifts in water chemistry when compared to historical data can indicate adverse impacts from the plant management activities.

Bantam Lake has historically experienced high concentrations of cyanobacteria beginning between the midsummer and fall portions of the recreational season. High cyanobacteria concentrations, or harmful algae blooms, have become a key issue in lake management due to the risk they present to ecosystem and public health. In addition to depletion of oxygen from the water column following a bloom, many genera of cyanobacteria are capable of synthesizing toxins. These cyanotoxins are generally grouped into one of several categories: hepatotoxin that cause liver damage, neurotoxins that have been associated with neurological disorders like amyotrophic lateral sclerosis (ALS), and others in groups classified as dermatotoxins, cytotoxins, and endotoxins. The State of Connecticut provides a useful summary on cyanobacteria, the toxins they produce, and standards by which municipal health department can assess conditions at public beaches (CT DPH & CT DEEP 2019).

Bantam Lake greatly benefits from the stewardship and active oversight of management activities by the Bantam Lake Protective Association (BLPA). The BLPA likewise benefits from the environmental expertise of the nearby White Memorial Foundation and Center as will be evidenced later in this report. The BLPA leverages aquatic herbicide programs to manage aquatic invasive plants including *Myriophyllum spicatum* (Eurasian watermilfoil), *Cabomba caroliniana* (Fanwort), and *Potamogeton crispus* (Curly-leaf pondweed). The BLPA also utilizes copper sulfate treatments during the summer to control cyanobacteria populations that threaten the recreational uses of

the lake. Another important BLPA initiative is the public communications program whereby water quality and cyanobacteria concentration data are electronically made available. This affords the recreational public the tools to make informed decisions with regards to use of the lake.

In 2018, the BLPA contracted with Aquatic Ecosystem Research (AER) to implement a monthly water quality monitoring program and a program to collect and analyze water samples biweekly from April through October to quantify cyanobacteria populations. Results of that biweekly program are the basis of communications to the public about lake conditions. AER was also hired in 2019 to perform the same services. This report presents the results of the two years of study, interprets those results, and provide recommendations for future management strategies.

METHODS

Monthly Water Quality Monitoring

Four sites were visited monthly from April through October in 2018 and 2019. Dates of the 2018 visits were April 22nd, May 21st, June 18th, July 16th, August 16th, September 24th, and October 22nd. A second visit in July of 2018 occurred on the 30th. The 2019 dates were April 22nd, May 21st, June 18th, July 15th, August 12th, September 9th, and October 7th. An additional visit occurred on August 26th to collect water samples that were not collected on August 12th. Sites were identified as North Bay (NB), Center Lake (CL), Folly Point (FP), and South Bay (SB; see Fig. 1). Maximum depths were approximately 6 meters (m), 8m, 6.5m, and 4.5m at the NB, CL, FP, and SB sites, respectively.

During each site visit, Secchi transparency was measured with a 26cm diameter Secchi disk. Additionally, vertical profile data for six parameters were collected using a Eureka Manta II Sensor. Profiled data were measured at 0.5m from the surface and at one meter intervals to 0.5m above the bottom, and included the following variables: temperature (°C), dissolved oxygen (mg/L), percent oxygen saturation (% O₂), specific conductance (µS/cm), pH, and relative cyanobacteria concentration. In 2019, oxidation-reduction potential was added to the list of parameters collected in this manner.

Water samples were collected at NB and CL during site visits and analyzed for the variables listed in Table 1 by a State-certified laboratory with the exception of algae samples, which were analyzed by AER. Water samples were collected using two different methods and at several depths in the water column. For nutrient and alkalinity analyses, samples were collected with a horizontal Van Dorn water sampler at 1m below the surface (epilimnion), at approximately 0.5m above the sediment water interface (hypolimnion), and at the thermocline, which was determined using the vertical temperature profiles collected at each site on each sample date. For iron (Fe) and manganese (Mn), samples were collected with the Van Dorn sampler at 1m below the surface and 0.5m above the sediment water interface. For base cations of sodium (Na⁺), potassium (K⁺), calcium (Ca²⁺), magnesium (Mg²⁺), and the anion chloride (Cl⁻), samples were collected from 1m below the surface.



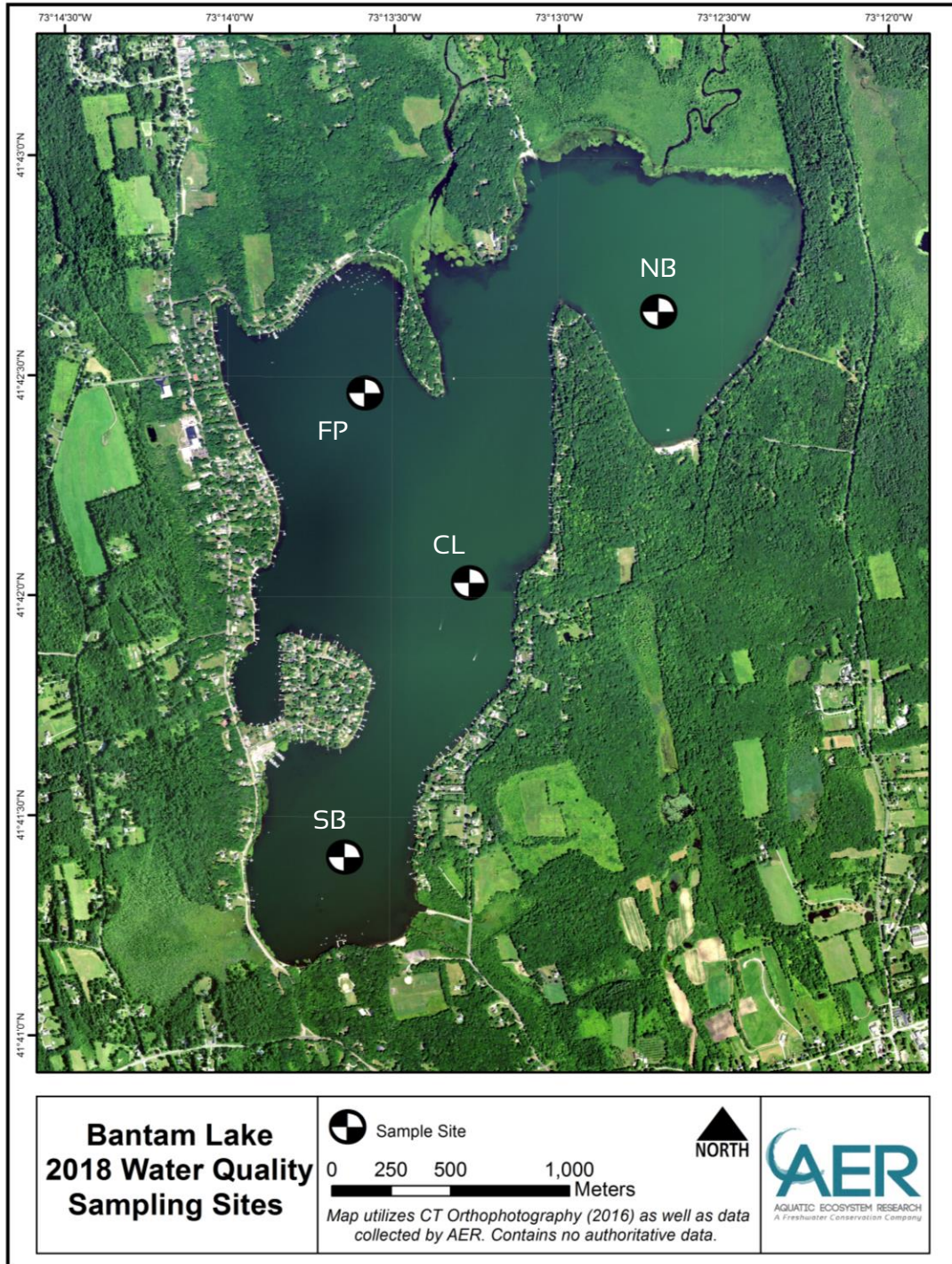


Figure 1. Locations of the sampling sites on Bantam Lake during the 2018 and 2019 seasons. NB = North Bay Site, FP = Folly Point Site, CL = Center Lake Site, and SB = South Bay Site.

Table 1. Summary of data collections for Bantam Lake in 2018 and 2019 used in this report. NB = North Bay Site, CL = Center Lake Site, FP = Folly Point Site, and SB = South Bay Site. Chl-*a* = chlorophyll-*a*.

2018 Dates	Profiles and Secchi ¹	Algae ²	Nutrients & Alkalinity ³	Iron & Manganese ⁴	Chl- <i>a</i> , Cations, Chloride ⁵
22-Apr-18	NB, CL, FP, SB	NB, CL	NB, CL	NB, CL	NB, CL
8-May-18	NB, CL, FP, SB	NB, CL			
21-May-18	NB, CL, FP, SB	NB, CL	NB, CL	NB, CL	NB, CL
1-Jun-18*	NB, CL, FP				
4-Jun-18	NB, CL, FP, SB	NB, CL			
18-Jun-18	NB, CL	NB, CL	NB, CL	NB, CL	NB, CL
26-Jun-18*	NB, CL, FP, SB				
2-Jul-18	NB, CL, FP, SB	NB, CL			
5-Jul-18*	NB, CL, FP, SB				
6-Jul-18*	NB, CL, FP, SB				
11-Jul-18*	NB, CL, FP, SB				
16-Jul-18	NB, CL, FP, SB	NB, CL, SB	NB, CL	NB, CL	NB, CL
19-Jul-18*	NB, CL, FP, SB				
30-Jul-18	NB, CL, FP, SB	NB, CL	NB, CL		
2-Aug-18*	NB, CL, FP, SB				
10-Aug-18*	NB, CL, FP, SB				
16-Aug-18	NB, CL, FP, SB	NB, CL			NB, CL
24-Aug-18*	NB, CL, FP, SB				
27-Aug-18	NB, CL, FP, SB	NB, CL, SB	NB, CL	NB, CL	
5-Sep-18*	NB, CL, FP, SB				
11-Sep-18	NB, CL, FP, SB	NB, CL, SB			
20-Sep-18*	NB, CL, FP, SB				
24-Sep-18	NB, CL, FP, SB	NB, CL, SB	NB, CL	NB, CL	NB, CL
4-Oct-18*	NB, CL, FP, SB				
9-Oct-18	NB, CL, FP, SB	NB, CL			
22-Oct-18	NB, CL, FP, SB	NB, CL	NB, CL	NB, CL	NB, CL
8-Nov-18	NB, CL, FP, SB	NB, CL			

¹ Profile data include temperature, oxygen, specific conductance, pH, and relative cyanobacteria concentration measured at 0.5m and every meter below to 0.5m above the bottom.

² Algae data included a comprehensive genus list and algal cell enumeration from samples collected in the top 3m of the water column.

³ Nutrients include total phosphorus, total Kjeldahl nitrogen, nitrate, nitrite, and ammonia from samples collected at 1m below the surface, 0.5m above the bottom, and at the thermocline.

Table 1 (continued). Summary of data collections for Bantam Lake in 2018 and 2019 used in this report. NB = North Bay Site, CL = Center Lake Site, FP = Folly Point Site, and SB = South Bay Site. Chl-*a* = chlorophyll-*a*.

2019 Dates	Profiles and Secchi ¹	Algae ²	Nutrients & Alkalinity ³	Iron & Manganese ⁴	Chl- <i>a</i> , Cations, Chloride ⁵
22-Apr-19	NB, CL, FP, SB	NB, CL	NB, CL	NB, CL	NB, CL
6-May-19	NB, CL, FP, SB	NB, CL			
15-May-19*	NB, CL, FP, SB				
22-May-19	NB, CL, FP, SB	NB, CL	NB, CL	NB, CL	NB, CL
31-May-19*	NB, CL, FP, SB				
4-Jun-19	NB, CL, FP, SB	NB, CL			
7-Jun-19*	NB, CL, FP, SB				
14-Jun-19*	NB, CL, FP, SB				
19-Jun-19	NB, CL, FP, SB	NB, CL	NB, CL	NB, CL	NB, CL
27-Jun-19	NB, CL, FP, SB	NB, CL			
1-Jul-19*	NB, CL, FP, SB				
8-Jul-19*	NB, CL, FP, SB				
15-Jul-19	NB, CL, FP, SB	NB, CL	NB, CL	NB, CL	NB, CL
24-Jul-19*	NB, CL, FP, SB				
29-Jul-19	NB, CL, FP, SB	NB, CL			
31-Jul-19*	NB, CL, FP, SB				
1-Aug-19	NB, CL, FP, SB	NB, CL			
2-Aug-19*	NB, CL, FP, SB				
6-Aug-19*	NB, CL, FP, SB				
7-Aug-19*	NB, CL, FP, SB				
12-Aug-19	NB, CL, FP, SB	NB, CL	NB, CL	NB, CL	NB, CL
20-Aug-19*	NB, CL, FP, SB				
26-Aug-19	NB, CL, FP, SB	NB, CL			
9-Sep-19	NB, CL, FP, SB	NB, CL	NB, CL	NB, CL	NB, CL
23-Sep-19	NB, CL, FP, SB	NB, CL			
7-Oct-19	NB, CL, FP, SB	NB, CL	NB, CL	NB, CL	NB, CL
21-Oct-19	NB, CL, FP, SB	NB, CL			

⁴ Samples collected at 1m below the surface and 0.5m above the bottom.

⁵ Chlorophyll-*a* samples are an integration of the top 3m of the water column. Cation (sodium, potassium, calcium, and magnesium) samples are collected at 1m of depth.

* Data collections by James Fischer of the White Memorial Conservation Center. All others by AER.

For chlorophyll-*a* and algal analyses, a weighted tube sampler was used to collect and integrate water from the top three meters of the water column at the NB and CL sites. Additionally, a 10µm mesh plankton net was used to collect from within the top 3m of the CL water column for a concentrated algal sample. Chlorophyll-*a* was analyzed by a State-certified laboratory.

Biweekly Algal Monitoring

In addition to the sampling schedule described above, nine extra visits occurred between April 22nd and November 8th of 2018; eight additional visits occurred between April 22nd and October 22nd in 2019. All visits were scheduled on a biweekly basis which formed the basis of the program to monitor the algal community and determine cyanobacteria cell concentrations (Table 1).

During each visit, Secchi transparency and vertical profile data were collected at NB, CL, FP, and SB. A total of 15 samples for algal analyses were collected at NB and CL each season following methods discussed below.

Portions of the 10µm mesh plankton net sample were analyzed microscopically before preservation with Lugol's solution to establish a comprehensive genus list (Appendix 1). The whole water samples were also preserved with Lugol's solution and later treated with hydrostatic pressure to collapse gas vesicles that might have been created by cyanobacteria cells in the sample for buoyancy regulation (Lawton et al. 1999). Measured volumes of the preserved whole water samples were concentrated into smaller measured volumes with centrifugation and a vacuum pump / filtration flask system. A known portion of those concentrates were pipetted into a counting chamber and genus-level algal cell enumerations were performed by counting algae cells in a subset of fields within the counting chamber slide using an inverted Nikon Diaphot research microscope. Those counts were then corrected to be reflective of the whole sample.

Additional Data Collections

Additional Secchi transparency and profile data were collected by James Fischer, Director of Research for the White Memorial Conservation Center. The White Memorial Conservation Center is a partner and advisor to the Bantam Lake Protective Association. The data collected by Mr. Fischer facilitated a much higher temporal resolution in assessments of seasonal Secchi transparencies, and temperature/oxygen dynamics in the water column. These data have been incorporated into the results and discussion below. Specific dates of AER's and Mr. Fischer's site visits and types of data collections undertaken are provided in Table 1.

Mixing and Stratification

Patterns of water column mixing and resistance to mixing (or stratification) were assessed using most temperature profile data collected. Where temperature profile data was collected by both AER and Mr. Fischer on the same date, the AER data was used. Resistance to mixing, which is an assessment of the ability of two different water volumes – that differ in temperature and density – to mix, was calculated using the Relative Thermal Resistance to Mixing (RTRM) formula: $(D_1 - D_2)/(D' - D^0)$, where D_1 is the density of upper water volume, D_2 is the density of the lower water volume, D' is the density of water at 5°C, and D^0 is the density of water at 4°C.

TEMPERATURE AND OXYGEN DYNAMICS

The biweekly and often weekly temperature and oxygen profile data were used to develop isopleth charts, which provide graphic representations of the seasonal dynamics within the water column. In isopleth charts, temperature and oxygen profile data for a site are plotted and interpolate between data collections throughout the water column; the result is a graphical display of the full season's data. Isopleths provide a view of seasonal patterns in water quality data that might not be evident in the individual sampling's graphical displays.

Temperature and oxygen isopleths varied from site to site, which was due to site differences such as depth and spatial location. Differences were also detected between the year-specific sites where water temperature warmed earlier in the 2018 season, reached higher mid-season temperatures, and remained warmer later into the season (Figs. 2-5). Differences in seasonal stratification patterns were observed between sites and between years at the same sites.

The CL site was the deepest (i.e. 8m); seasonal temperature and oxygen dynamics were distinctive at this site compared to the other sites. This portion of the water column stratified earlier in 2018 compared to 2019. Stratification broke down after August 27th in 2018 and September 9th in 2019 (Fig. 3).

The CL water column contained a concentration $\geq 5\text{mg/L}$ oxygen, which is a critical value for aquatic life, in April and throughout May in both 2018 and 2019. However, by early June, oxygen concentrations of $< 1\text{mg/L}$ were observed from 6m of depth to the bottom in 2018 and at the 8m stratum in 2019. In 2018, $< 1\text{mg/L}$ of oxygen was recorded from 6m to the bottom from June 4th through July 11th and from 5m to the bottom on July 16th and 19th. The period of time between July 19th and July 30th was significant for 2018 water quality. It was during that time that the thermocline migrated down to between 6 and 7m of depth.

The upper boundary of the anoxic waters continued to fluctuate between the 5m and 6m strata until August 24th when it was observed at the 7m strata. By September 11th a thermally mixed water column reintroduced $> 7\text{mg/L}$ of oxygen throughout the water

column. For the remainder of the 2018 season, anoxic conditions were observed at the bottom one to two meters of the water column on September 20th and October 22nd.

In 2019 at the CL site, the bottom of the water column fluctuated above and below 1mg/L of oxygen from early- to mid-June. The upper boundary of anoxic waters moved from between the 7m to 8m strata on June 14th to between the 5 and 6m strata on July 1st and to between the 4 and 5m strata by July 8th. Similar to 2018, mid- to late- July oxygen concentrations of <1mg/L extended from the bottom, above the thermocline, up to 5m of depth in 2019. These conditions persisted into early August with the upper anoxic boundary reaching to the 4m stratum on August 1st. The upper boundary was then observed at greater depths until September 3rd at which time, the entire water column contained >6mg/L oxygen. Anoxic conditions at the very bottom of the CL did occur afterwards but were not of the duration or water volume as those in July and early August.

The temperature and oxygen isopleth diagrams for the NB and FP sites for 2018 and 2019 shared a number of similarities (Figs. 2 & 4). At the CL site, the water columns at NB and FP warmed earlier, reached higher temperatures, and stayed warmer longer in 2018 than they did in 2019. Dissimilar to CL, periods of continuous stratification at NB and FP were of shorter duration and complete mixing events were more common. At both NB and FP – in both years – the first signs of stratification were observed near the end of May. In 2018 the water columns remained stratified until June 18th at NB and August 16th at FP before mixing. Site NB would stratify again from July 2nd to July 19th, mix, and again stratify from August 10th to August 16th.

Between May 22nd and June 19th in 2019, the water columns at both the NB and FP sites were periodically mixed between short episodes of stratification. At NB, a period of continuous stratification was observed from June 19th through August 7th. At FP continuous stratification occurred between June 27th and August 12th.

Similar to CL, the first signs of anoxia at NB and FP occurred in early June at the bottom of the water column in both 2018 and 2019. In 2018, anoxic conditions persisted at the bottom strata, but were not anoxic in the strata just above. This continued until June 26th. Afterwards the bottom 1.5-2.0m of the NB water column contained <1mg/L oxygen, which persisted until August 2nd when mixing returned concentrations to 1.9mg/L at 6m and 4.3mg/L at 5m of depth. Oxygen concentrations at the very bottom (6m) of NB were <1mg/L for most of August through September 11th. The exception was August 24th when mixing replenished levels to 1.8mg/L. Concentrations throughout the water column from September 20th to November 8th were all >1mg/L.

Oxygen levels in 2018 at FP were similar to those at NB. One exception was the duration of midseason anoxic conditions at the bottom of FP, which lasted throughout July to August 16th.

In 2019 anoxic conditions near the bottom at NB and FP occurred between June 19th and August 20th. Of the remaining seven sampling dates after August 20th, oxygen

concentrations of <1mg/L were only observed at the very bottom on September 9th and 23rd.

Conditions at SB were unique due to the maximum depth of 4.5m and its location at the south end of the lake where the long fetch may have contributed to mixed conditions. In both years, the water column was rarely stratified based on RTRM values. The dates in 2018 when it was stratified were June 18th, July 2nd to July 6th, August 10th, and October 4th. In 2019, the SB site was stratified on May 31st, June 27th through July 1st, and August 2nd. On all other dates, the water column was largely mixed (Fig. 5). Resultingly, anoxic conditions were rare.

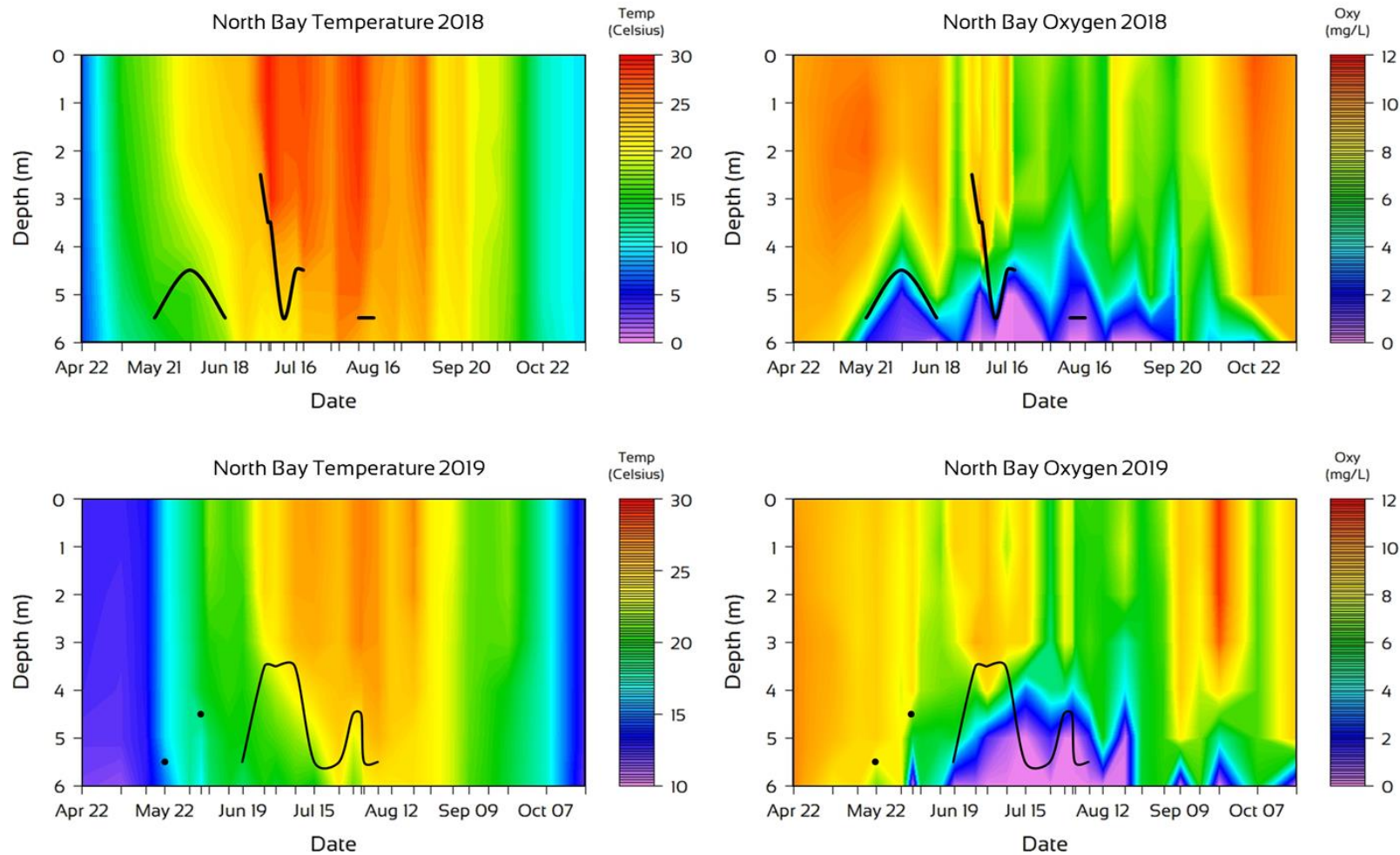


Figure 2. Temperature and oxygen isopleth diagrams for the North Bay site in 2018 (top) and 2019 (bottom). The black lines and dots represent the location of a thermocline in the water column. Lines represent continuous observation of a thermocline over time while dots represent isolated events of stratification separated by mixed conditions.



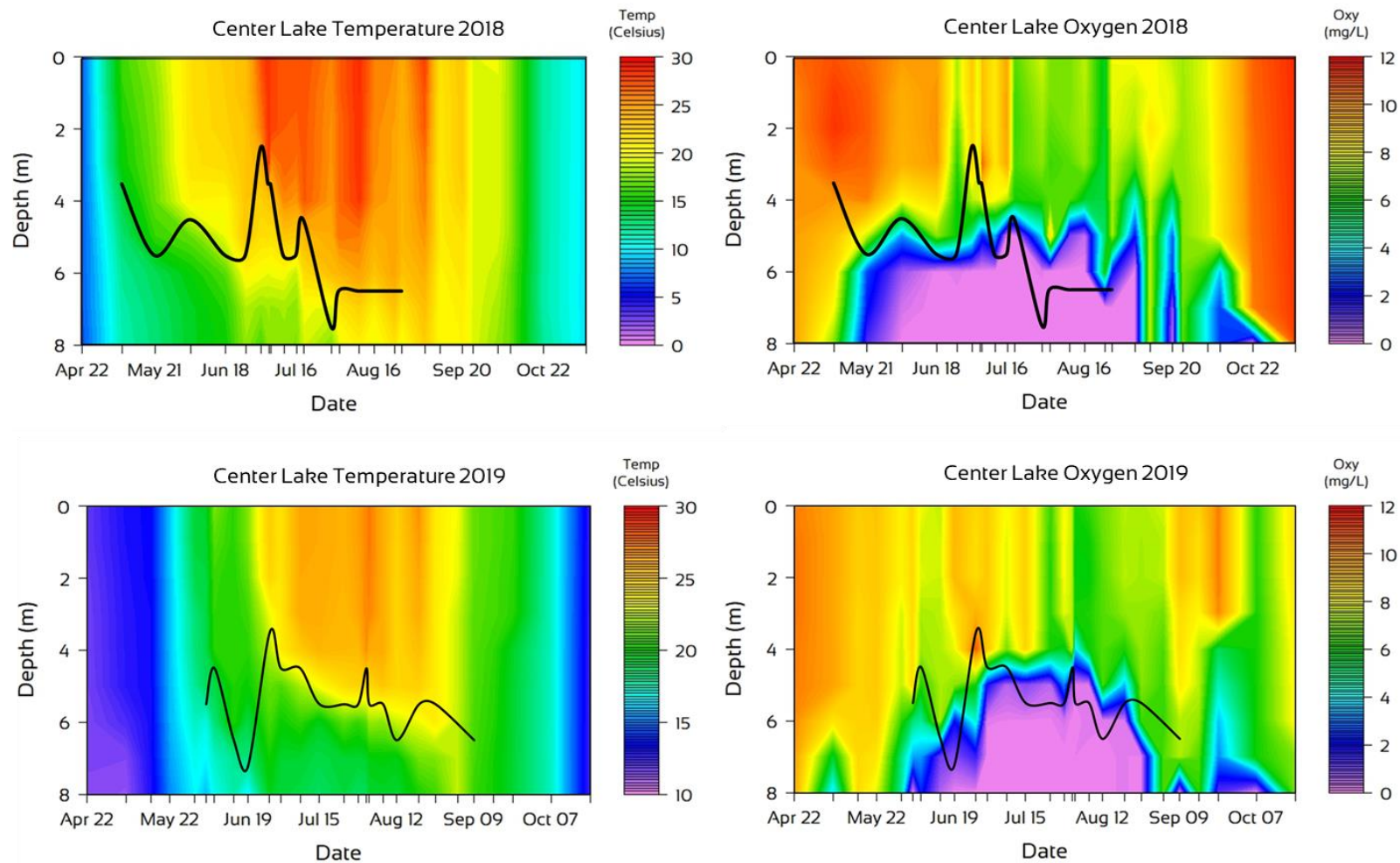


Figure 3. Temperature and oxygen isopleth diagrams for the Center Lake site in 2018 (top) and 2019 (bottom). The black lines and dots represent the location of a thermocline in the water column. Lines represent continuous observation of a thermocline over time while dots represent isolated events of stratification separated by mixed conditions.

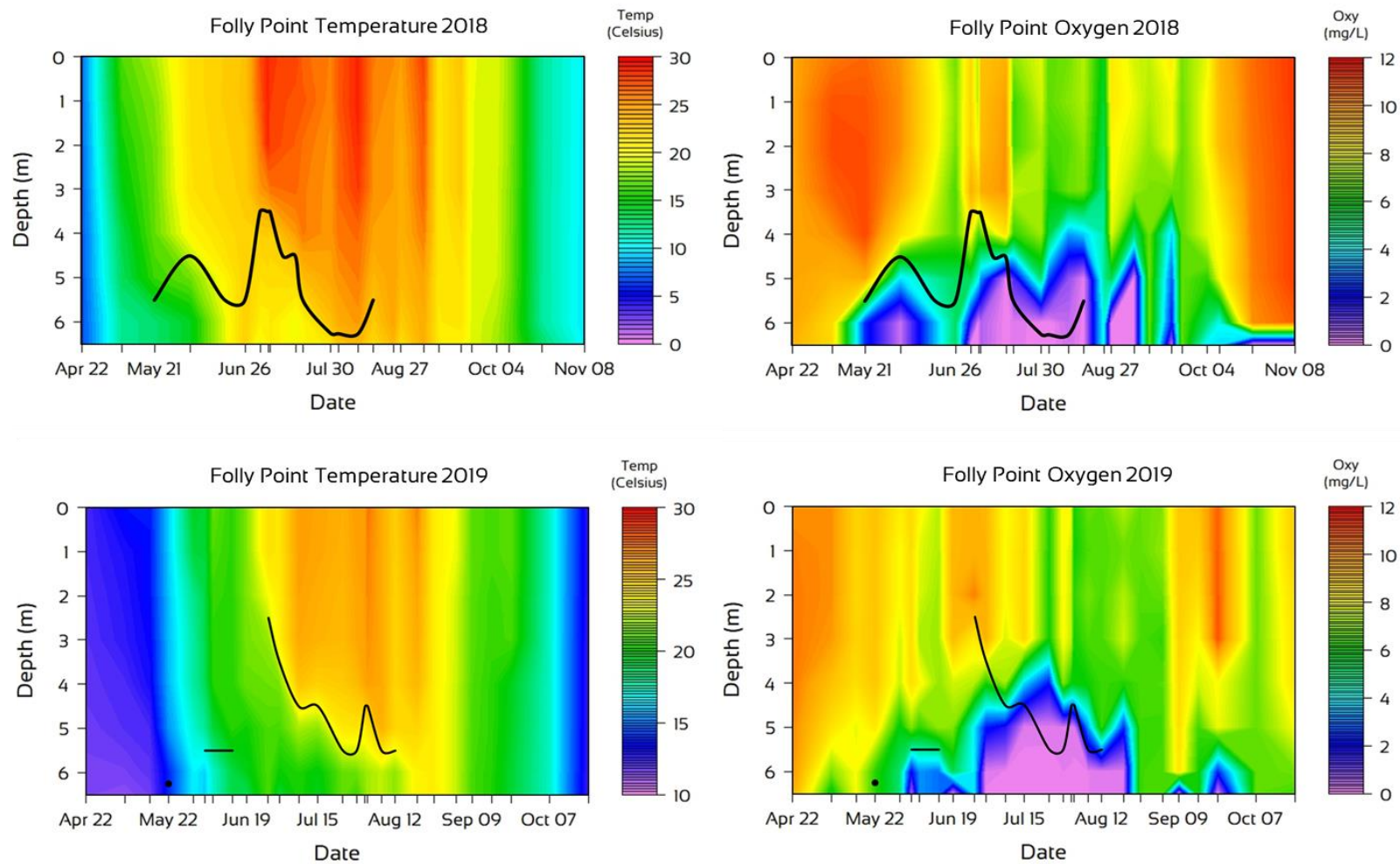


Figure 4. Temperature and oxygen isopleth diagrams for the Folly Point site in 2018 (top) and 2019 (bottom). The black lines and dots represent the location of a thermocline in the water column. Lines represent continuous observation of a thermocline over time while dots represent isolated events of stratification separated by mixed conditions.

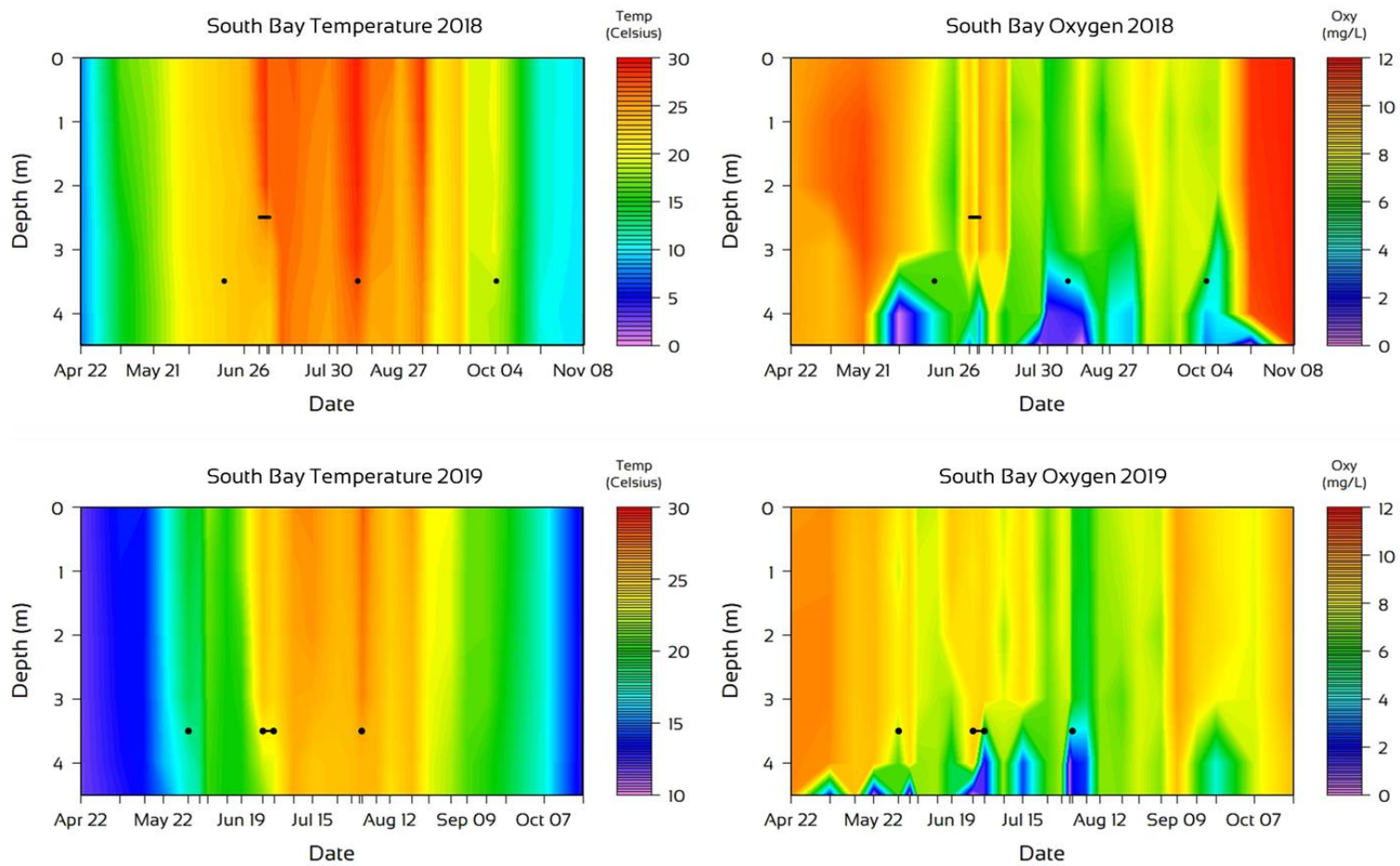


Figure 5. Temperature and oxygen isopleth diagrams for the South Bay site in 2018 (top) and 2019 (bottom). The black lines and dots represent the location of a thermocline in the water column. Lines represent continuous observation of a thermocline over time while dots represent isolated events of stratification separated by mixed conditions.

BIOLOGICAL ASSESSMENTS

Secchi Transparencies

Variables used to assess biological productivity at Bantam Lake included Secchi transparencies, chlorophyll-*a* concentrations, algae concentrations – including cyanobacteria cell concentrations – and relative cyanobacteria levels. Between April 22nd and November 8th of 2018, Secchi transparency was measured 27 times at the NB, CL, and FP sites, and 26 times at SB for a total of 107 readings. Between April 22nd and October 21st of 2019, Secchi measurements were taken 27 times at each site for a total of 108 readings.

The Bantam Lake average over the two seasons was 2.47m. The 2018 season average was 2.28m; in 2019 it was greater with an average clarity of 2.66m. Season low measurements of 0.98 and 0.99m in 2018 and 2019, respectively occurred in the later part of September both years. Season highs occurred between late May and early June in both years when it ranged between 3.48 and 3.70m in 2018, and from 3.43 to 4.95m in 2019.

In most cases the individual site averages in 2018, 2019, and the combined 2018-2019 averages were not statistically different with a few exceptions, e.g. the 2018 average Secchi transparency at NB was statistically higher than the average at SB. While not the case in 2019, the combined 2018-2019 average at NB was also significantly higher than the SB average. The combined 2018-2019 average at FP was significantly higher than the two-season average at SB; however, the FP and SB site averages were not significantly different from each other in either 2018 or 2019.

In 2018, Secchi transparencies of ≥ 3 m represented 15% of all measurements and all occurred between May 8th and July 6th with most occurring between May 21st and June 18th (Fig. 6). The largest class of 2018 Secchi measurements were those ranging from >2 m and <3 m, which accounted for 50% of the total. All but 7 of the 52 measurements taken between June 26th and August 27th fell within this range. Thirty-five percent of all Secchi transparencies were ≤ 2 m and 25% were ≤ 1.5 m (Fig. 6). All of the measurements of ≤ 2 m occurred after July 16th, with most occurring in the months of September and October. Twenty-seven of the 32 readings between September 5th and November 8th were ≤ 1.5 m.

In 2019, Secchi transparencies of ≥ 3 m comprised 36% of all measurements. As in 2018, most occurred between early May through early July; the remainder occurred between August 1st and August 20th (Fig. 6). Thirty-eight percent of all Secchi measurements in 2019 were >2 and ≤ 3 m, with most occurring between April 22nd and July 31st. Secchi transparencies of ≤ 2 m constituted the remaining 26% of all 2019 measurements. Measurements in this range occurred from the middle to the latter part of July, and from August 26th through the end of the monitoring season. All Secchi transparencies from September 23rd to October 7th, or 11% of all measurements, were <1.5 m.

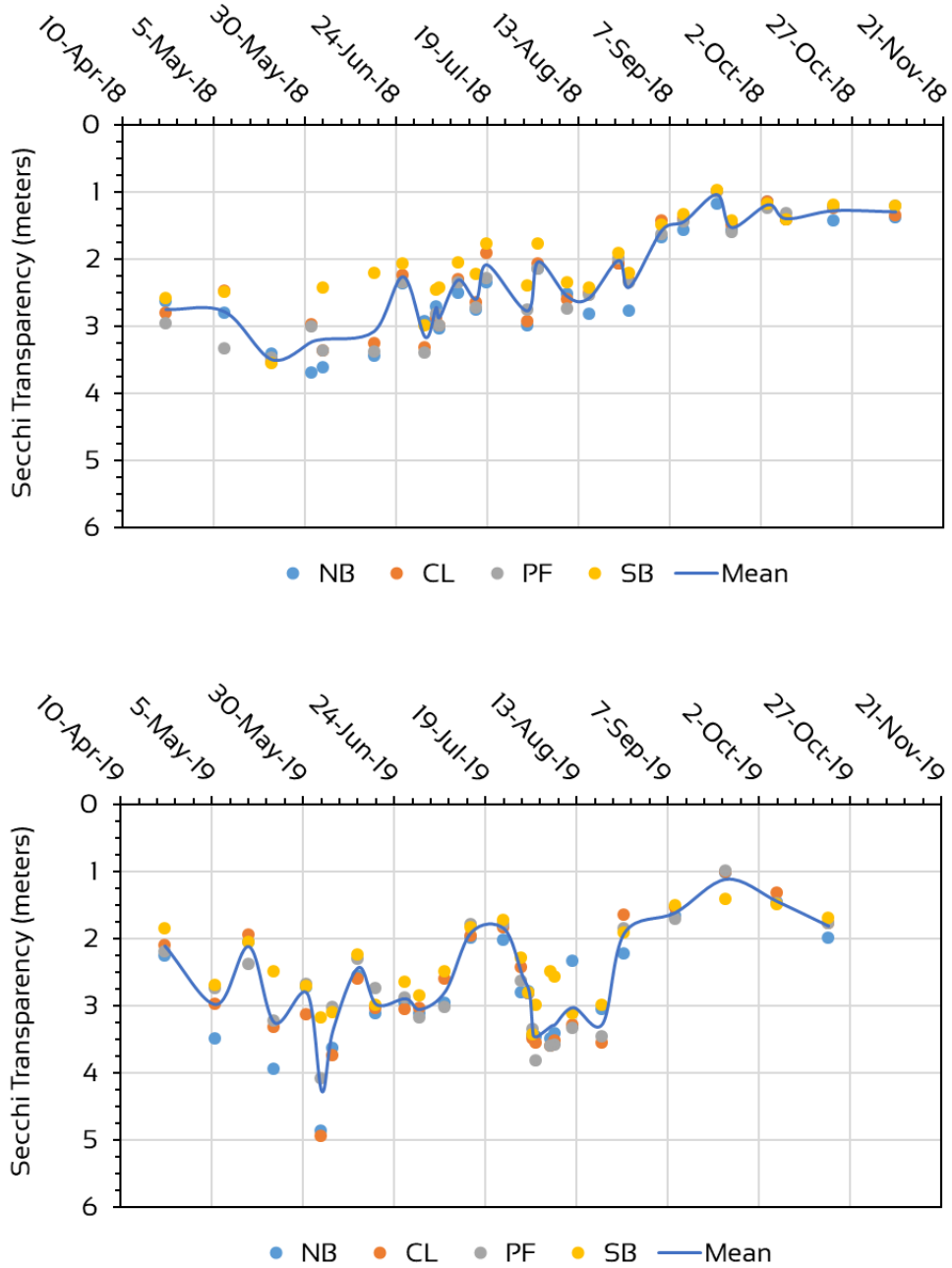


Figure 6. Secchi transparency measurements in the 2018 (top) and 2019 (bottom) season at the North Bay (NB), Center Lake (CL), Folly Point (PF), and South Bay (SB) sites. The blue line connects the means for the lake.

Chlorophyll-*a* Concentrations

Modestly elevated chlorophyll-*a* concentrations on April 22nd in both 2018 and 2019 were reflective of spring algal productivity (Fig. 7). In 2018, levels gradually decreased through early summer as a spring algal community diminished and transitioned to an early summer community, with levels fluctuating between 2.5 and 7 $\mu\text{g/L}$ through August 16th (Fig. 6). Between August 16th and September 24th chlorophyll-*a* concentrations increased significantly. September 24th levels were 21 and 17 $\mu\text{g/L}$ at NB and CL, respectively. Concentrations increase further at the CL site to 28 $\mu\text{g/L}$ by October 22nd.

In 2019, season lows occurred at both the NB and CL sites on May 21st, then increased through July 15th with concentrations ranging from 2.1 to 7.9 $\mu\text{g/L}$ during that time period (Fig. 6). Although concentrations tended to be higher at the NB site, the means for both sites during that period of time were not significantly different. August 26th concentrations decreased to May 21st levels before increasing to the highest levels of the season, which were encountered on September 9th and October 7th.

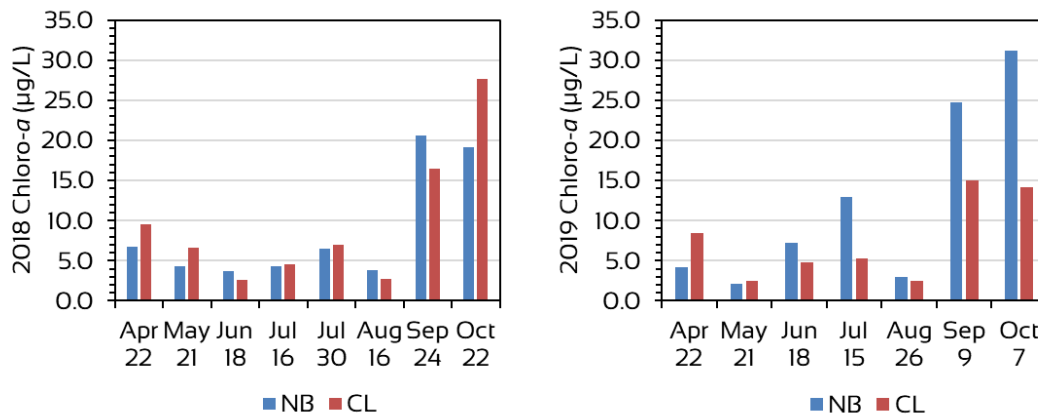


Figure 7. Chlorophyll-*a* concentrations at the North Bay (NB) and Center Lake (CL) sites in 2018 (left) and 2019 (right) seasons.

Secchi Transparency and Chlorophyll-*a*

In open water environments, Secchi transparency is most commonly related to the density of the algal populations. Greater algal productivity results in less clarity; less productivity yields greater transparency. Since chlorophyll-*a* is a photosynthetic pigment common to all algal taxa, including cyanobacteria, it is an excellent indicator of open water productivity and biomass.

To understand the relationship between the two variables at Bantam Lake, Secchi transparencies were regressed against corresponding chlorophyll-*a* concentrations collected at the NB and CL sites on 15 different dates over the two seasons (n=30). The two variables exhibited a strong correlation indicating that Secchi transparency has good predictive value for algal productivity as expressed by chlorophyll-*a* concentration (Fig. 8).

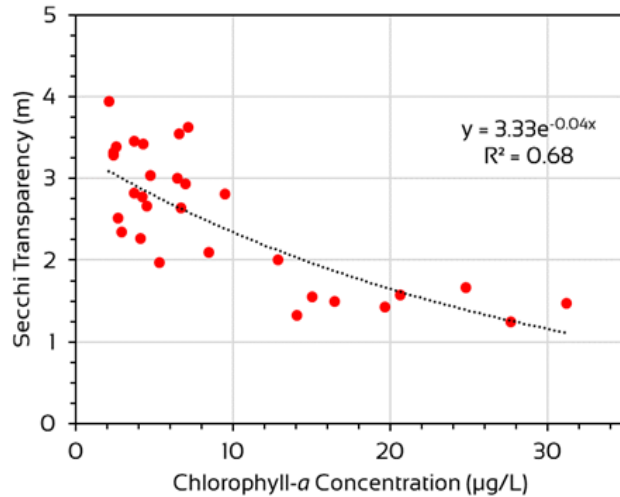


Figure 8. Regression analysis of paired Secchi transparency and chlorophyll-*a* data collected at the North Bay and Center Lake sites during the 2018 and 2019 sampling season. Each point represents both a Secchi transparency and chlorophyll-*a* concentration for one of the two sites on one of fifteen sampling dates.

Data points along the regression line were distributed into two groups. The first group contained points in which Secchi transparencies were between 2 and 4 meters and chlorophyll-*a* levels were between 2 and 10µg/L. This group exhibited greater variability, i.e. they were more loosely distributed around the regression line (Fig. 8). The second group was characterized by Secchi transparencies of ≤2 meters and chlorophyll-*a* concentrations of >12µg/L; these data were for the timeframe of September and October in both seasons. The relationship between Secchi transparency and chlorophyll-*a* concentration in this group was very strong, i.e. the points were more tightly distributed along the regression line.

Algal Community Structure

A total of 57 and 59 algal genera were identified in the Bantam Lake plankton in 2018 and 2019, respectively (Appendix A). The richest taxon was the Chlorophyta or *Green Algae*, which was represented by 25 genera over the two seasons. The most common genera included *Eudorina spp.*, *Gloeocystis spp.*, *Scenedesmus spp.*, *Anikistrodesmus spp.*, *Elakatothrix spp.*, *Pediastrum spp.*, and *Staurastrum spp.*

Cyanobacteria (aka *Blue-green Algae*) were the next most rich taxon and was represented by 14 genera over the two seasons. Seven cyanobacteria genera were common. The most common genera include *Dolichospermum spp.* (formerly *Anabaena spp.*), *Aphanizomenon spp.*, *Microcystis spp.*, *Woronichinia spp.*, *Pseudoanabaena spp.* and *Coelosphaerium spp.*

Nine genera of Bacillariophyta (aka *Diatoms*) were encountered in samples over the study period. Only two diatoms genera were observed nine or more times with *Au-locoseria spp.* occurring in 14 of the 15 samples sets each season. The only times it was not observed was in late August in 2018 and early August in 2019. Other common diatoms included *Tabellaria spp.*, *Stephanodiscus spp.*, *Asterionella spp.*, *Fragilaria spp.*, and *Synedra spp.*

Two of the five Chrysophyta (aka *Golden Algae*) genera observed were very common. These were *Mallomonas spp.* and *Uroglenopsis spp.* A listing of all genera observed in both seasons is provided in Appendix 1.

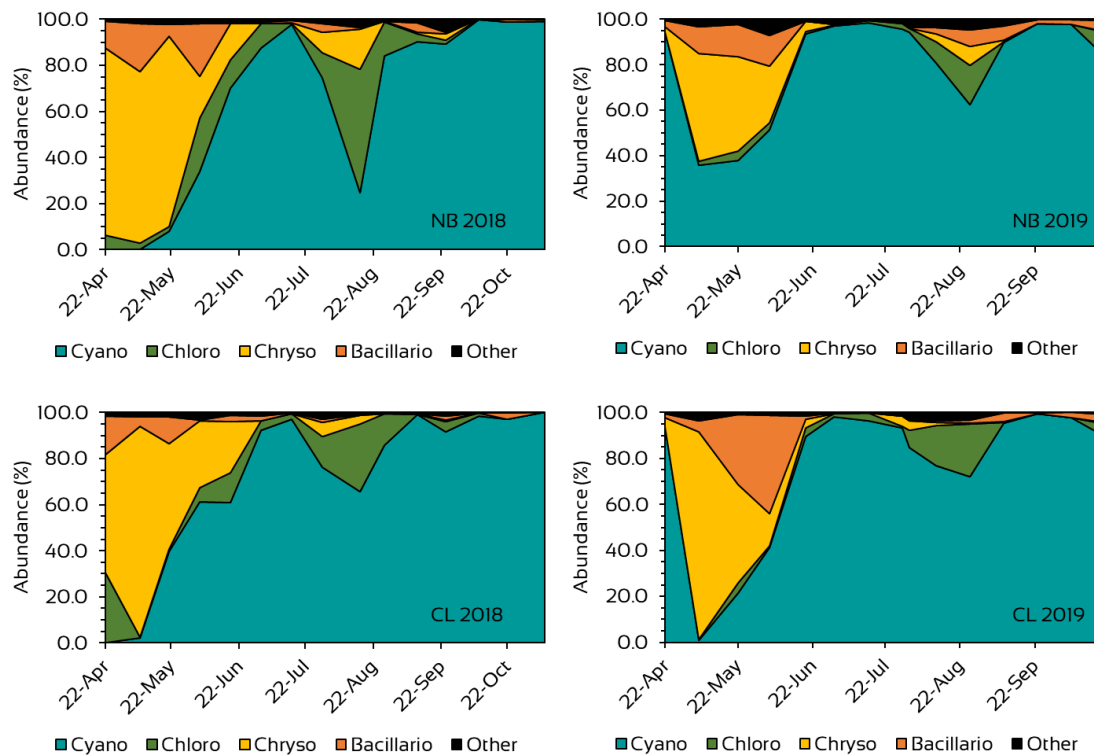


Figure 9. Relative abundance of algae taxa at the NB (top) and CL (bottom) sites on Bantam Lake in 2018 (left) and 2019 (right). Cyano = Cyanobacteria (Blue-green Algae); Chlo = Chlorophyta (Green Algae); Chryso = Chrysophyta (Golden Algae); Bacillario = Bacillariophyta (Diatoms).

For most of both seasons, Cyanobacteria was the dominant algal genera counted in samples (Fig. 9).¹ In 2018, Cyanobacteria were dominant between late May and early

¹ Cyanobacteria are technically not algae, but rather are photosynthetic bacteria. For purposes of discussion of productivity in the open water, they are grouped with the algae.

June. Prior to that Golden Algae (Chrysophyceae) was the dominant taxa followed in importance by the Diatoms (Bacillariophyceae). By mid-June of 2018, the relative abundance of Cyanobacteria was >60% at both sites.

In 2019, the April 22nd algal community was dominated by the Cyanobacteria before giving way to the Golden Algae and Diatoms. At the NB site the relative abundance of Cyanobacteria was never <35%. By June 19th the relative abundance of Cyanobacteria was >90% at both sites; it would never be lower than 62% for the remainder of the season (Fig. 9).

In addition to the overall dominance by Cyanobacteria and the importance of Golden Algae and Diatoms early in the season, there was one other characteristic of the algal community structure common in both seasons and at both sites. This was the emergence of Green Algae (Chlorophyceae) as an important component of the community from mid to late August.

Cell Concentrations and Biological Surrogates

In 2018, total algal cells at NB ranged from 1,048 cells/mL on April 22nd to 107,357 cells/mL on October 9th. The cyanobacteria portion of those concentrations ranged from 0 cells/mL on April 22nd and May 8th to 107,269 cells/mL on October 9th. At the CL site, total algal cell concentrations ranged from 177 cells/mL on May 8th to 189,339 cells/mL

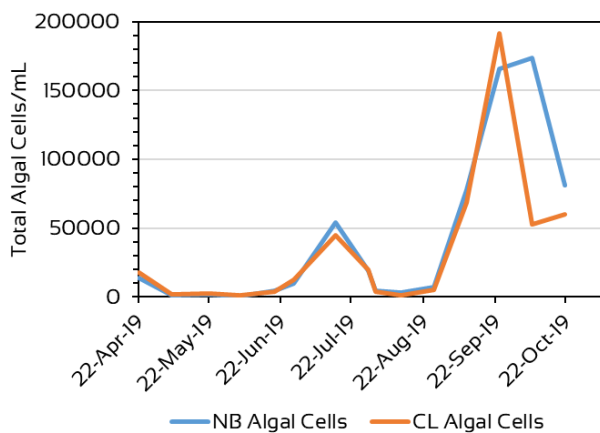
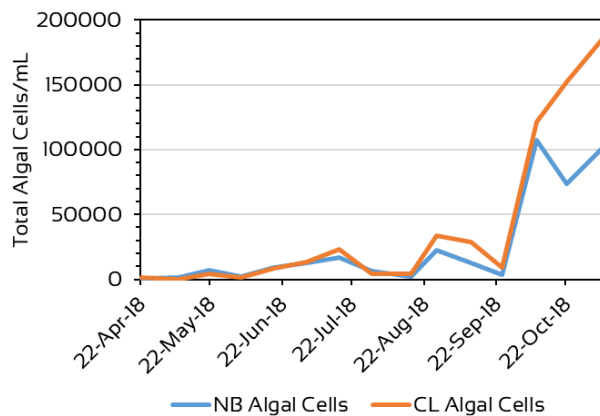
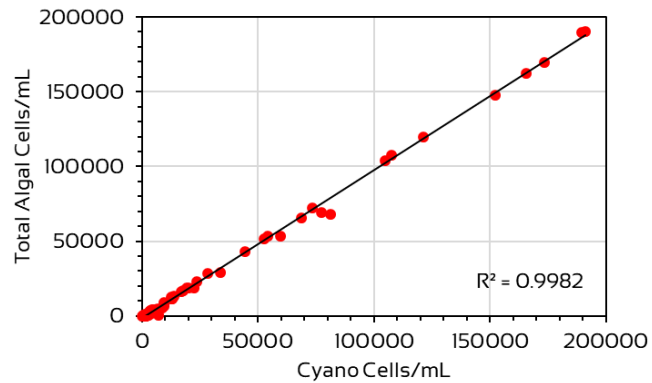


Figure 10. The 2018 and 2019 algal community dynamics. Top panel is a linear regression of total cell and cyanobacteria cell concentrations in each count at both sites on all dates. The middle and bottom panels are total cell concentrations at North Bay (NB) and Center Lake (CL) sites in 2018 and 2019, respectively.

on November 8th; cyanobacteria concentrations ranged from 0 on May 8th to 189,339 cells/mL on November 8th.

In 2019, NB total cell concentrations ranged from 548 cells/mL on June 4th to 173,507 cells/mL on October 7th; NB cyanobacteria cell concentrations ranged from 281 to 169,446 cells/mL on the same dates. At CL in 2019, the total cell concentration minimum was 1,338 cells/mL on June 4th, and the maximum was 191,223 cells on September 23rd. Cyanobacteria cell concentrations at CL in 2019 ranged from 14 cells/mL on May 6th to 190,387 cells/mL on September 23rd.

As inferred from cell concentration data described above and shown in the top panel of Fig. 10, there were no statistical difference between the total algal cell concentration and cyanobacteria cell concentration in a count at either site or either season ($p > 0.05$). Most counts, particularly after the spring, were largely comprised of cyanobacteria.

In 2018, cell concentrations gradually increased through late September before increasing by two orders of magnitude by October 9th at both sites. Concentrations at CL continued to increase through early November while remaining more constant at NB (Fig. 10). In 2019, low algal cell concentrations increased to between 44,000 to 54,000 cells/mL by July 15th then decreased precipitously and remained low through August 26th. The low numbers of algal cells during this time period is likely a result of the copper sulfate treatment on July 30th; however, cell concentrations increased to 165,000 to 191,000 cells/mL by September 23rd. Concentrations remained high at NB through October 7th.

Variability is inherent to algal and cyanobacteria cell counts due to small cell sizes, colonial cell arrangement that make counting individual cells challenging, differences in microscopes, and enumeration techniques. To check our cell count findings, we performed regression analyses to assess relationships between the cell concentrations and the other biological variables of Secchi transparency and chlorophyll-*a* concentrations.

For all regressions, Coefficients of Determination, aka R^2 values, were calculated to assess the portion of variability in cell concentrations explained by the other biological data (Table 2). Coefficients of Determination closer to the maximum of 1 denotes that more of variability was explained. We

Table 2. Relationships between total algae cell concentrations and cyanobacteria cell concentrations with chlorophyll-*a* concentrations and Secchi transparencies.

Regression Analyses	Function	n	R^2	p
Chloro vs Algal Cells	Linear	30	0.70	<0.05
Chloro vs Cyano Cells	Linear	30	.070	<0.05
Secchi vs Algal Cells	Linear	60	0.47	<0.05
Secchi vs Cyano Cells	Linear	57	0.47	<0.05

also determined p-values to assess the predictability of cell concentrations based on the biological variables. P-values of >0.05 were interpreted as the biological variables

not predictive of algae cell concentrations; whereas p-values of <0.05 meant that biological variables were useful in predicting cell concentrations.

Regressions of algal and Cyanobacteria cell concentrations against chlorophyll-*a* concentrations were performed since it is the cells that contain the chlorophyll-*a*. Using all data points where both chlorophyll-*a* data and corresponding cell concentration data existed ($n=30$), the R^2 values were 0.70 and p-values were <0.05 . The number of times Secchi transparency and total cell concentrations data pairs existed was 60. On three of those, no Cyanobacteria cells were counted so for that regression the number of data points was 57. The R^2 values using Secchi transparency to predict cell concentrations ranged from 0.46 to 0.47 and p-values were <0.05 (Table 2).

Although chlorophyll-*a* concentrations explained more variability in the cell counts, both chlorophyll-*a* concentrations and Secchi transparencies were useful predictors of total algae and cyanobacteria cell concentrations. These analyses also provided evidence of precision, if not accuracy, in algae cell enumerations.

Cyanobacteria Profiles

Isopleth diagrams were created of the relative cyanobacteria concentrations at NB, CL, FP, and SB using profile data collected between May 8th to November 8th of 2018 and April 22nd to October 21st of 2019 (Fig. 11 & 12). Fifteen profiles over that time were used to construct the 2018 NB, CL, and SB diagrams; 14 profiles were used to construct the 2018 FP diagram. The set of profile data missing in the FP isopleth chart but in the others was from June 18th and due to complications with the field meter. Fifteen profiles were used for all sites in 2019.

Data in each profile were collected with the fluorimeter incorporated into the sensor array of the Eureka Manta II instrumentation. Fluorimeters work on the principal that a particular substance fluoresces at a specific wavelength when light of another wavelength is directed on that substance. The fluorimeter in AER's field instrumentation emits a wavelength that interacts with a photosynthetic pigment unique to cyanobacteria (phycocyanin). This sensor is not calibrated to known concentrations of phycocyanin so measurements are not quantitative; instead the measurements are relative to other measurements in the water column or to other sites. It should be noted that the relative level ranges were different in the two seasons with 0 – 400 the range in 2018 and 0 – 3,500 the range in 2019. This occurred following factory calibration of the instrument in the Spring of 2019.

The conspicuous result from the cyanobacteria isopleth diagrams were the shift from lower levels to higher concentrations of phycocyanin as the season progressed. In 2018, increases were more gradual from May to September (Fig. 11). In 2019, increases through late July were followed by a decrease after the copper sulfate treatment on

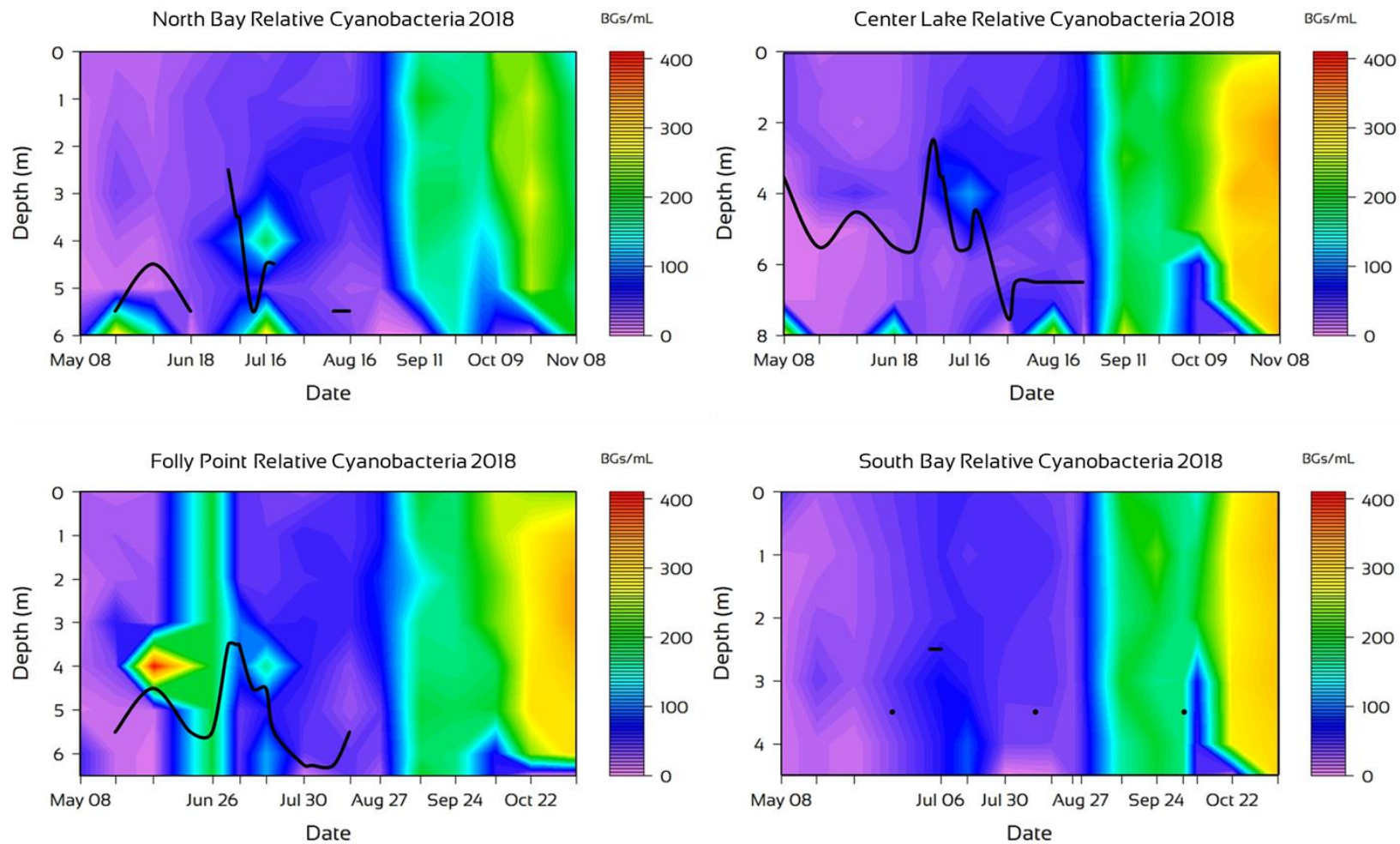


Figure 11. Relative cyanobacteria isopleth diagrams for the North Bay, Center Lake, Folly Point, and South Bay sites in 2018. The black lines and dots represent the location of a thermocline in the water column. Lines represent continuous observation of a thermocline over time while dots represent isolated events of stratification separated by mixed conditions.

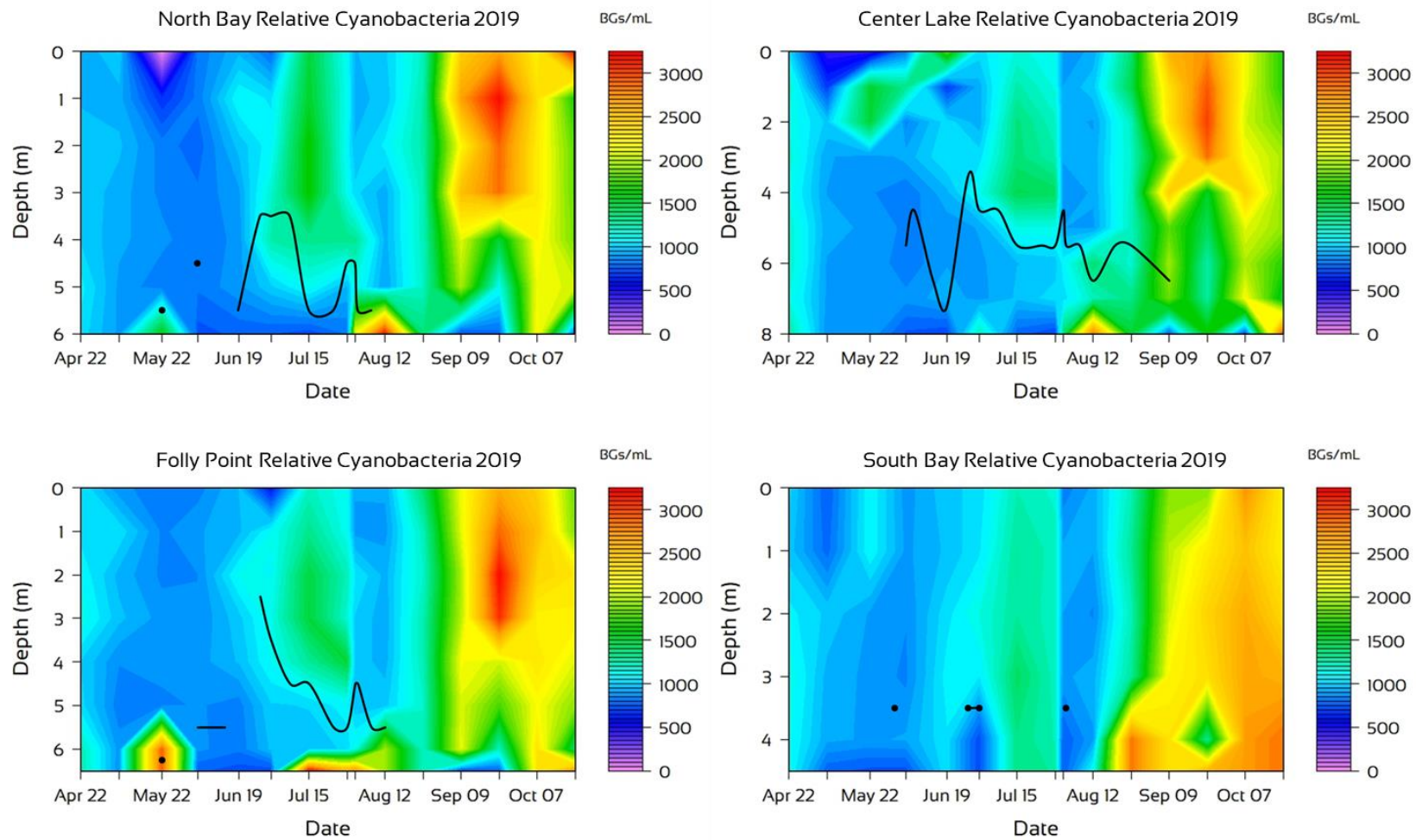


Figure 12. Relative cyanobacteria isopleth diagrams for the North Bay, Center Lake, Folly Point, and South Bay sites in 2019. The black lines and dots represent the location of a thermocline in the water column. Lines represent continuous observation of a thermocline over time while dots represent isolated events of stratification separated by mixed conditions.

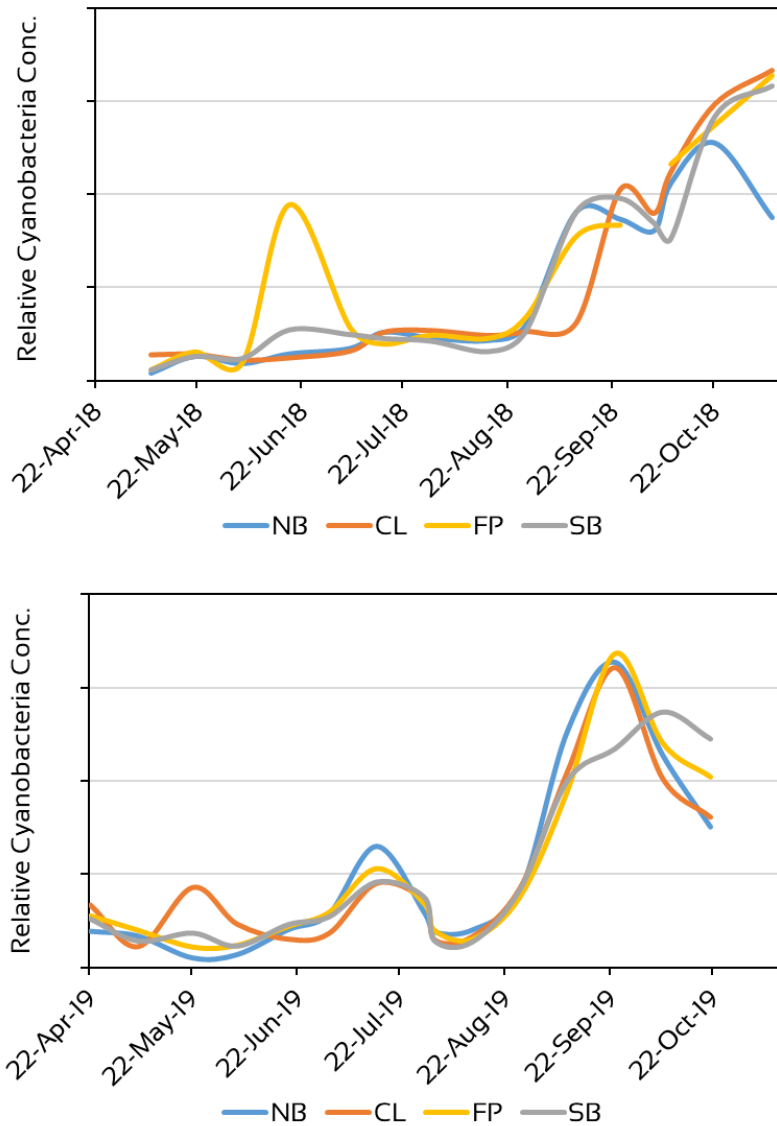


Figure 13. Changes in relative cyanobacteria concentrations over time in 2018 and 2019 at North Bay (NB), Center Lake (CL), Folly Point (FP) and South Bay (SB). Each point along the time line represents the average relative concentration based on measurements from 1 to 3m of depth at each site.

July 30th; and, then by an increase from late August through October (Fig. 12). On October 21st, the final sampling date in 2019, relative concentrations were lower in much of the water columns at three of the four sites; the SB site was the exception.

A decrease in relative cyanobacteria concentrations following the 2018 copper sulfate treatment on July 26th was not captured in the isopleth diagrams of that year. To confirm that, we averaged the relative concentrations recorded from 1 to 3 meters from each profile and plotted those over time for all sites in both 2018 and 2019 (Fig. 13).

These analyses corroborated the pattern of an increase in cyanobacteria through late July of 2019 followed by a decrease, and the lack of a similar pattern in 2018.

Other isopleth diagrams indicated that higher concentrations of cyanobacteria were found at depth and near the thermocline, particularly in the early part of the season through mid-July of 2018. The most distinctive of these events occurred at FP on June 4th of 2018 when the relative concentration at 4m of depth was >2000% higher than the average concentration between 1 and 3m of depth. Higher concentrations were also sometimes observed at the lower reaches of the water column. This may be reflective of benthic mats of cyanobacteria inhabiting the sediments at the bottom.

Table 3. Microcystin concentrations from samples collected on July 16th, July 30th, and August 16th of 2018. Results included toxin concentration from the whole water sample (WLW), the cyanobacteria size class of <53µm diameter, and from the bloom forming fraction of the WLW sample that were induced to bloom.

Date	Site	Size Class	Conc.	Site	Size Class	Conc.
16-Jul-18	NB	<53	0.584	CL	<53	0.518
16-Jul-18	NB	<53	0.488	CL	<53	0.570
16-Jul-18	NB	WLW	0.401	CL	WLW	0.301
16-Jul-18	NB	WLW	0.339	CL	WLW	0.317
16-Jul-18	NB	BFC	1.151	CL	BFC	1.054
16-Jul-18	NB	BFC	1.033	CL	BFC	1.182
30-Jul-18	NB	<53	0.489	CL	<53	0.599
30-Jul-18	NB	<53	0.472	CL	<53	0.621
30-Jul-18	NB	WLW	0.482	CL	WLW	0.423
30-Jul-18	NB	WLW	0.429	CL	WLW	0.384
30-Jul-18	NB	BFC	0.514	CL	BFC	1.171
30-Jul-18	NB	BFC	0.523	CL	BFC	1.080
16-Aug-18	NB	<53	0.598	CL	<53	0.641
16-Aug-18	NB	<53	0.508	CL	<53	0.647
16-Aug-18	NB	WLW	0.768	CL	WLW	0.554
16-Aug-18	NB	WLW	0.587	CL	WLW	0.615
16-Aug-18	NB	BFC	0.975	CL	BFC	1.356
16-Aug-18	NB	BFC	0.996	CL	BFC	1.441

Cyanotoxins

As part of a regional research project on microcystin levels in Connecticut lakes, AER in conjunction with Dr. Edwin Wong at the Biological and Environmental Department of Western Connecticut State University (WCSU), collected samples and measured microcystin concentrations at the NB and CL sites on July 18th, July 30th, and August 16th of 2018. Microcystin is one of the more prevalent toxins produced by blue-green algal blooms and is produced by a number of cyanobacteria genera including *Microcystis spp.* and *Dolichospermum spp.*

The collaborative AER/WCSU research initiative is modeled after the work being conducted at the University of New Hampshire Center for Freshwater Biology. There, microcystin levels are measured in samples of varying algal size classes. The first size class is “all sizes” in the whole lake water (WLW) sample. The second size class are the “Bloom Forming Cyanobacteria” (BFC) which are the cyanobacteria cells in the WLW sample that are induced to become positively buoyant and form a bloom using specialized laboratory instrumentation. The toxins in the induced “bloom” are measured. The last size class are the cyanobacteria from the WLW sample that are $\leq 53\mu\text{m}$ in diameter. The results presented below are preliminary and part of a more comprehensive report now in progress.

In 2018, the Connecticut Department of Public Health (CT DPH) and Connecticut Department of Energy and Environmental Protection (CT DEEP) used a microcystin threshold of 4 $\mu\text{g/L}$ which is based on the US EPA’s standards for recreational waters (CT DPH 2017, US EPA 2016). Samples measured from Bantam Lake on all dates and regardless of size class, never exceeded the 4 $\mu\text{g/L}$ threshold. Microcystin levels in the BFC samples were the only samples to exceed 1 $\mu\text{g/L}$ levels. These occurred on samples collected at NB on July 16th and at CL from samples collected on July 16th, July 30th, and August 16th (Table3).

In 2019, the microcystin threshold in CT was raised to 8 $\mu\text{g/L}$ (CT DPH & CT DEEP 2019). The BLPA continued its relationship with WCSU to collect additional data on microcystin levels at Bantam Lake in 2019, but over a longer portion of the season and with only whole lake water samples.

Table 4. Microcystin concentrations measured in samples collected at the North Bay and Center Lake sites in 2019.

Date	North Bay	Center Lake
22-May-19	0.657	0.807
4-Jun-19	0.632	1.171
18-Jun-19	1.336	0.742
1-Jul-19	1.293	0.093
15-Jul-19	0.124	0.157
29-Jul-19	0.144	0.162
12-Aug-19	0.108	0.091
26-Aug-19	0.184	0.144
9-Sep-19	0.247	0.259
23-Sep-19	0.293	0.304
7-Oct-19	0.425	0.348
21-Oct-19	0.204	0.15

Results of the 2019 analyses are presented in Table 3. Similar to 2018, almost all the whole lake water samples collected in 2019 did not exceed 1µg/L of microcystin. Exceptions were June 4th at CL, and June 18th/July 1st at NB. In general, levels were higher in May, June and early July, were lowest from mid-July through late August, then modestly increased through early October before diminishing again. No result exceeded the State threshold of 8µg/L.

Cyanotoxins vs Cyanobacteria Counts and Relative Concentrations

To understand the relationship between the cell counts, relative measures of cyanobacteria and the amount of microcystin toxins in samples, we regressed these variables measured in samples collected in 2019 against each other. As noted earlier, samples for analyses of cyanobacteria cell concentrations and microcystin levels were collected by integrating the top three meters of the water column. Likewise, relative cyanobacteria levels used in these analyses were an average of fluorometer readings from the 1 to 3m strata of the water column.

There was good correlation between actual cyanobacteria counts and the relative levels of cyanobacteria measured fluorometrically (Fig. 14a). There was also good correlation between actual cell concentrations and microcystin levels in samples (Fig. 14b). The strongest relationship observed was between relative cyanobacteria levels and microcystin concentrations (Fig. 14c).

The good correlation between cyanobacteria cell concentrations and relative cyanobacteria levels implies consistency in cell counts, which can be susceptible to inconsistencies due to cell sizes, types of cell arrangements, and analytical methods. The relative cyanobacteria levels are based on intensity of specific fluoresced light determined by the fluorimeter and averaged from readings at 1, 2, and 3 meters in the water column. This aided in reducing variability. For these reasons, the variable with the strongest correlation with microcystin concentrations was relative cyanobacteria levels measured fluorometrically. This correlation may be useful in providing an additional measure of assessing public health risk in the future.

Lastly, we plotted microcystins measured in 2019 at NB and CL over time. Microcystin levels in July and August ranged between 0.1 and 0.2µg/L. Levels increased to approximately 0.3µg/L by late September, and peaked in early October reaching 0.35µg/L at CL and 0.43µg/L at NB. On the final sample collection on October 21st, concentrations decreased to between 0.1 and 0.2µg/L.

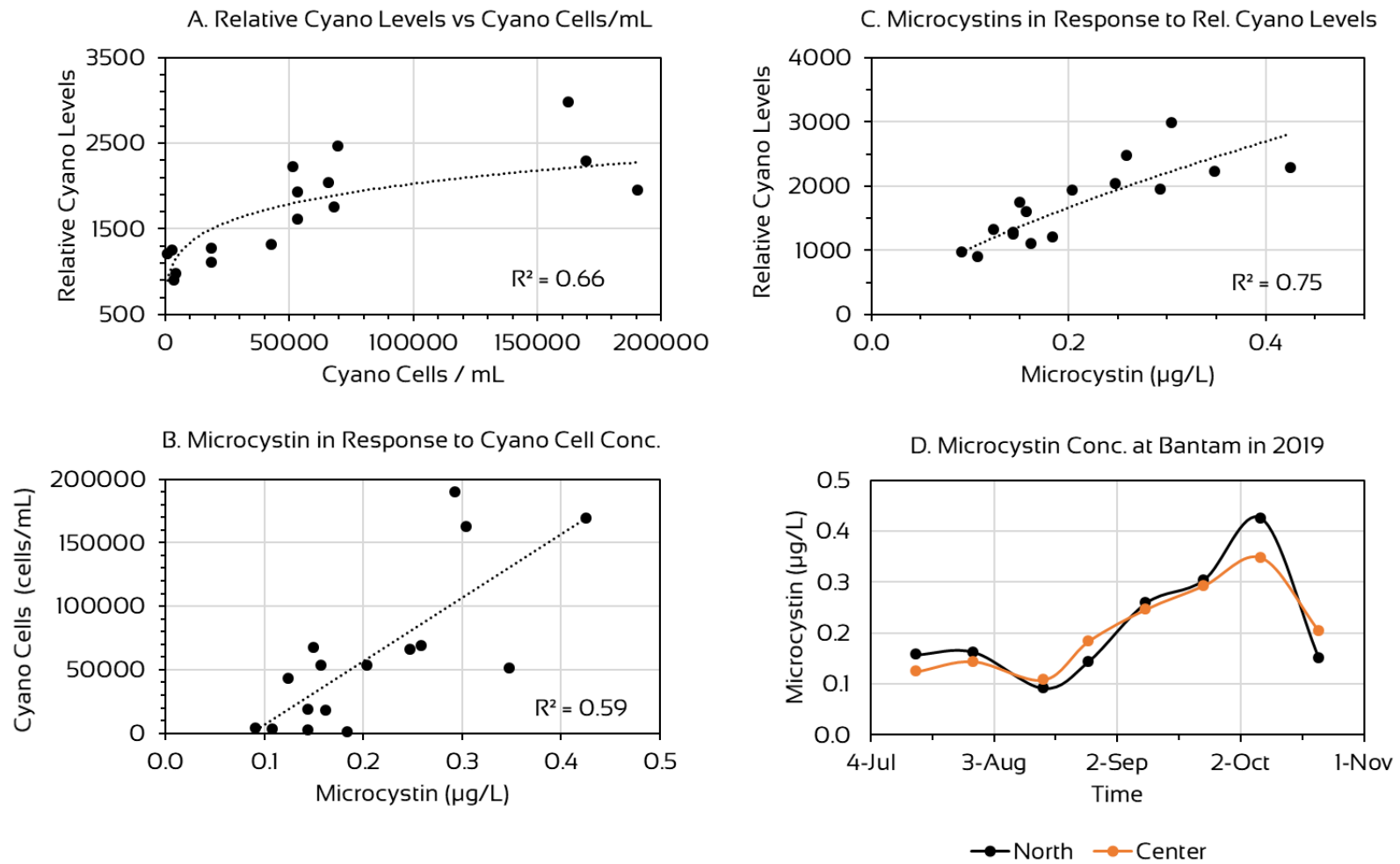


Figure 14. Relationships between A) cyanobacteria cell concentration and relative cyanobacteria levels, B) microcystin concentrations and cyanobacteria cell concentrations, C) microcystin concentrations and relative cyanobacteria levels, and D) microcystin concentration and dates the samples were collected.

NUTRIENT ASSESSMENTS

Total Phosphorus

Phosphorus in freshwater systems is most commonly the nutrient in shortest supply and in greatest demand by the algae; therefore, it often limits algal productivity. Sources of phosphorus can be from external sources (e.g. from the watershed or atmosphere), or internal sources (e.g. released from bottom sediments under anoxic conditions). Total phosphorus represents all forms of phosphorus in a sample, i.e. particulate and soluble forms.

The lowest total phosphorus levels of both years and at both the NB and CL sites occurred in April and May, and ranged from *not detectable* (e.g. in the epilimnion and hypolimnion at NB and CL in April of 2018) to 19 $\mu\text{g/L}$ (in the hypolimnion at CL in April of 2019). Marked differences between sites, the three depths or seasons were not observed (Fig. 15).

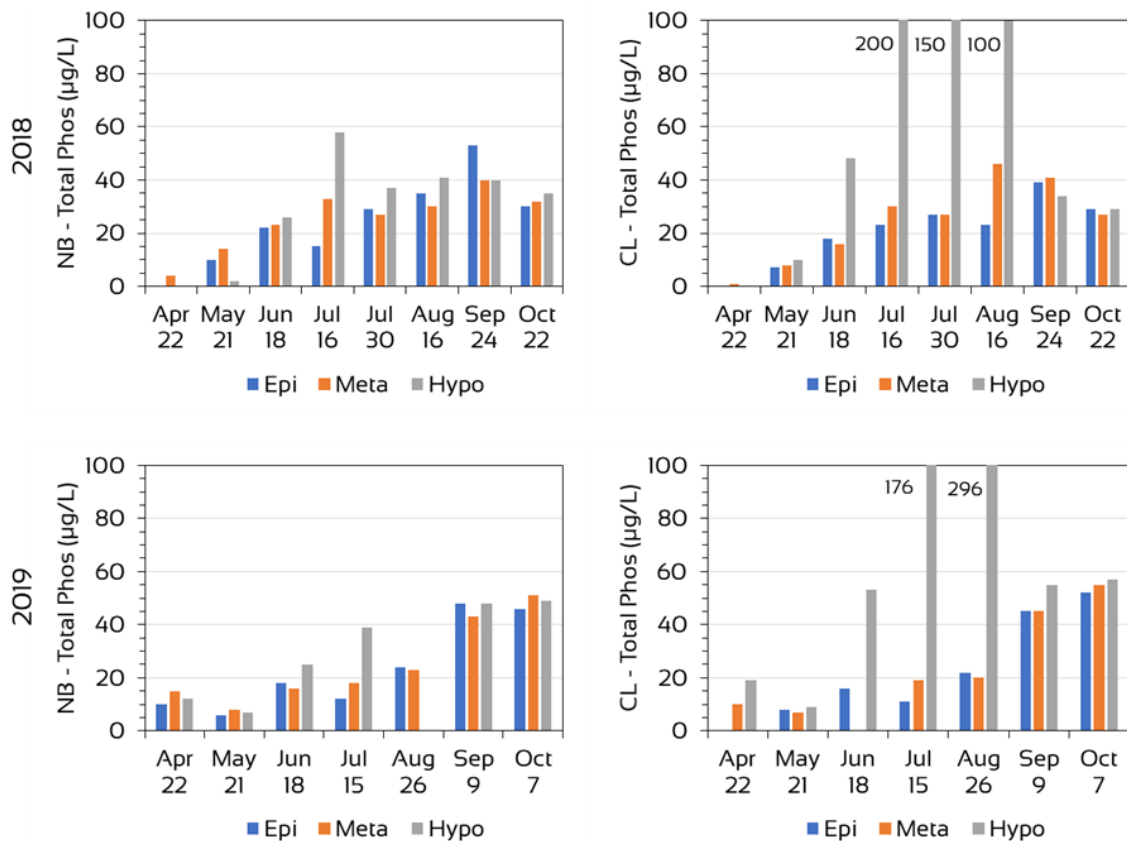


Figure 15. Total phosphorus concentrations at the North Bay (NB) and Center Lake (CL) sites in the 2018 (top) and 2019 (bottom) seasons. Epi = epilimnion; Meta = metalimnion; Hypo = hypolimnion.

By mid-June in both years, differences between sites were observed. Hypolimnetic concentrations were two to three times higher than epilimnetic and metalimnetic concentrations at CL, while concentrations in the three strata at NB were similar. Stated differently, internal loading of phosphorus was occurring at CL by mid-June in both seasons, but not occurring at NB.

By mid-July of 2018 and 2019, phosphorus concentrations in the hypolimnion of NB were two to three times higher than those measured in the epilimnion and metalimnion (i.e. phosphorus was being released from the sediments). The NB hypolimnetic concentration in mid-July were 58 and 39 $\mu\text{g/L}$ in 2018 and 2019, respectively. The CL site continued to internally load but by mid-July hypolimnetic concentrations were an order of magnitude greater than epilimnetic levels, reaching 200 and 176 $\mu\text{g/L}$ in 2018 and 2019, respectively.

An additional set of phosphorus data was collected on July 30th of 2018. The July 30th hypolimnetic concentration at NB site was down from the July 16th level while the epilimnetic concentration increased to the highest level up to that point in the 2018 season (i.e. 29 $\mu\text{g/L}$). The concentrations of all three strata at the CL site varied little between July 16th and July 30th but hypolimnetic concentrations were very high (i.e. 150 $\mu\text{g/L}$).

On August 16th of 2018, concentrations of all three strata were between 30 and 41 $\mu\text{g/L}$ at NB. However, CL total phosphorus concentrations in the epilimnion, metalimnion, and hypolimnion were 23, 46, and 100 $\mu\text{g/L}$. In late August of 2019, the NB epilimnetic and metalimnetic concentrations were relatively low; hypolimnetic data was not collected. At CL in August of 2019, the epilimnetic and metalimnetic levels were relatively low but the hypolimnetic concentration was 296 $\mu\text{g/L}$, which was the highest concentration recorded during the two-year study period.

By September 24th of both 2018 and 2019, the water columns of NB and CL were mixed (Fig. 2). Resultantly, similar concentrations of phosphorus were measured at the top, middle, and bottom of the water column at each site. Epilimnetic and metalimnetic concentrations were generally greater than those measured in August. Hypolimnetic concentrations had decreased from highly elevated August levels at CL, but were similar to hypolimnetic August levels at NB in 2018. October concentrations were similar to those measured in September in both 2018 and 2019.

Phosphorus Mass Balance

Estimations of the total mass of phosphorus in the water column, and in each layer of the water column (epilimnion, metalimnion, and hypolimnion) from May through October of 2018 and from April through October in 2019 were performed to better understand nutrient dynamics, i.e. where is the phosphorus coming from and how much. This was done by using the NB and CL averaged total phosphorus concentration

measured at each layer during each site visit, extrapolating mass by applying that concentration to the averaged volume of the entire layer within the water column, and then averaging mass for each layer for the lake over the season.

These analyses make some assumptions which may require further investigation, e.g. it assumes that the concentration of phosphorus at 0.5 meters from the bottom is the same throughout the hypolimnion; the same is true of the other layers. For these analyses it was necessary to integrate water volumes of each layer to make any estimation with the phosphorus data. Despite the assumptions, these calculations are useful to understand the general dynamics of the system.

It is clear from these analyses that the phosphorus mass in Bantam Lake increased from spring to fall (Fig. 16). This is indicative of an internal source of phosphorus. Most of that mass was in the epilimnion where the majority of the volume was located.

Phosphorus in the hypolimnion reached its greatest mass on July 16th in 2018 and August 26th in 2019. Afterwards in both years the epilimnetic mass substantially increases while hypolimnetic mass decreases.

Nitrogen

Nitrogen is commonly the second most limiting nutrient for algae in freshwater systems. It can be present in a number of forms in lake water. Ammonia – a reduced form of nitrogen – is important because it can affect the productivity, diversity, and dynamics of the algal and plant communities. Ammonia can be indicative of internal nutrient loading since bacteria will utilize other forms of nitrogen (e.g. nitrite and nitrate) in lieu of oxygen for cellular respiration under anoxic conditions, resulting in ammonia enrichment of the hypolimnion. Total Kjeldahl nitrogen (i.e. TKN) is a measure of the reduced forms of nitrogen (including ammonia) and total organic proteins in the water column. Since TKN accounts for biologically derived, nitrogen-rich proteins in the water column, it is useful in assessing the productivity of the lentic system. Nitrate and nitrite are often below detectable levels in natural systems because they are quickly cycled by bacteria and aquatic plants. Total nitrogen is the sum total of TKN, nitrate and nitrite. Since the latter two are often below detectable limits, TKN levels are often similar or equal to total nitrogen levels.

Concentrations of ammonia at the surface, mid-depths, and 0.5m above the bottom at NB ranged in both seasons from *not detectable* to 0.16mg/L (Fig. 17). Surface and mid-depth concentrations of ammonia at CL over the two seasons were similar to those at NB, ranging from *not detectable* to ≤ 0.23 mg/L. Conditions at the bottom of the CL water column were different. In both years, concentrations notably increased starting in May of 2018 and in June of 2019 then peaked in August of both years (Fig. 17). The concentration maximums in 2018 and 2019 were 1.13 and 1.49mg/L, respectively.

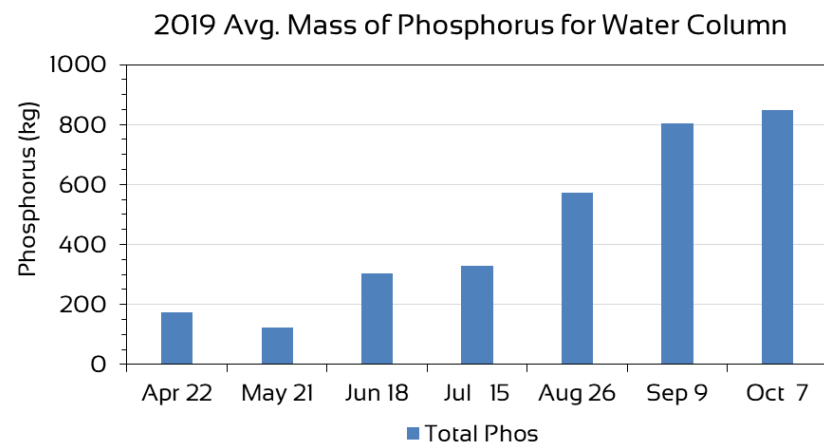
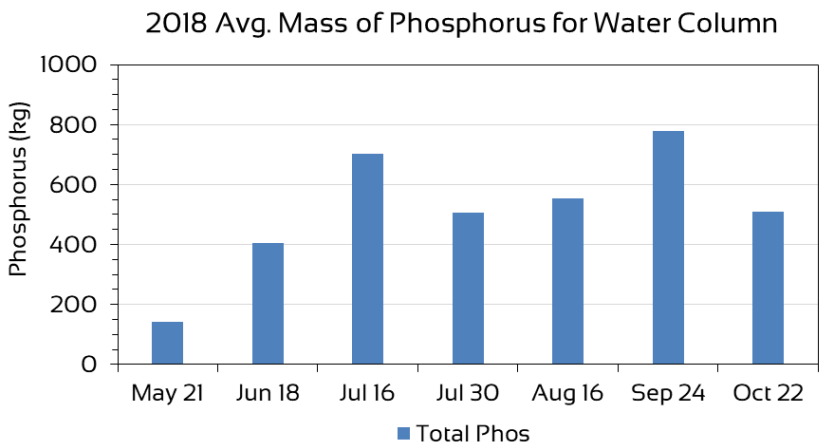
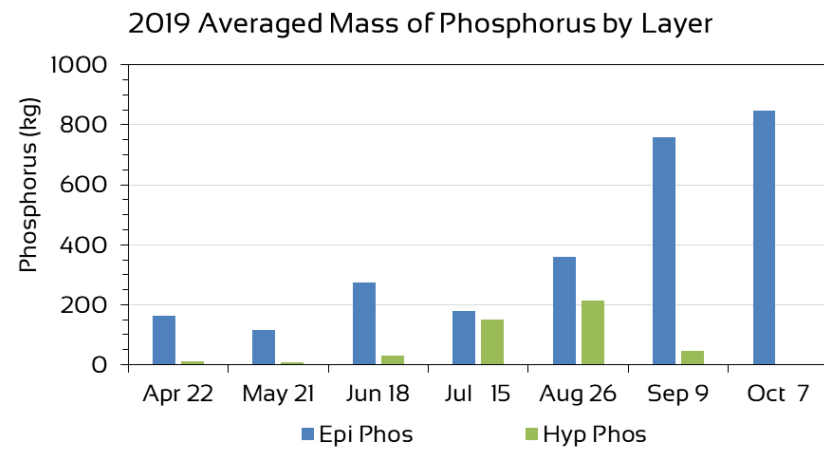
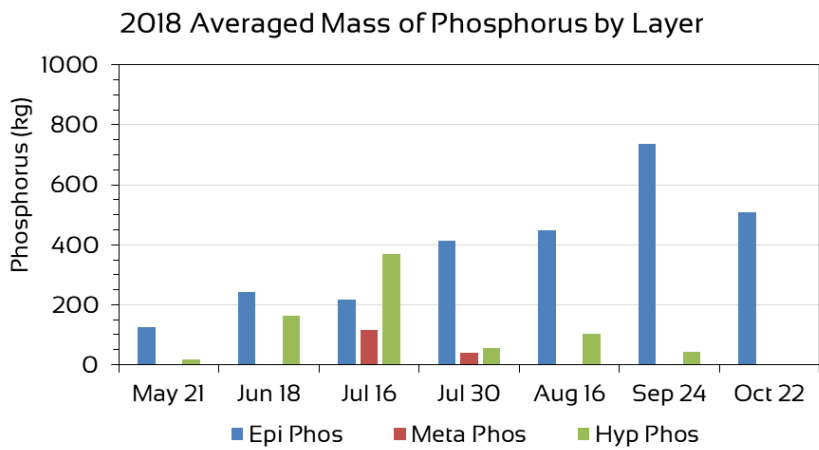


Figure 16. The top panels display the averaged phosphorus mass in the epilimnion (Epi), metalimnion (Meta), and hypolimnion (Hypo) in 2018 (left) and 2019 (right). The bottom panel displays the total mass of phosphorus in the water column from May 21st to October 22nd of 2018.



These measured increases of hypolimnetic ammonia concentration was most discrete at CL in 2018 for several reasons. First, the water column warmed and stratified earlier in 2018. That resulted in bottom waters becoming anoxic sooner, resulting in the shift from oxygen to other final electron acceptors such as nitrogen compounds for anaerobic cellular respiration. The water column was continuously stratified at CL through early September (Fig. 2), which prevented mixing and dilution. When the lake mixed later in September, ammonia levels became undetectable.

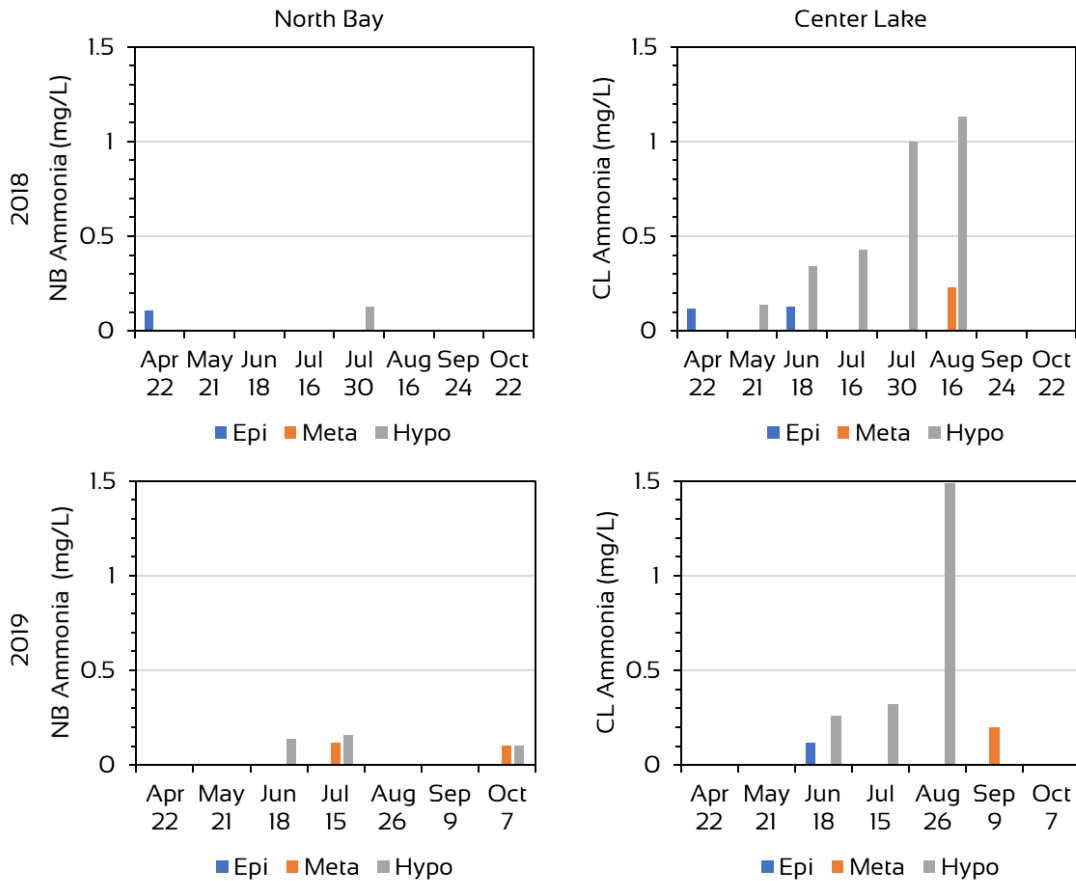


Figure 17. Ammonia concentrations in the 2018 (top panels) and 2019 (bottom panels) seasons at the North Bay (NB; right panels) and Center Lake (CL; left panels) in the epilimnion (Epi or 1m from the surface), metalimnion (Meta or mid-level depths when not stratified), and hypolimnion (Hypo or 0.5m from the bottom).

Other reduced forms of nitrogen measured as TKN, including that in organic proteins, were consistently detectable within the water column at the NB and CL sites in 2018. TKN levels at the NB site most often ranged from 0.4 to 0.6mg/L regardless of collection depth. April 22nd and July 30th levels were modestly lower while August 16th and October 22nd levels were modestly higher (Fig. 18). A similar pattern was observed at

the CL site with the exception of the much higher TKN levels in the hypolimnion measured between June 18th and August 16th which were due, in large part, to the high ammonia concentration at that depth during that time period.

In 2019, TKN was *not detectable* in surface samples collected on April 22nd at both sites and on June 18th and August 26th at the NB site. When it was detected, surface and mid-depth concentrations at both sites ranged from 0.12 to 0.36mg/L with one exception. That was the mid-depth concentration at NB on June 18th which was 0.62mg/L; data on the mid-depth sample from CL was not available.

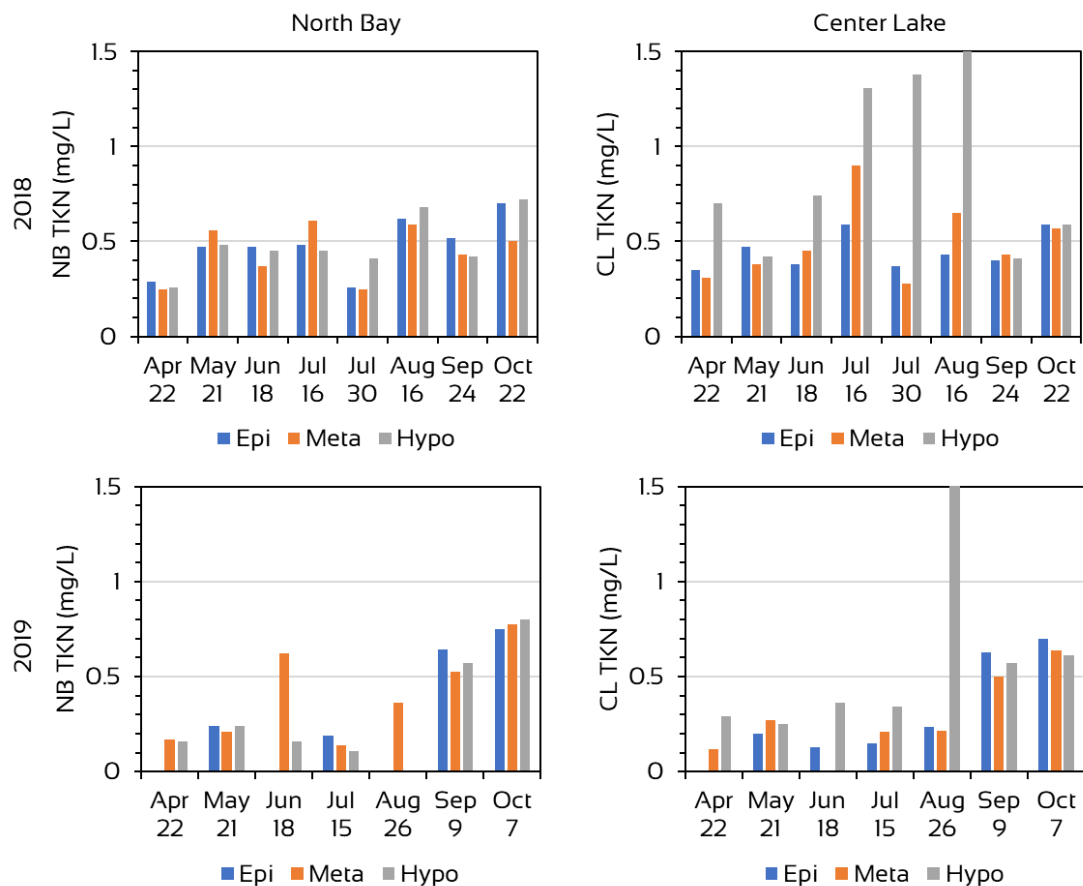


Figure 18. Total Kjeldahl nitrogen (TKN) concentrations in the 2018 (top panels) and 2019 (bottom panels) seasons at the North Bay (NB; right panels) and Center Lake (CL; left panels) in the epilimnion (Epi or 1m from the surface), metalimnion (Meta or mid-level depths when not stratified), and hypolimnion (Hypo or 0.5m from the bottom).

Hypolimnetic TKN levels at both sites in 2019 were low from April through July and ranged from 0.11 to 0.36mg/L. The June 18th and July 15th TKN levels appear to be driven by ammonia as was the hypolimnetic TKN maxima of 2.47mg/L on August 26th

(data for the NB hypolimnion on August 26th was not available). The 2019 September 24th and October 7th TKN levels at both sites were similar to the respective 2018 September and October levels, were generally high, similar at all sample depths, and not related to ammonia levels.

Total Nitrogen to Total Phosphorus Ratios

As stated above, total nitrogen is a variable used to assess trophic and nutrient dynamics in lake; it is the sum of TKN, nitrate/ nitrite, and is often the same as TKN levels since nitrate and nitrite are frequently at concentrations that are not detectable by analytical techniques. Total nitrogen levels at Bantam were closely correlated with TKN levels. Almost all the total nitrogen / TKN paired data from all dates, all depths, and sites where levels were detected fit closely on a 1:1 line (Fig. 19). This indicated that most times total nitrogen was equal or very similar to TKN. The one exception occurred on a sample collected from the metalimnion of NB on July 17, 2018 when the single greatest nitrate level measured in the two-year period of 1.06mg/L drove the total nitrogen levels to 1.63mg/L. That data point could be an error in laboratory quantification.

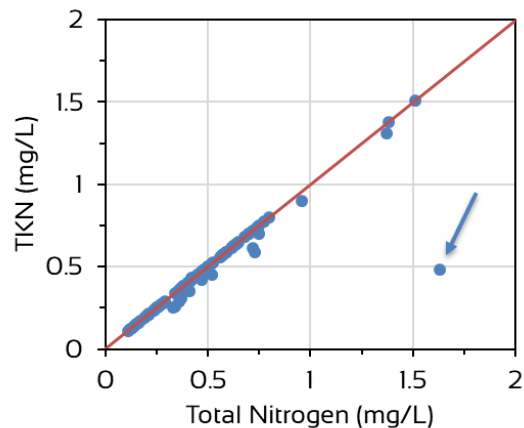


Figure 19. Regression of all total Kjeldahl nitrogen (TKN) levels against total nitrogen levels from both sites, all depths, and both seasons. The arrow points to one data point when nitrate levels of 1.06mg/L resulted in a total nitrogen level that far exceeded the TKN levels.

Although nitrogen is normally the second most limiting nutrient in freshwater systems, it can sometimes be the primary nutrient limiting productivity. Nitrogen limitation in a system favors certain cyanobacteria over other algae because those cyanobacteria can assimilate the available atmospheric nitrogen diffused in the water whereas other algal taxa cannot.

Limnologists frequently used the Redfield ratio of 16 (16:1 of nitrogen to phosphorus) to determine whether nitrogen or phosphorus is limiting in a freshwater system (Redfield 1958). Ratios below 16 (i.e. 7.2mg/L) indicate nitrogen limitation while ratios above 16 indicate phosphorus limitations. The Redfield ratios were calculated for all sites and depths for samples collected in May through October of both years.

Ratios in both seasons were more often above 7.2. However, in some instances the ratios neared 7.2, e.g. July 30th and September 24th in 2018 implying that nitrogen limitation was a potentiality. In general, ratios in 2018 were higher from May through mid-July then move closer to nitrogen limitation later in the season (Fig. 20).

The 2019 season exhibited a similar TN:TP pattern as that seen in 2018. In 2019 the shift from phosphorus limitation toward nitrogen limitation appeared to occur earlier in the season (Fig. 20).

In summary, ratios were much higher than 7.2 early in the seasons of both years and closer to 7.2 after the middle of the season, which suggests a shift toward nitrogen limitation (Fig. 20).

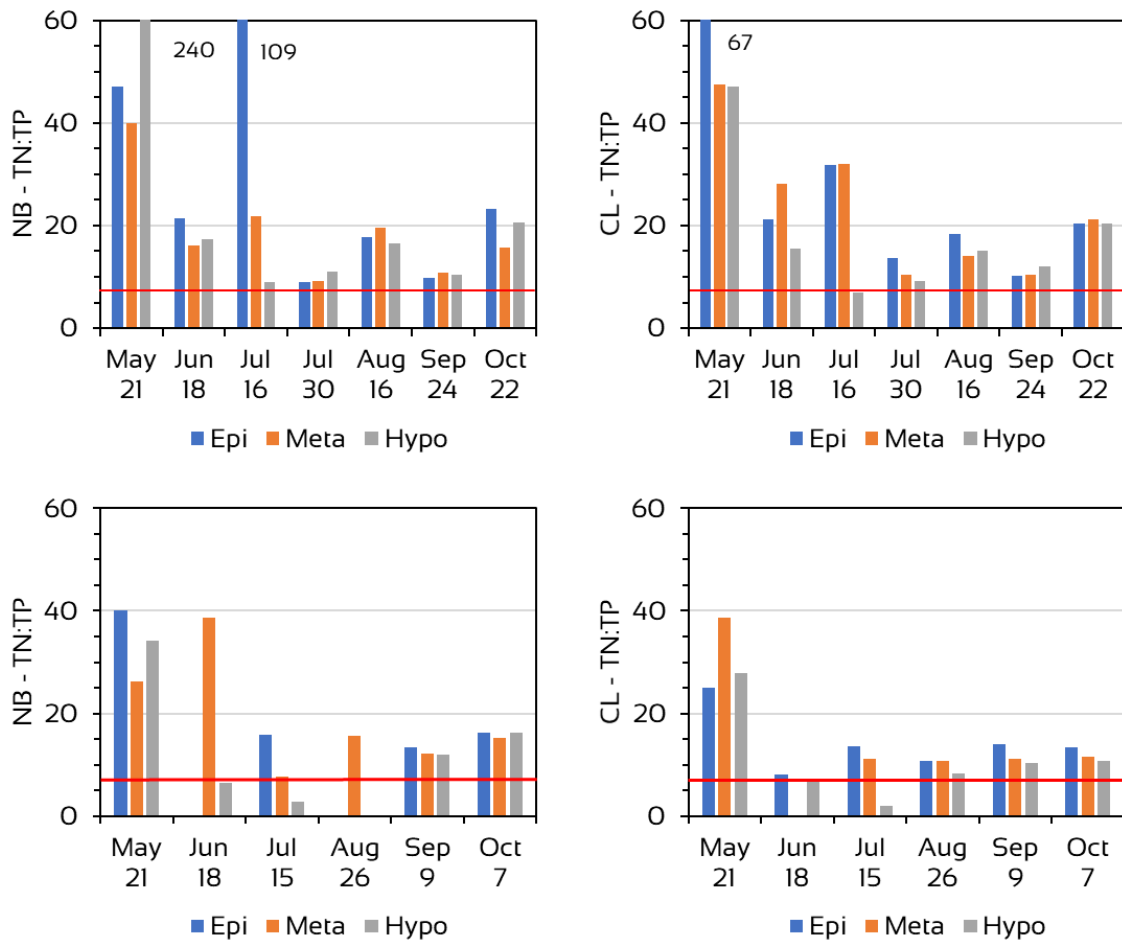


Figure 20. Redfield ratios (total nitrogen: total phosphorus) at the North Bay (NB) and Center Lake (CL) sites from May to October in 2018 and 2019. The red horizontal lines mark a ratio of 16. Phosphorus is theoretically limiting when above 7.2; nitrogen is theoretically limiting when below 7.2.

CHEMICAL ASSESSMENTS

AER assessed a number of in situ water chemistry parameters during the 2018 and 2019 seasons. The proceeding chemical characteristics are useful for understanding the lake processes, anthropogenically driven changes, and why certain plant and algal flora are found at a particular lake.

Specific Conductance

Conductivity is a surrogate measurement for the ionic concentration of water; simply, it is a measure of water's ability to transmit an electrical current. Specific conductance levels are conductivity measurements standardized to water temperature, which varies with depth and/or season. Specific conductance is an important metric in limnological studies due to its ability to detect pollutants and/or potential nutrient loadings.

It can also be useful in understanding patterns of stratification and mixing of lake water columns. Conductivity/specific conductance can also have an influence on organisms that inhabit a lake or pond; particularly, algae. Species within taxa of algae have been shown to change over time in a lake as the conductivity changes.

In 2018, specific conductance in the surface water depths (top three meters) of the water column average $189\mu\text{S}/\text{cm}$. With the exception of levels on July 30th, the specific conductance in the surface waters from April 22nd through September 11th ranged 185 to $208\mu\text{S}/\text{cm}$. The maxima of both sites occurred on July 30th and were 218 to $219\mu\text{S}/\text{cm}$. From September 20th through November 8th, surface water specific conductance was modestly lower and ranged from 145 to $181\mu\text{S}/\text{cm}$.

The 2019 specific conductance average in the top 3m of water was $176\mu\text{S}/\text{cm}$. Surface water specific conductance gradually increased over the season. Early season (April to June) levels were between 160 and $170\mu\text{S}/\text{cm}$; most concentrations between early August through October 7th were between 180 and $186\mu\text{S}/\text{cm}$. On October 22nd of 2019, levels decreased modestly to 175 to $176\mu\text{S}/\text{cm}$ except at NB where levels were approximately $184\mu\text{S}/\text{cm}$.

There existed a great deal of variability in specific conductance in the bottom 1 to 2m of the water column between dates and sites. To illustrate those differences, the 2018 and 2019 specific conductance profiles were used to create isopleth charts for the four sites (Figs. 21 & 22). Isolated spikes in specific conductance levels were observed at the bottom 0.5 to 1m of the water column at NB, FP, and SB. Between events when bottom levels were elevated, hypolimnetic water specific conductance would return to surface water concentrations; these were most likely the result of mixing events (e.g. wind or storm events).

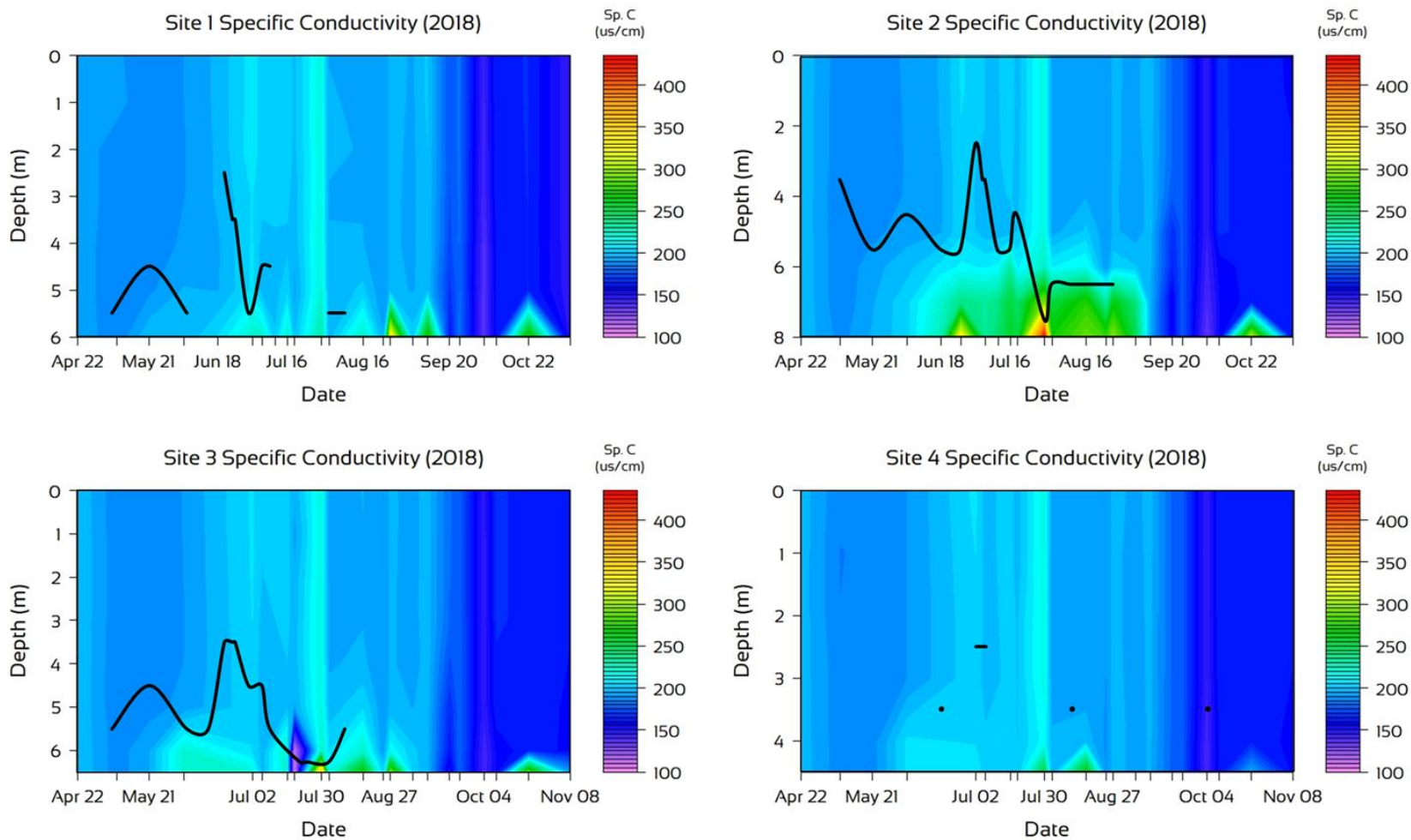


Figure 21. Specific conductance isopleth diagrams for the North Bay, Center Lake, Folly Point, and South Bay sites in 2018. The black lines and dots represent the location of a thermocline in the water column. Lines represent continuous observation of a thermocline over time while dots represent isolated events of stratification separated by mixed conditions.

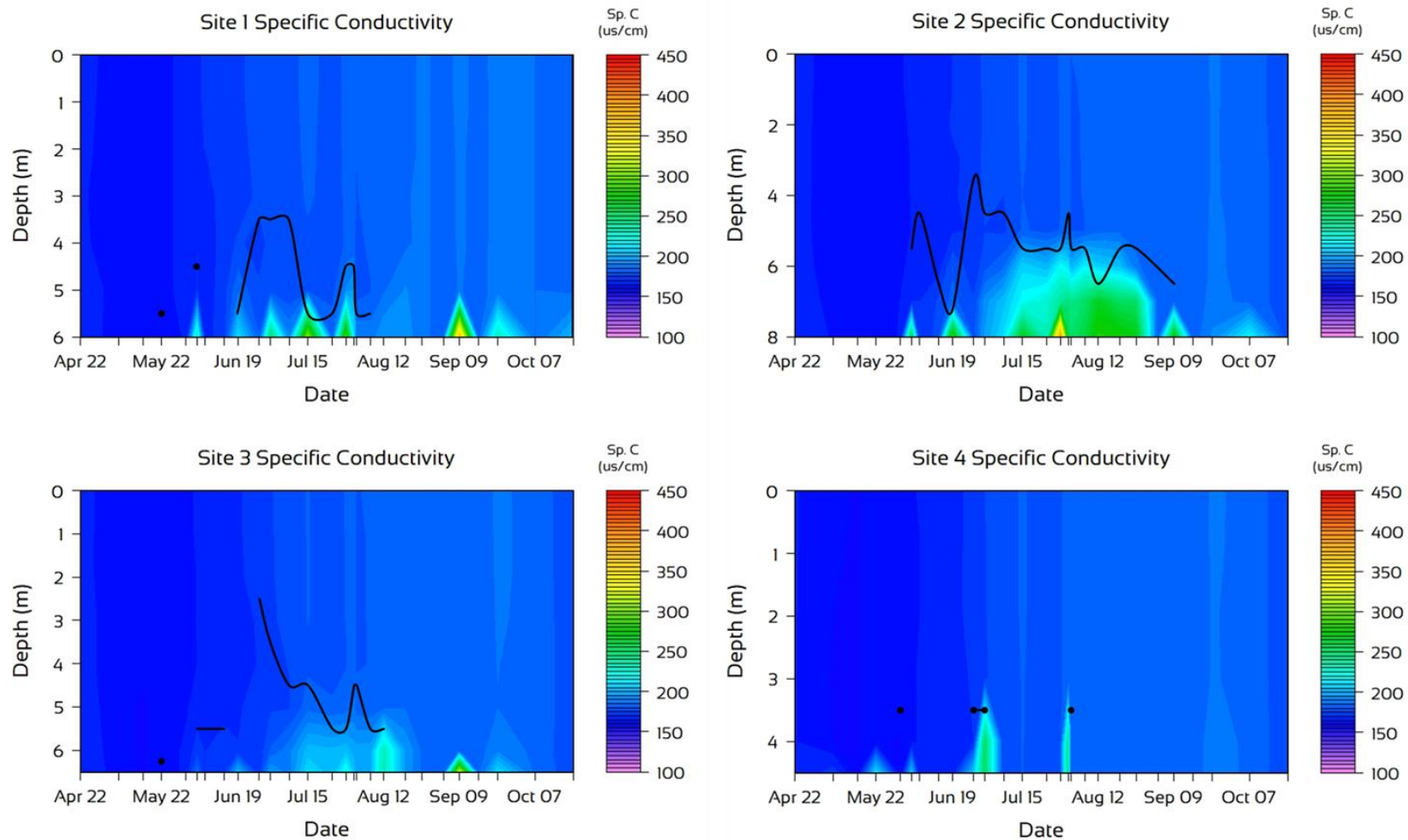


Figure 22. Specific conductance isopleth diagrams for the North Bay, Center Lake, Folly Point, and South Bay sites in 2019. The black lines and dots represent the location of a thermocline in the water column. Lines represent continuous observation of a thermocline over time while dots represent isolated events of stratification separated by mixed conditions.

Specific conductance at the bottom of the CL water column differed from the other three sites. Specifically, there were extended periods of elevated specific conductance in the 7 and 8m strata from mid-June to early September in 2018 and from early July to late-August in 2019 (Figs. 21 & 22). In addition, the highest specific conductance measurements each season were from the 8m strata at CL. These were 434 μ S/cm on July 30, 2018 and 395 μ S/cm on July 29, 2019.

pH and Alkalinity

The pH of lake water is important for several reasons. Firstly, very low or very high pH levels will not support diverse lentic plant and animal communities. Algal communities are influenced by pH due in part to the form of dissolved carbon in the water column at a given pH. For example, at a pH greater than 8.3, bicarbonate is the dominant form of carbon available to the pelagic algal community; the blue-green algae have adaptive advantages over other algal groups in that they are better equipped to utilize this form of carbon. Other algal groups are dependent upon carbon dioxide, which is not available in water above pH of 8.3.

The pH data from 1m below the surface (surface) and approximately 0.5m above the bottom (bottom) at the NB and CL sites were compiled from the dates in 2018 and 2019 when water samples were collected for laboratory analyses (see Table 1) and used for these analyses. In 2018, average surface pH at both NB and CL was 7.8. Levels at both sites ranged from 7.2 on September 24th to 8.6 on July 16th. The average pH at the bottom of the water column in 2018 was 7.2 and 7.4 at NB and CL, respectively. Ranges of pH levels were slightly lower at NB with a minimum and maximum of 6.8 and 7.6, respectfully compared to respective levels of 7.0 and 7.7 at CL. The only pH >8.0 from this set of data was from July 16th from surface waters at both sites.

In 2019, pH levels were slightly higher than those observed in 2018. Average surface pH was 8.1 and 8.0 at NB and CL, respectively. Seasonal minimum and maximum levels at the two sites in 2019 were similar. These were 7.6 and 9.1 at NB; and 7.6 and 8.7 at CL. Similar to 2018, the seasonal maximums occurred in mid-July. The surface pH levels also exceeded 8.0 on September 9th and were 8.5 and 8.3 at NB and CL, respectively. The average pH at the bottom of NB and CL were 7.4 and 7.5, respectively. Bottom pH ranged from 7.2 to 7.6 at NB; and 7.4 to 7.6 at CL.

Alkalinity is a measure of calcium carbonate, and reflects the acid neutralizing capacity of water (i.e. buffering capacity). Alkalinity of surface waters is largely influenced by the geology and other watershed phenomenon. Alkalinity at the bottom of a lake can be generated internally from the dissimilatory reduction reactions of sulfate by bacteria found in the anoxic lake sediments (Siver et al. 2003).

Alkalinity over the 2-year period at the 1m strata (epilimnion or surface) and mid-depth (metalimnion) strata were constant. Average NB and CL surface and mid-depth alkalinities in 2018 were both 41mg/L. In 2019, average NB surface and mid-level concentrations were 40 and 42mg/L, respectively; and average CL surface and mid-level concentrations were both 39mg/L.

Alkalinity concentrations at the bottom of the NB and CL water columns were more variable. In 2018, the concentrations at the bottom of NB in April through June, September, and October were similar to concentrations at the surface and middle depths (Fig. 23). In July and August of 2018, the NB concentrations at the bottom were modestly higher than surface and mid-depths levels. At CL, differences between bottom alkalinities and those in the upper strata exhibited more contrast in June through August than was observed at NB (Fig. 23).

Similar seasonal trends were observed in 2019. At NB, bottom alkalinity was similar to alkalinity at mid-depths and the surface on all dates except September 8th when it was 8mg/L higher (note that August 26th bottom alkalinity data was not collected). At CL, July and August alkalinity at the bottom was notably higher than concentrations in other strata; April through June, September and October levels were more comparable (Fig. 23).

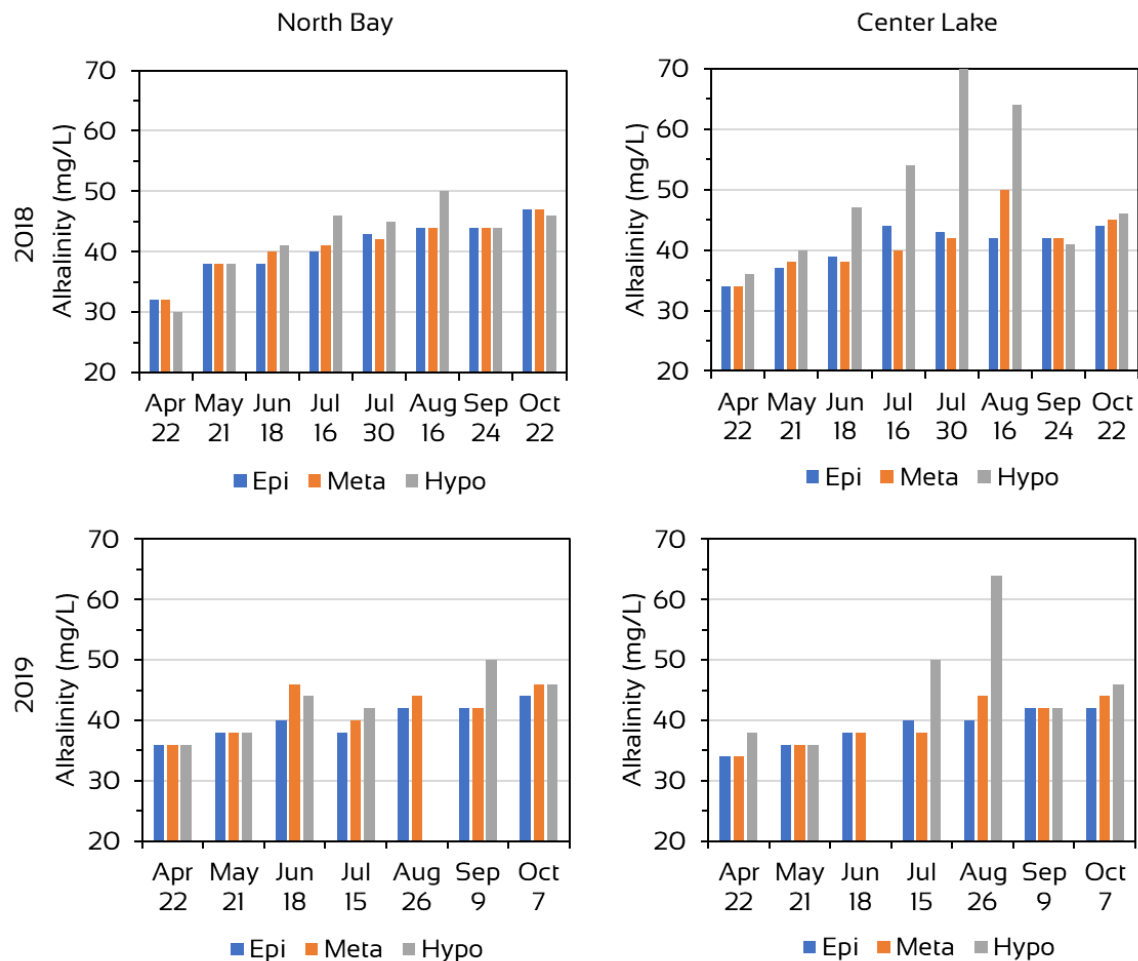


Figure 23. Alkalinity in the epilimnion at 1m (Epi), metalimnion or mid-depths (Meta), and hypolimnion (Hypo) at the North Bay and Center Lake sites in 2018 and 2019.

Iron and Manganese

Iron and manganese concentrations in lake waters can provide important insights into the role of the internal loading in lake phosphorus dynamics. In New England, oxidized iron compounds sequester phosphorus in lake sediments making it unavailable to the algae community. After oxygen is consumed in aerobic cellular respiration and not replenished at the bottom of the water column during stratification, the biological processes and composition of the organisms carrying out those processes shift. A series of other oxidizing agents are used in anaerobic respiration until the iron compounds binding the phosphates are used, thus becoming reduced. Once iron is reduced, that species of iron and its associated phosphates become soluble then accumulate in waters overlying the sediments. Although oxidized manganese compounds do not sequester phosphorus to the extent iron does, they are the compounds used before iron in the series of oxidizing agent used in anaerobic respiration; therefore, useful in understanding nutrient dynamics.

Iron and manganese were measured in samples collected at the bottom of NB and CL to understand the aforementioned environmental dynamics, and in corresponding samples collected at 1m from the surface to provide a baseline. Paired samples were collected at both sites on the seven occasions in 2018 when water samples for nutrient analyses were collected (see Table 1). In 2019, iron and manganese were analyzed in samples collected monthly at both sites from April 22nd to July 15th.

Manganese levels in surface waters at Bantam Lake ranged from *not detectable* to 0.05mg/L and averaged 0.03mg/L based on the available data from both seasons. The average of 0.03mg/L is used as the baseline in analyses below. In 2018, manganese levels at the bottom of the water column were similar to baseline levels in April, May, August, September, and October (Fig. 24). June and July hypolimnetic levels at NB were approximately 33x and 47x higher than the baseline concentrations.

At the bottom of CL in 2018, no discernable difference was observed between the baseline and hypolimnetic manganese concentrations on April 22nd. By May 21st, hypolimnetic concentrations were approximately 20x greater than the baseline concentration. The difference increased through August 16th until the hypolimnetic concentration was approximately 90x greater than the baseline concentration (Fig. 24). Differences in manganese concentrations between the baseline and bottom strata in the water column returned to being negligible in samples collected in September and October.

Similar trends in hypolimnetic manganese concentrations were observed in the limited 2019 data. Very small differences between the baseline and hypolimnetic concentrations were observed on April 22nd and May 21st at NB; by June 18th and July 15th hypolimnetic concentrations were 16x and 47x greater than the baseline levels. At CL in 2019, the July 15th hypolimnetic concentration was 69x greater than the baseline. Hypolimnetic data was not available for CL on June 18th.

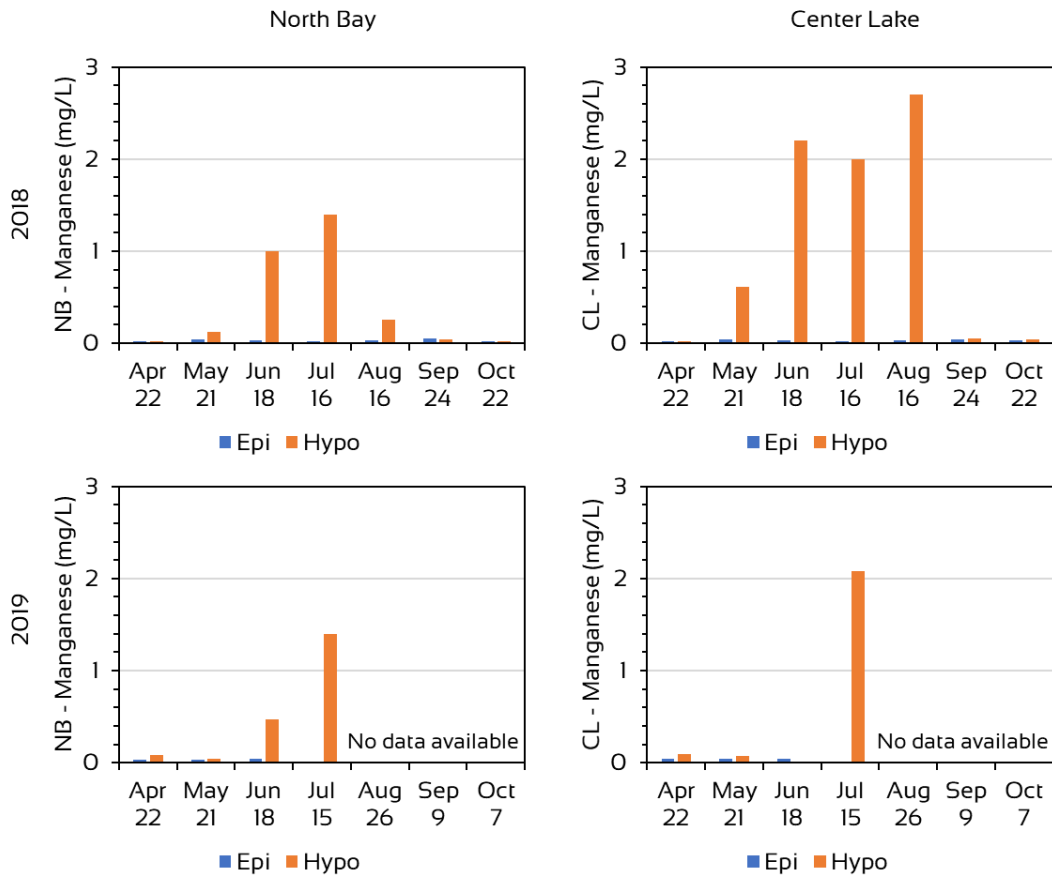


Figure 24. Manganese in the epilimnion at 1m (Epi) and hypolimnion (Hypo) at the North Bay and Center Lake sites in 2018 and 2019.

Iron concentrations measured in surface waters at both sites ranged from *not detected* to 0.18mg/L and averaged 0.10mg/L over the two years. The 0.10mg/L average is used below as the baseline level. In 2018 at NB, iron levels in the hypolimnion were at approximately baseline levels in April and May, the increased to approximately 7x the baseline level by June 18th. They continued to increase until approximately 21x greater than the baseline level on June 18th before decreasing to approximately 6x the baseline level on August 16th and baseline levels afterwards (Fig. 25).

At CL in 2018, hypolimnetic levels reached 21x the baseline level on June 18th, 54x baseline levels on July 16th, and 74x the baseline levels on August 16th. Hypolimnetic levels at CL on September 24th and October 22nd were very similar to baseline levels (Fig. 25).

In 2019, very little difference was observed between hypolimnetic and baseline iron concentrations at either site through June 18th. By July 15th the NB hypolimnetic concentrations was 36x the baseline concentration and over twice that at 82x the baseline concentration at CL.

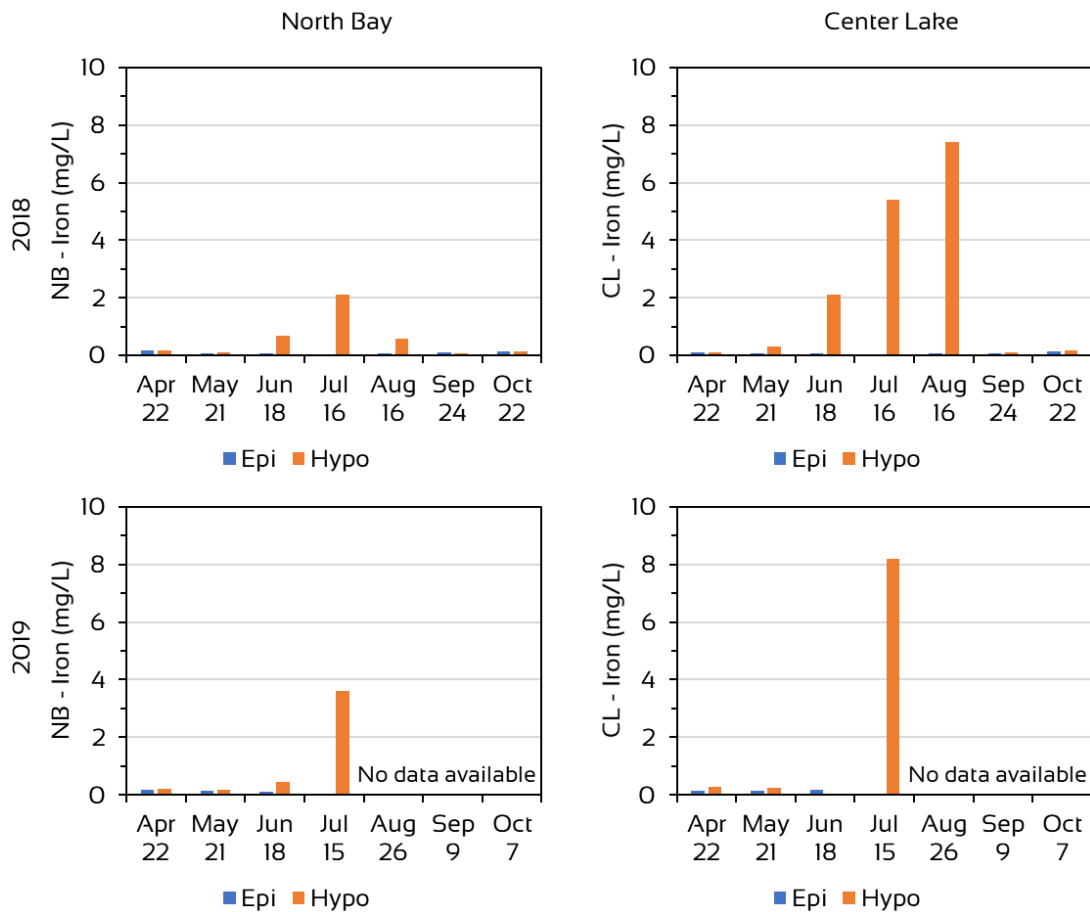


Figure 25. Ferrous iron in the epilimnion at 1m (Epi) and hypolimnion (Hypo) at the North Bay and Center Lake sites in 2018 and 2019.

Oxidation-Reduction Potential

Midway through the 2018 season, AER added another parameter to those measured in the field throughout the water column. The oxidation-reduction potential (otherwise known as redox potential or ORP) in lakes refers to the oxidative or reductive state in a particular stratum of the water column and can aid in understanding phosphorus dynamics in the lentic system. In general, when ORP is ≥ 200 millivolts (mV) phosphate remains bound to iron; at ORP values of < 200 mV, iron becomes reduced and phosphate is released (Søndergaard 2009). In some cases, a sudden mixing of phosphate-laden waters to the upper reaches of the water column during a storm event could trigger a harmful algal bloom. Below we present isopleth diagrams of ORP in the water columns of the four sites in 2019 (Fig 26) and report on them below since in the 2019 season we collected a full season of data.

At the three sites with a maximum depth of ≤ 6.5 m (NB, CL, and FP), the top 5 m of the water column generally had ORP levels ranging from 200 to 300 mV, particularly in data collections in June through October. A range of 100 to 300 mV was observed at

those depths and sites in April through May with higher ORP closer to the bottom. A similar trend was observed from the surface to the 4m strata at the South Bay site, where maximum depth was 4.5m.

The ORP ranges near the bottom of the water column at NB, FP and SB were more variable (Fig. 26). For example, at NB the ORP at the 6m strata (bottom) was -81mV on June 4th, 121mV on June 19th, then ranged from -78 to -123mV for the month of July before increasing to 12mV by August 12th. During the period between July 15th and August 1st, the ORP at the 5m strata ranged between 39 and 95mV. On August 12th and August 26th, the ORP throughout the entire water column ranged from 260 to 313mV

In September, ORP at the 6m stratum ranged from -89 to -136mV before increasing to nearly 300mV by October 7th.

Similar patterns of alternating high and low ORP at the bottom depths of FP and SB were observed (Fig. 26). On very rare occasions at FP the ORP at the 5 or 6m strata <200mV. These occurred on July 15th when the ORP at the respective strata were 114 and 41mV; and on August 12th at 6m when ORP was -86mV. The ORP was also -86mV at 6.5m on August 12th; but on sampling events of August 1st and August 26th, ORP it was 280 and 285mV, respectively. ORP at 6.5m of depth at FP was also <200mV on June 4th through July 29th, and September 9th and 23rd. At SB, ORP levels at the 4m and/or 4.5m strata ranged from -47 to -156mV on May 6th through June 4th, July 1st and August 1st. All other ORP levels at those depths were >200mV.

The ORP trends at the 8m deep CL site were different. All ORP readings from the surface to 5m deep in June through October ranged between 222 and 330mV. At the 6m stratum, all ORP measures were in the same range with the exception of those from July 15th through August 1st which ranged from -57 to -87mV and from August 12th, which was 129mV. At the 7m stratum, a range of -2 to -172mV existed between July 1st and August 26th. At the 8m stratum ORP range from -21 to -175mV from June 4th through September 9th and again on October 7th. All other ORP measurements at 6m, 7m, or 8m of depth were >240mV.

In summary, very low ORP persisted uninterrupted at the bottom of the CL site from June 4th through September 9th; those conditions extended upwards to the 6m stratum between July 1st and August 26th and ultimately up to the 5m strata between July 15th and August 1st

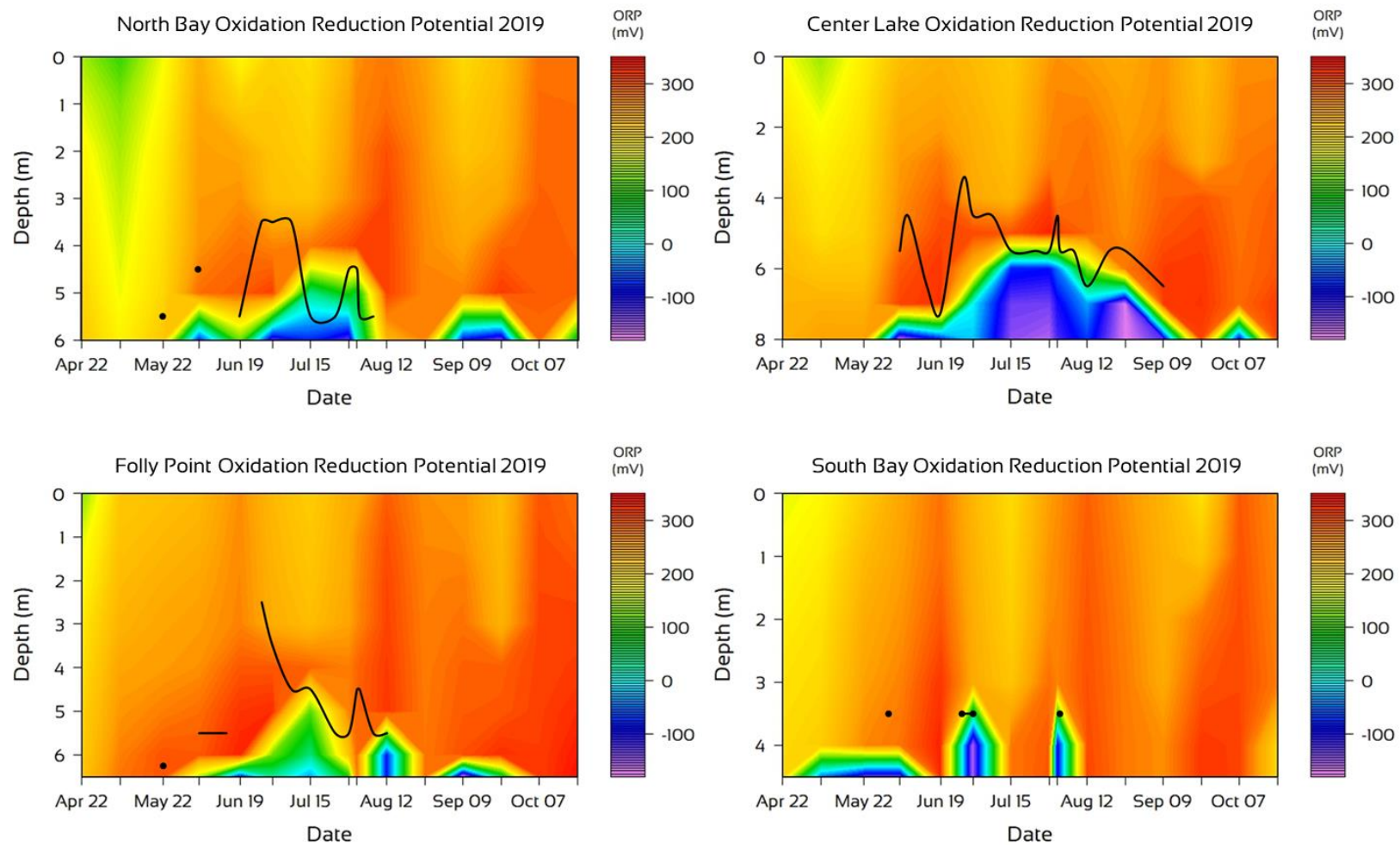


Figure 26. Oxidation reduction potential isopleth diagrams for the North Bay, Center Lake, Folly Point, and South Bay sites in 2019. The black lines and dots represent the location of a thermocline in the water column. Lines represent continuous observation of a thermocline over time while dots represent isolated events of stratification separated by mixed conditions.

Table 5. Summary statistics for the base cations, chloride, and alkalinity data collected at North Bay (NB) and Center Lake (CL) sites in 2018 and 2019. n = number of samples; SD = standard deviation.

Analyte	Site	Year	n	Mean (mg/L)	SD (mg/L)	Analyte	Site	Year	n	Mean (mg/L)	SD (mg/L)
Sodium (Na ⁺)	NB	2018	7	17.1	2.4	Magnesium (Mg ²⁺)	NB	2018	7	4.9	0.4
	CL	2018	7	17.3	2.4		CL	2018	7	4.8	0.5
	NB	2019	5	14.9	1.0		NB	2019	5	4.2	0.6
	CL	2019	5	15.5	0.9		CL	2019	5	4.2	0.7
Potassium (K ⁺)	NB	2018	7	1.9	0.5	Chloride (Cl ⁻)	NB	2018	7	33.0	4.8
	CL	2018	7	1.9	0.4		CL	2018	6	34.5	3.6
	NB	2019	5	1.4	0.2		NB	2019	5	28.0	2.0
	CL	2019	5	1.4	0.2		CL	2019	5	27.8	2.8
Calcium (Ca ²⁺)	NB	2018	7	11.9	1.0	Alkalinity (CaCO ₃)	NB	2018	7	39.9	4.0
	CL	2018	7	11.9	0.6		CL	2018	7	40.1	3.4
	NB	2019	5	10.4	0.5		NB	2019	7	40.0	2.6
	CL	2019	5	10.6	0.9		CL	2019	7	38.9	2.8



Base Cations and Chloride

Base cation and anion concentrations are important in understanding natural influences (e.g. dissolved salts from bedrock geology) as well as anthropogenic influences from the watershed (e.g. road salts). In lakes of the Northeast, the dominant base cations in lake waters are calcium (Ca^{2+}), magnesium (Mg^{2+}), sodium (Na^+) and potassium (K^+). Dominant anions include chloride (Cl^-), sulfate (SO_4^{2-}), carbonate (CO_3^{2-}), and bicarbonate (HCO_3^-). In this assessment we examined the base cations, chloride, and alkalinity anions (carbonate and bicarbonate).

In 2018, samples for these analyses were collected monthly from April to October at NB and CL for a total of seven samples. In 2019, samples were collected monthly at both sites, but August and October data were not available, yielding five samples from each site for the season. A table with summary statistics of the results of analyses from samples collected is provided above in Table 5.

In general, ionic concentrations were slightly higher in 2018 than in 2019. This is consistent with average specific conductance each year. Very little differences between sites each year were observed. There was a strong correlation between total ionic concentration and specific conductance in samples. This was determined by converting milligrams per liter to milliequivalents per liter for each dissolved mineral listed above totaling the milliequivalents for each sample, and regressing each against the specific conductance of that sample (Fig. 27).

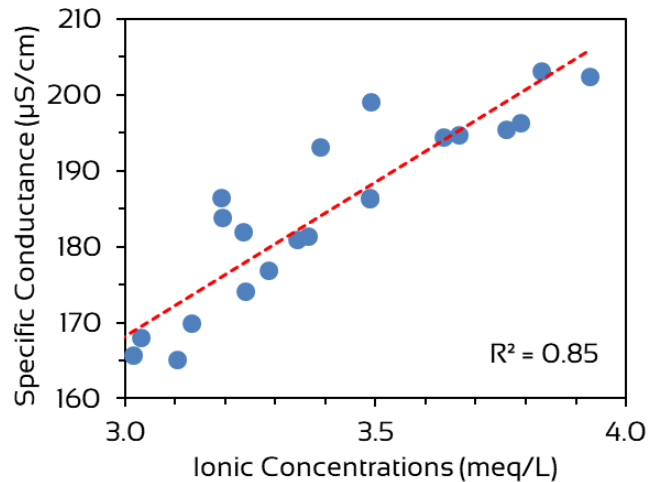


Figure 27. Regression of the sum total of ion concentration against the corresponding specific conductance in samples collected at the North Bay and Center Lake sites in 2018 and 2019.

GENERAL TRENDS

Trophic Trends

As noted earlier, Bantam Lake has been part of several state-wide surveys of Connecticut Lakes. Below we provide a comparison of data collected at Bantam Lake in 2018 and 2019 to that from a survey conducted in the early 1990s (Canavan and Siver 1994, 1995; Table 6). We also provide below criteria used in Connecticut to assess the trophic conditions of lakes (Table 7). Based on the 2018 and 2019 season averages, Bantam Lake total phosphorus levels are characteristic of mesotrophic conditions. However, phosphorus concentrations observed from late July and afterwards in both 2018 and 2019 are characteristic of eutrophic conditions.

Table 6. Comparisons of the 2018 and 2019 Bantam Lake season averaged water quality variables to averages in an early 1990s and to ranges observed in lakes located in the Connecticut Western Uplands (Canavan and Siver 1995) conducted in the early 1990s. All measures with the exception of Secchi transparency were from 1 meter depth.

Parameter	Units	Bantam Lake			Western Uplands Lakes*		
		90's*	2018	2019	Min	Max	Mean
Total Nitrogen	µg/L	714	550	276	208	714	364
Total Phosphorus	µg/L	42	22.5	22.7	10	57	33
Chlorophyll- <i>a</i>	µg/L	19.7	9.2	9.8	0.7	19.7	5.1
Secchi Disk	meters	1.7	2.28	2.66	1.7	7.6	3.5
pH	pH units	7.8	7.8	8.0	4.6	8.1	7.2
Sp. Conductivity	µS/cm	122	189	176	25	188	96
Alkalinity	mg/L	30.5	40.7	39.4	23.7	44	21
Chloride (Cl ⁻)	mg/L	10.3	33.7	27.9	0.7	24.1	9.2
Calcium (Ca ²⁺)	mg/L	8.2	11.9	10.5	2.8	11.4	6.8
Magnesium (Mg ²⁺)	mg/L	7.8	4.8	4.2	1	5.2	4.1
Sodium (Na ⁺)	mg/L	7.4	17.2	15.5	1.4	10.4	5.3
Potassium (K ⁺)	mg/L	1.2	1.9	1.5	0.2	0.9	0.5

Table 7. Trophic classification criteria used by the Connecticut Experimental Agricultural Station (Frink and Norvell, 1984) and the CT DEP (1991) to assess the trophic status of Connecticut lakes. The categories range from oligotrophic or least productive to highly eutrophic or most productive.

Trophic Category	Total Phosphorus (µg / L)	Total Nitrogen (µg / L)	Summer Chlorophyll- <i>a</i> (µg / L)	Summer Secchi Disk Transparency (m)
Oligotrophic	0 - 10	0 - 200	0 - 2	>6
Early Mesotrophic	10 - 15	200 - 300	2 - 5	4 - 6
Mesotrophic	15 - 25	300 - 500	5 - 10	3 - 4
Late Mesotrophic	25 - 30	500 - 600	10 - 15	2 - 3
Eutrophic	30 - 50	600 - 1000	15 - 30	1 - 2
Highly Eutrophic	> 50	> 1000	> 30	0 - 1

The average 2018 and 2019 chlorophyll-*a* and Secchi transparency levels were characteristic of mesotrophic to late mesotrophic conditions but late season levels were characteristic of eutrophic conditions. The late July copper sulfate treatments also biased conditions to appear less eutrophic.

Bantam Lake’s trophic condition in the 1990s survey were based on single date data collections in early August of 1991, late July in 1992, and late July and late August of 1993. The conditions in the late August date of 1991 exhibited the most enriched conditions at Bantam Lake in the survey due to the concentrations of chlorophyll-*a* (34.8µg/L), total phosphorus of 58µg/L, and Secchi transparency of 1m. These collectively indicate eutrophic conditions and are similar to the late season conditions at Bantam Lake in 2018/2019.

Dissolved Salts on the Rise

Differences in ion concentrations and specific conductance between the 1990s data and recent data are more evidenced by concentrations of sodium, potassium, calcium, chloride, alkalinity, and specific conductance, which are all 24 to 67% higher now than in the 1990s.

Increases in the specific conductivity and most ion concentrations – most notable chloride – over the last 50 years are not uncommon to Connecticut lakes and largely due to changes in cultural land use practices (e.g. loss of forested watershed), use of deicing road salts, soil erosion, agriculture, etc.

MANAGEMENT CONSIDERATIONS

Copper Sulfate Treatments

Bantam Lake experienced declining water quality starting sometime after mid-July during both seasons. These conditions were characterized by decreasing Secchi transparency, increasing cyanobacteria concentrations, increasing relative cyanobacteria levels, and increasing chlorophyll-*a* concentrations. To mitigate the deteriorating conditions the BLPA contracted with a certified pesticide applicator for a late-July copper sulfate treatment.

The efficacies of treatments in each year were similar but might have appeared more effective in 2019 because the mid- to late July water quality was poorer. In 2019, Secchi transparency improved from a lake average of 1.85m on July 24th to over 3.4m by early August. There was also a corresponding decrease in average chlorophyll-*a* concentrations from 9.1 to 2.7µg/L between July 15th and August 12th of 2019; both of those variables reflect an effective treatment. Cyanobacteria cell counts also decreased following the July 24th treatment (Fig. 10) as did relative cyanobacteria levels (Fig. 13). In 2018, the August 2nd average Secchi transparency of 2.04m increased to 2.58m by August 16th and average chlorophyll-*a* decreased from 6.7µg/L on July 30th to 3.2 on August 16th.

In both seasons, improved conditions persisted through late August but degraded by early November in 2018 and late September in 2019. It was during these times when cyanobacteria cell concentrations exceeded 100,000 and – in some instances – approached 200,000 cells/mL (Fig. 10).

Stratified and Mixed Water Columns

There were important differences in seasonal patterns of stratification and mixing among the four sites. These patterns were demonstrated in the isopleth diagrams created for temperature, oxygen, specific conductance, and oxidation-reduction potentials. The differences were likely due to the depths at each site and the location's orientations with respect to wind directions. Based on data from the White Memorial Weather Station, winds directions during the 2018 and 2019 monitoring seasons tended to come out of the south or north-north-east (Fig. 28).

The Center Lake site is centrally located along the lake's north to south axis nearer

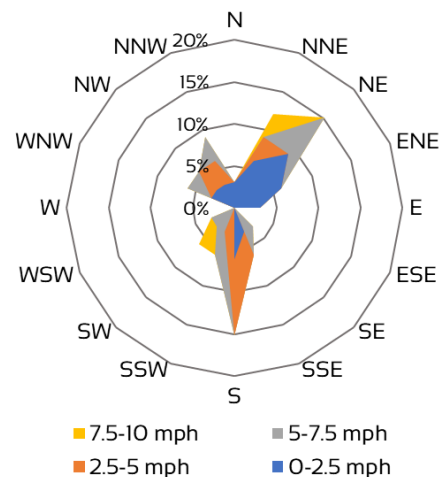


Figure 28. Wind directions and speeds on selected sampling dates. Data from the White Memorial Weather Station.

to the eastern shore (Fig. 1); and, theoretically more prone to mixing from winds from the north or south. However, it is the deepest site, which decreased its tendency to mix completely during periods of strong thermal stratification. It was the only site with continuous stratification from early in the season until August (Fig. 3).

In direct contrast, the South Bay site, which has a maximum depth of 4.5m, was rarely stratified over the two-year period (Fig. 5). This site was hypothetically less subject to winds coming out of the south than other sites; but it would be more affected by winds out of the north due to the north/south orientation of the lake. The North Bay and Folly Point sites had intermittent and/or shorter periods of continuous stratification compared to the Center Lake site in both seasons (Figs. 2 & 4).

The patterns of mixing and stratification impact the distribution of oxygen and thus the oxidation-reduction potential throughout water column. Under stratified conditions, the depletion of oxygen near the bottom of the lake at deeper sites exceeds the replenishment rate below the thermocline. The thermocline acts as a barrier preventing diffusion of oxygen between the oxygenated waters above and the oxygen depleted waters below.

Once oxygen is depleted, ORP decreases and elements such as iron and manganese in the sediments are reduced and become soluble in water; ultimately, this coincides with a release of phosphorus. Oxidation-reduction potentials increase once water column mixing enriches oxygen to lower depths. Soluble minerals precipitate back out to the sediments in the compounds they were once part of normally.

Internal Loading of Phosphorus and Depth

To investigate the sequence of oxidation-reduction reactions at the bottom of Bantam Lake, we determined the ratios of hypolimnetic to epilimnetic concentrations for ammonia, manganese, iron, total phosphorus, and alkalinity at the North Bay and Center Lake sites during the 2018 season (Fig. 29). The results from Center Lake, where the water column was stratified from early May through late August, exhibited in order all of the redox reactions discussed above. At North Bay, the reactions appeared to stop just after reduction of iron. Based on alkalinity ratios, the reduction of sulfur compounds at North Bay appear minimal. Higher hypolimnetic: epilimnetic ratios of manganese, iron, and total phosphorus at North Bay were only observed through mid-July. This was likely due to a late July mixing of the water column at North Bay (see Fig. 2).

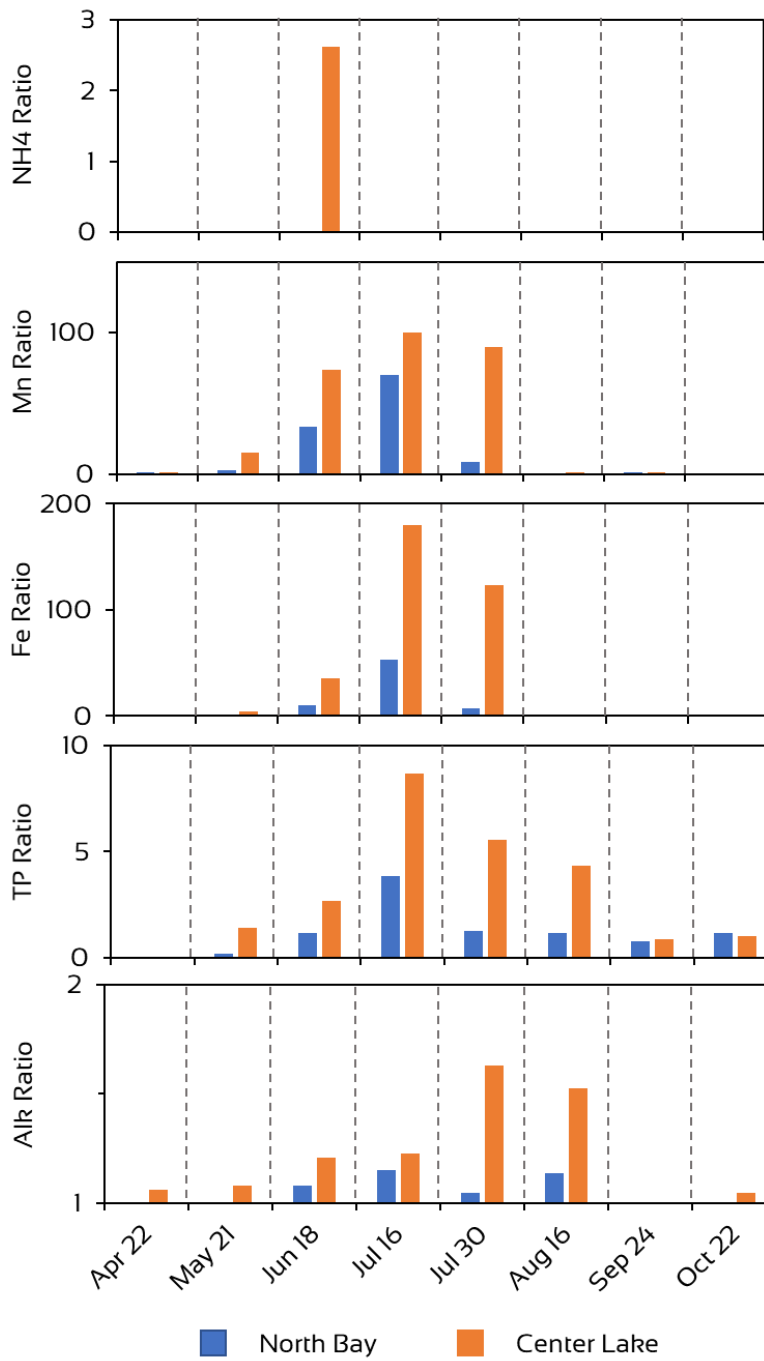


Figure 29. Ratios of ammonia (NH₄), manganese (Mn), iron (Fe), total phosphorus (TP), and alkalinity measured in the surface and bottom of the North Bay and Center Lake sites in 2018.

Several significant management considerations can be deduced from these analyses. First, internal loading of phosphorus is an important contributor to the phosphorus budget at Bantam Lake. This was also supported by the nutrient budget model presented in Fig. 15. In addition, higher rates of loading occur at the Center Lake site due to the greater depth that results in prolonged stratification.

The other significant consideration is the theoretical loss of iron as pyrite in lake sediments that might otherwise bind phosphate under oxidizing conditions. The proportionally higher levels of alkalinity at the bottom of the Center Lake site is the result of dissimilatory reduction of sulfur, which then binds with soluble iron, forming pyrite. That iron is then unavailable to bind with phosphates once the environment becomes more oxidized. The long-term impact of loss of phosphate binding iron should be explored further.

We discussed earlier in this document that the 8m deep Center Lake site was prone to longer periods of stratification, lower ORP, and higher concentrations of internally derived total phosphorus concentrations compared to the 6m deep North Bay site. Theoretically, other areas of the lake that were between >6 to 8m deep would exhibit similar characteristics to those at Center Lake. Based on available bathymetric data for Bantam Lake, we have graphically delineated those areas that were ≥ 7 m deep (Fig. 30). These areas theoretically contribute higher influxes of phosphorus from the lake sediments. We calculated the size of that area as 119.5 acres or approximately 12% of the bottom surface.

We also noted that while the North Bay site might not exhibit the levels of internal loading compared to the Center Lake, it did contribute to the loading of phosphorus intermittently throughout the season. This may explain the higher concentrations throughout the water column at North Bay after July (Fig. 14). After loading under stratified conditions, the water column was mixed thereby increasing the phosphorus concentration at all depths.

Cyanobacteria at Bantam Lake

We reported that the Bantam Lake phytoplankton community is largely dominated by Cyanobacteria. One of the water quality characteristics during this study is a shift at Bantam Lake from phosphorus limitation to nitrogen limitation between June and July. Nitrogen limitation provides an adaptive advantage to certain Cyanobacteria over other algal taxa. Cyanobacteria genera like *Dolichospermum spp.* and *Aphanizomenon spp.* are capable of utilizing atmospheric nitrogen (N_2) if nitrogen compounds like nitrate or nitrite are unavailable. Many create specialized cells where nitrogen fixation occurs (Fig. 31). Other taxa (e.g. Green or Golden Algae, Diatoms, etc.) are not able to utilize atmospheric nitrogen. Both *Dolichospermum spp.* and *Aphanizomenon spp.* are important components of the pelagic algal community at Bantam.

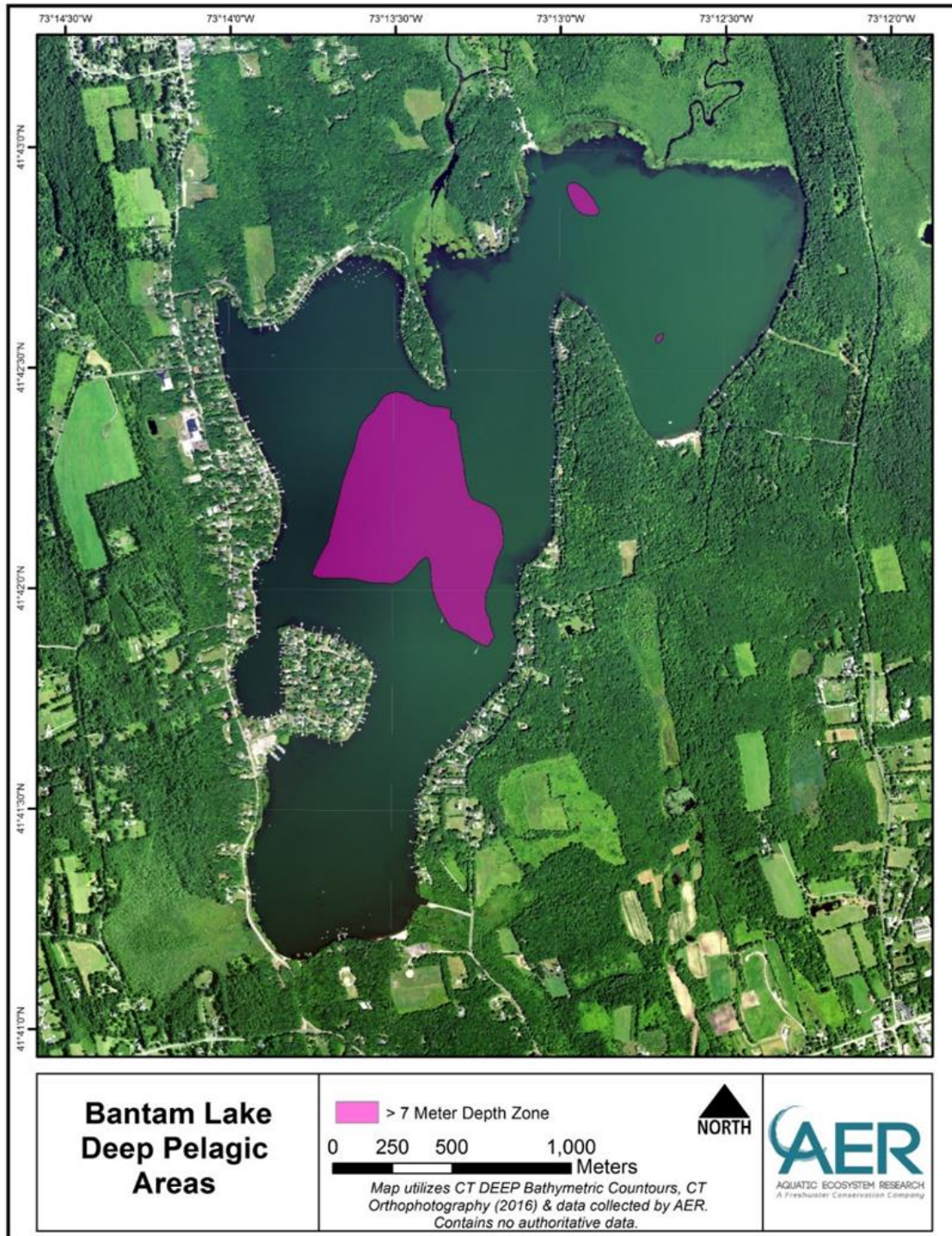


Figure 30. Map of Bantam Lake with areas of >7 meters of depth delineated.



Figure 31. A filament of *Dolichospermum* spp. The yellow arrow points to the heterocyst in the filament; the red arrow points to the akinete.

In addition to possible nitrogen limitation we believe other characteristics of Bantam Lake, in conjunction with the life cycle cyanobacteria contribute to the success of cyanobacteria (Fig. 32). Cyanobacteria like *Dolichospermum* spp. and *Aphanizomenon* spp. also form other specialized cells called akinetes. These “resting cell” of cyanobacteria over-winter in lake sediments after senescence (Fig. 31). The akinetes that over-winter in sediments from 0 to 4m of depth germinate and provide the beginnings of the cyanobacteria population that will develop the following season. There is 353 acres of approximately 37% of the lake sediment surface that lies within the 0 – 4m depth range (Fig. 33).

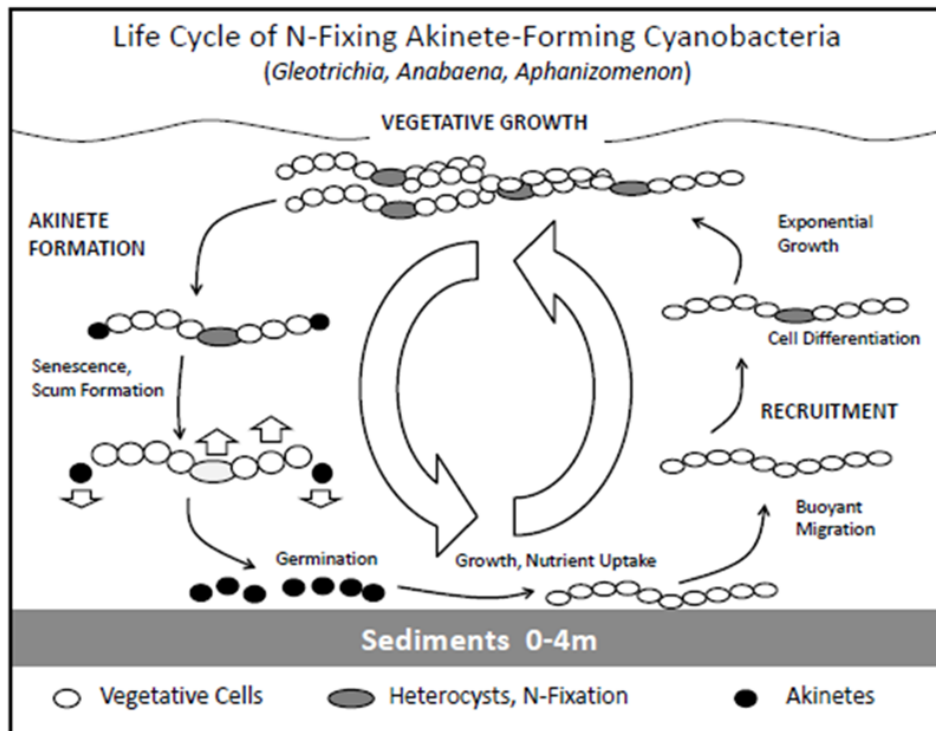


Figure 32. Generalized life cycle of *Anabaena* (aka *Dolichospermum*) spp., *Aphanizomenon* spp., and similar Cyanobacteria genera (Kortmann 2015). Printed with permission from Dr. Robert Kortmann.

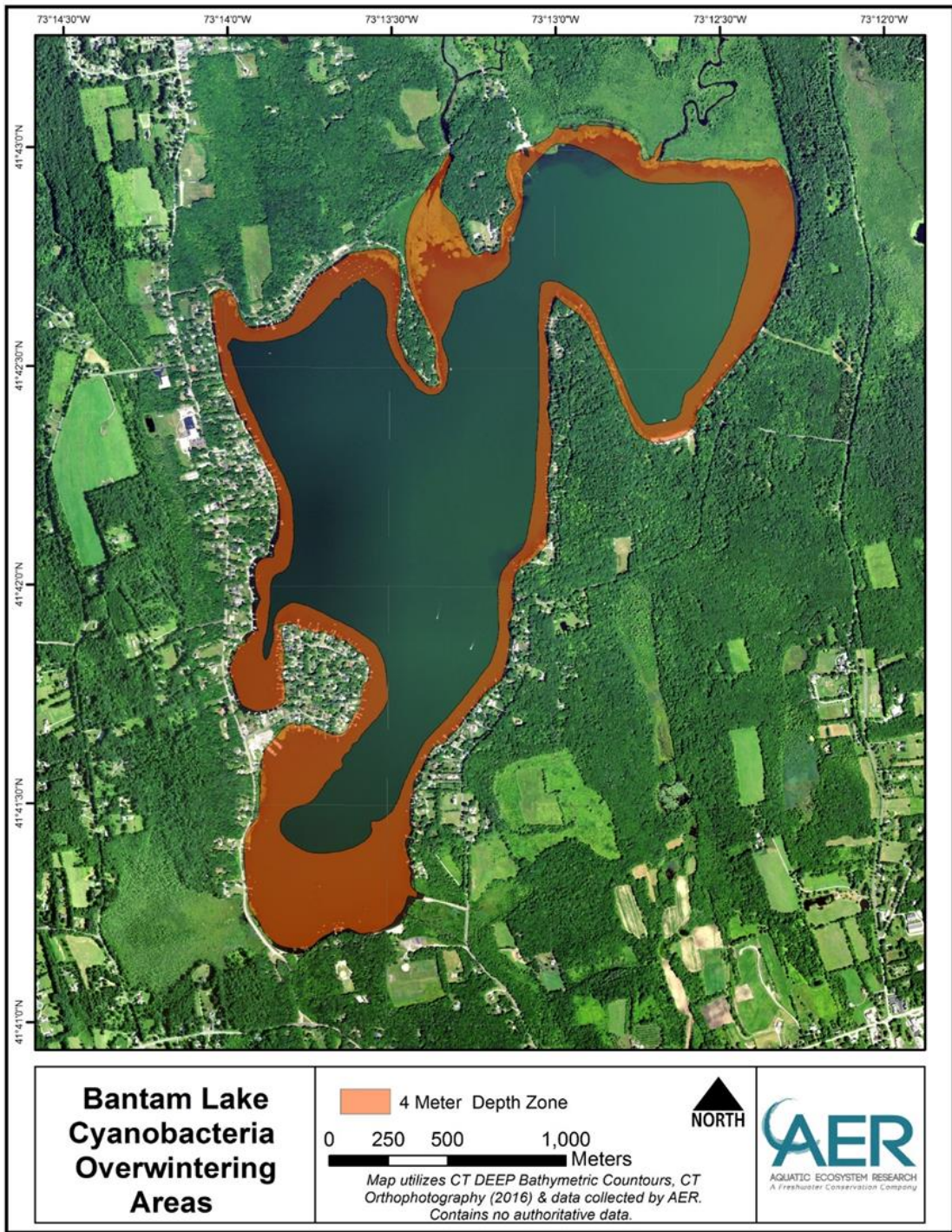


Figure 33. Map of Bantam Lake with areas of ≤ 4 meters of depth delineated.

Traditionally, algicides like copper sulfate are used in response to declining conditions from algae blooms. The life cycle of akinete-forming cyanobacteria may provide opportunities to gradually reduce the population in preemptive measures to mitigate blooms in future years. Theoretically, if many of the cyanobacteria are removed in late summer before the formation of akinetes, then the “seed bank” in subsequent years would be reduced. Likewise, if the cyanobacteria population is treated just after germination of akinetes in the area of the lake that is 0 – 4m deep, before cell division, that could reduce the population that year.

Based on our analyses, most winds are coming from a northerly or southerly direction. Because of their ability to regulate buoyancy, some cyanobacteria can collect at the surface and if wind conditions are right (i.e. not so strong as to cause vertical mixing) cyanobacteria can be concentrated in certain areas of the lake (i.e. bays, swim areas etc.). On several occasions in 2018 we observed surface scums at the State boat launch. Development of a bloom watch program at Bantam Lake that includes meteorological data could help better to understand cyanobacteria blooms at Bantam Lake.

RECOMMENDATIONS

Plan for an Alum Treatment

- Internal loading of phosphorus is an important contributor to the phosphorus budget, particularly in deeper areas of the lake. Alum treatments are a method of mitigating internal loading of phosphorus.
- Alum strips phosphate from the water column and can sequester phosphorus in the sediments for 10+ years.
- Reduction of phosphorus would reduce algal productivity and biomass and theoretically increase the TN:TP ratio thereby reducing the advantage heterocyst-forming cyanobacteria may have under nitrogen-limited conditions
- Several exploratory studies should be conducted in 2020:
 - Delineation of the transition zone between near-shore, inorganic sediments to deeper, organic sediments
 - Sediment sampling and analyses for concentrations of iron-bound phosphate and labile phosphorus.

Monthly Water Quality Monitoring

- A water quality monitoring program is fundamental to lake management efforts. It provides empirical data necessary for determining what strategies might be best suited to address the characteristics as determined by limnological assessments. It also provides a means of assessing if the implementation of a management strategy is effective or not, or deleterious or not.
- The Bantam Lake monitoring program should continue in its current form with some the following changes:
 - Base cation and chloride analyses can be reduced to three times in 2020 at the North Bay and Center Lake sites, e.g. May, July, and September.
 - Monthly nutrient analyses (ammonia, nitrate, nitrite, total Kjeldahl nitrogen, total phosphorus and alkalinity) should be expanded to include the Folly Point and South Bay sites to understand differences in phosphorus loading relative to site depth.
 - Increase the number of sites where profile data (temperature, oxygen, specific conductance, ORP, pH, relative cyanobacteria levels) is collected from 4 to 6 sites

Biweekly Cyanobacteria Monitoring

- This program has been successful at providing important public health information to users of Bantam Lake and should be continued.
- Sites could be expanded to include the public beaches.

Cyanotoxin Monitoring

- BLPA developed an agreement with the research laboratory of Dr. Edwin Wong of the Biological and Environmental Science Department at Western Connecticut State University to test samples for concentration of microcystin. AER collected those samples at North Bay and Center Lake as part of the biweekly sample collections for cyanobacteria cell enumerations.
- The current program should be implemented again with the following modifications:
 - Add the public beaches to collection sites, or
 - Add the public beaches to the collection sites and set frequency at the beaches to weekly from July 1st through Labor Day
 - Add analyses of saxitoxins to the microcystins that are already analyzed.
 - Saxitoxins (aka paralytic shellfish poison) are being found in samples from other lakes and are known to be produced by *Dolichospermum spp.* and *Aphanizomenon spp.* Both of these cyanobacteria genera are found in high concentrations at Bantam Lake.
 - Investigate the idea of adding the results of cyanotoxin analyses to information shared with the public

Statistical Analyses of Phycocyanin and Chlorophyll-a Data

- In 2019, data was regularly collected on phycocyanin and chlorophyll-a concentrations throughout the water columns at the NB, CL, FP, and SB sites. This data was collected by researchers at the White Memorial Conservation Center by collecting samples throughout the water column at each site, and analyzing samples with fluorimetry after sample treatment with a series of freeze/thaws.
- This type of data collection is currently being conducted by researchers at the Center for Freshwater Biology at the University of New Haven and used to develop predictive models for cyanobacteria blooms.
- The Bantam data should be thoroughly analyzed and used in multiple regression analyses and ordination analyses along with other corresponding water quality data to see if it can be used to predict blooms at Bantam Lake.

Forward-thinking Measures to Reduce Cyanobacteria Population

- Currently, the BLPA manages rising cyanobacteria concentrations with a responsive copper sulfate treatment in late July.
 - These treatments have had some success in extending the recreational use of the lake.
 - By mid to late August, cyanobacteria levels begin to return to higher concentrations.

- The life cycle of the akinete-forming cyanobacteria may provide opportunities for forward-thinking management to reduce cyanobacteria populations
 - Treating populations just prior to akinete formation in late summer and/or treating populations just after akinete germination are worthy of exploration.

Assess Watershed Management Strategies

- Increases in levels of dissolve salts and minerals and specific conductance since the early 1990s are indicative of a watershed influence on water quality at Bantam Lake.
- Continued increases in some of these chemical characteristics could:
 - Impact the aquatic plant and algal community structure,
 - Make Bantam Lake prone to other aquatic invasive species, including zebra mussels
 - Be a proxy for nutrient export to the lake
- Future stormwater investigations could include:
 - Compiling all historical stormwater data and analyzing it
 - Collect stormwater data in 2020 and add that to the analyses.

Cyanobacteria Bloom Watch

- Collection of data on bloom events at Bantam and their locations may aid in better understanding risks to public health. This kind of data could assist in answering questions like, "Do most blooms form in south or north facing coves or beaches?"

REFERENCES

- Canavan RW, Siver PA. 1994. Chemical and physical properties of Connecticut lakes, with emphasis on regional geology. LAKE RESERV MANAGE. 10(2):175-188.
- Canavan RW, Siver PA. 1995. Connecticut Lakes: A study of the chemical and physical properties of fifty-six Connecticut Lakes. New London (CT): Connecticut College Arboretum.
- Connecticut Department of Energy and Environmental Protection (CT DEEP). 1991. Trophic Classifications of Forty-nine Connecticut Lakes. CT DEEP, Hartford, CT. 98 pp.
- Deevey ES Jr. 1940. Limnological studies in Connecticut. V. A contribution to regional limnology. AM J SCI. 238(10):717-741.
- Frink CR, Norvell WA. 1984. Chemical and physical properties of Connecticut lakes. New Haven (CT): Connecticut Agricultural Experiment Station. Bulletin 817. 180 pp
- Lawton L, Marsalek B, Padisák J, Chorus I. 1999. DETERMINATION OF CYANOBACTERIA IN THE LABORATORY. In Toxic Cyanobacteria in Water: A guide to their public health consequences, monitoring and management. Chorus and Bartram, eds.
- Redfield A.C. 1958. The biological control of chemical factors in the environment. American Scientist. 46(3):205-221.
- Siver, P.A., Ricard, R., Goodwin, R. and A.E. Giblin. 2003. Estimating historical in-lake alkalinity generation and its relationship to lake chemistry as inferred from algal microfossils. J. Paleolimn. 29: 179-197.

APPENDIX 1. LIST OF ALGAL GENERA OBSERVED IN 2018 AND 2019.

2018

Taxa	Genera	22- Apr	8- May	21- May	4- Jun	18- Jun	2- Jul	16- Jul	30- Jul	16- Aug	27- Aug	11- Sep	24- Sep	9- Oct	22- Oct	8- Nov	
Cyanophyta	<i>Aphanizomenon sp.</i>				X	X	X	X	X	X	X	X	X	X	X	X	
	<i>Aphanothece sp.</i>				X	X			X	X	X	X	X				
	<i>Chroococcus sp.</i>						X										
	<i>Dolichospermum sp.</i>			X	X	X	X	X	X	X	X	X	X	X		X	
	<i>Gomphosphaeria sp.</i>							X									
	<i>Microcystis sp.</i>			X			X			X		X	X				
	<i>Snowella sp.</i>							X									
	<i>Woronichinia sp.</i>		X	X	X	X	X		X	X	X		X				
Chlorophyta	<i>Anikistrodesmus sp.</i>					X	X		X	X	X		X				
	<i>Coelastrum sp.</i>									X			X				
	<i>Crucigenia sp.</i>									X			X				
	<i>Dictyosphaerium sp.</i>								X	X			X				
	<i>Elakatothrix sp.</i>				X	X			X								
	<i>Eudorina sp.</i>						X	X	X								
	<i>Gloeocystis sp.</i>	X			X	X	X	X	X	X	X				X		
	<i>Gonium sp.</i>							X									
	<i>Mougiotia sp.</i>								X								
	<i>Nephrocytium sp.</i>											X					
	<i>Oocystis sp.</i>				X	X	X	X	X	X			X				
	<i>Padorina sp.</i>				X												
	<i>Pediastrum</i>			X													
	<i>Scenedesmus sp.</i>	X				X			X	X	X		X				
	<i>Schroederia sp.</i>		X	X		X			X	X	X						
	<i>Selenastrum sp.</i>								X				X	X			
	<i>Sphaerocystis sp.</i>									X	X						
<i>Tetraedron sp.</i>								X									



Chrysophyta	<i>Chrysophaerella sp.</i>																	X
	<i>Dinobryon sp.</i>		X			X												X
	<i>Mallomonas sp.</i>	X	X			X				X	X	X	X	X				
	<i>Synura sp.</i>	X	X							X								X
	<i>Uroglenopsis sp.</i>	X	X	X						X	X			X	X			X
Bacillariophyta	<i>Asterionella sp.</i>	X				X												
	<i>Aulocoseria sp.</i>	X	X				X	X	X	X	X				X			X
	<i>Fragilaria sp.</i>	X	X				X	X										
	<i>Stephanodiscus sp.</i>	X	X	X			X											
	<i>Synedra sp.</i>									X	X							X
	<i>Tabellaria sp.</i>	X								X			X					X
	<i>Pennate Diatom</i>	X			X													
Dinophyceae	<i>Ceratium sp.</i>						X	X	X	X	X	X	X					
	<i>Peridinium sp.</i>		X															
Cryptophyceae	<i>Cryptomonas sp.</i>			X	X	X	X			X	X	X			X			X
	<i>Rhodomonas sp.</i>		X	X	X	X	X				X							
Euglenophyceae	<i>Trachelomonas sp.</i>					X				X	X	X	X	X				
Total Genera		11	11	10	13	22	14	11	24	22	14	9	20	6	2	2	2	

2019

Taxa	Genera	22-Apr	6-May	22-May	4-Jun	19-Jun	1-Jul	15-Jul	29-Jul	1-Aug	12-Aug	26-Aug	9-Sep	23-Sep	7-Oct	23-Oct
Cyanophyta	Aphanizomenon sp.	X	X	X	X	X	X	X	X	X	X	X	X	X	X	X
	Aphanocapsa sp.			X	X	X			X	X		X	X	X	X	X
	Aphanothece sp.				X	X	X				X	X				
	Chroococcus sp.			X							X	X				
	Coelosphaerium sp.				X		X	X	X	X	X	X	X	X	X	X
	Dolichospermum sp.				X	X	X	X	X		X	X	X	X	X	X
	Gomphosphaeria						X									
	Merismopedia sp.											X				
	Microcystis sp.				X	X	X	X				X	X	X		
	Oscillatoria sp.											X				
	Pseudoanabaena sp.		X	X	X			X		X		X		X		
	Snowella sp.							X	X	X	X					
	Woronichinia sp.			X	X	X	X	X	X	X	X	X	X	X	X	X
Chlorophyta	Anikistrodesmus sp.				X		X		X	X	X					
	Chlamydomonas sp.								X							
	Closterium sp.				X											
	Coelastrum sp.					X	X				X	X				X
	Dictyosphaerium sp.						X		X	X	X	X	X		X	X
	Elakatothrix sp.		X		X	X	X		X	X	X	X		X		
	Eudorina elegans			X						X		X	X		X	
	Gloeocystis sp.		X	X	X	X	X	X		X	X	X	X	X		
	Gonium sp.								X	X						
	Gonium sp.								X				X			
	Mougiotia sp.							X								
	Nephrocytium sp.			X	X				X		X		X			
	Oocystis				X	X	X	X		X	X				X	



	Padorina sp.														
	Pediastrum sp.	X			X			X	X				X		X
	Quadrigula sp.				X	X	X	X		X					
	Scenedesmus sp.		X							X	X	X	X		
	Schroederia sp.					X						X			
	Selenastrum sp.			X				X	X			X			
	Sphaerocystis sp.										X				
	Staurastrum sp.			X	X	X	X			X	X	X			
	Tetraedron sp.							X			X	X			
	Ulothrix sp.												X		
Chrysophyta	Chrysosphaera sp.					X									
	Chrysosphaerella sp.								X				X		
	Dinobryon sp.	X	X	X		X				X					
	Mallomonas sp.	X	X	X	X	X		X	X	X	X	X	X	X	X
	Synura sp.	X	X	X	X	X						X			
	Uroglenopsis sp.	X	X	X	X	X	X	X	X		X	X	X	X	X
Bacillariophyta	Asterionella sp.		X	X	X	X	X					X		X	X
	Aulocoseria sp.	X	X	X	X	X	X	X	X		X	X	X	X	X
	Cyclotella sp.	X	X						X			X			
	Fragilaria sp.			X	X							X	X		X
	Rhizosolenia sp.								X						
	Stephanodiscus sp.		X	X	X	X	X					X	X	X	X
	Synedra sp.	X	X	X					X	X			X	X	
	Tabellaria sp.	X	X	X	X						X	X			X
Pennate Diatom	X		X											X	
Dinophyceae	Ceratium sp.		X	X	X	X	X	X	X	X	X	X	X	X	X
	Glenodinium sp.	X			X			X	X	X					
	Gymnodinium sp.									X		X	X		
	Peridinium sp.		X	X						X		X			



Cryptophyceae	Cryptomonas sp.	X	X		X				X	X		X	X	X	X	X
	Rhodomonas sp.															
Euglenophyceae	Euglena sp.			X			X	X		X		X		X	X	
	Phacus sp.					X					X	X				
	Trachelomonas sp.	X	X	X	X	X	X	X	X	X	X	X	X	X	X	X
Raphidophyceae	Gonystrogonum sp.												X			
Phaeothamniophyceae	Stichogloea sp..								X		X	X				
	Total	14	19	25	29	24	24	19	27	28	24	37	28	17	19	18



APPENDIX 2. 2018 AND 2019 NUTRIENT AND CHEMICAL DATA

Abbreviations: Alk = alkalinity; NH4 = ammonia; NO3 = nitrate; NO2 = nitrite; TKN = total Kjeldahl nitrogen; TN = total nitrogen; and TP = total phosphorus.

North Bay Site 2018

Date	Depth (m)	Alk (mg/L)	NH4 (mg/L)	NO3 (mg/L)	NO2 (mg/L)	TKN (mg/L)	TN (mg/L)	TP (µg/L)
22-Apr-18	1	32	0.11	0.07	0	0.29	0.36	0
	Meta	32	0	0.08	0	0.25	0.33	40
	6	30	0	0	0	0.26	0.26	0
Date	Depth (m)	Alk (mg/L)	NH4 (mg/L)	NO3 (mg/L)	NO2 (mg/L)	TKN (mg/L)	TN (mg/L)	TP (µg/L)
21-May-18	1	38	0	0	0	0.47	0.47	10
	Meta	38	0	0	0	0.56	0.56	14
	6	38	0	0	0	0.48	0.48	2
Date	Depth (m)	Alk (mg/L)	NH4 (mg/L)	NO3 (mg/L)	NO2 (mg/L)	TKN (mg/L)	TN (mg/L)	TP (µg/L)
18-Jun-18	1	38	0	0	0	0.47	0.47	22
	Meta	40	0	0	0	0.37	0.37	23
	6	41	0	0	0	0.45	0.45	26
Date	Depth (m)	Alk (mg/L)	NH4 (mg/L)	NO3 (mg/L)	NO2 (mg/L)	TKN (mg/L)	TN (mg/L)	TP (µg/L)
16-Jul-18	1	40	0	1.06	0	0.48	1.54	15
	Meta	41	0	0.11	0	0.61	0.72	33
	6	46	0	0.07	0	0.45	0.52	58
Date	Depth (m)	Alk (mg/L)	NH4 (mg/L)	NO3 (mg/L)	NO2 (mg/L)	TKN (mg/L)	TN (mg/L)	TP (µg/L)
30-Jul-18	1	43	0	0	0	0.26	0.26	29
	Meta	42	0	0	0	0.25	0.25	27
	6	45	0.13	0	0	0.41	0.41	37
Date	Depth (m)	Alk (mg/L)	NH4 (mg/L)	NO3 (mg/L)	NO2 (mg/L)	TKN (mg/L)	TN (mg/L)	TP (µg/L)
16-Aug-18	1	44	0	0	0	0.62	0.62	35
	Meta	44	0	0	0	0.59	0.59	30
	6	50	0	0	0	0.68	0.68	41

Date	Depth (m)	Alk (mg/L)	NH4 (mg/L)	NO3 (mg/L)	NO2 (mg/L)	TKN (mg/L)	TN (mg/L)	TP (µg/L)
24-Sep-18	1	44	0	0	0	0.52	0.52	53
	Meta	44	0	0	0	0.43	0.43	40
	6	44	0	0	0	0.42	0.42	40

Date	Depth (m)	Alk (mg/L)	NH4 (mg/L)	NO3 (mg/L)	NO2 (mg/L)	TKN (mg/L)	TN (mg/L)	TP (µg/L)
22-Oct-18	1	47	0	0	0	0.7	0.7	30
	Meta	47	0	0	0	0.5	0.5	32
	6	46	0	0	0	0.72	0.72	35

Center Lake Site 2018

Date	Depth (m)	Alk (mg/L)	NH4 (mg/L)	NO3 (mg/L)	NO2 (mg/L)	TKN (mg/L)	TN (mg/L)	TP (µg/L)
22-Apr-18	1	34	0.12	0.06	0	0.35	0.41	0
	Meta	34	0	0.06	0	0.31	0.37	1
	6	36	0	0.05	0	0.70	0.75	0

Date	Depth (m)	Alk (mg/L)	NH4 (mg/L)	NO3 (mg/L)	NO2 (mg/L)	TKN (mg/L)	TN (mg/L)	TP (µg/L)
21-May-18	1	37	0	0	0	0.47	0.47	7
	Meta	38	0	0	0	0.38	0.38	8
	6	40	0.14	0.05	0	0.42	0.47	10

Date	Depth (m)	Alk (mg/L)	NH4 (mg/L)	NO3 (mg/L)	NO2 (mg/L)	TKN (mg/L)	TN (mg/L)	TP (µg/L)
18-Jun-18	1	39	0.13	0	0	0.38	0.38	18
	Meta	38	0	0	0	0.45	0.45	16
	6	47	0.34	0	0	0.74	0.74	48

Date	Depth (m)	Alk (mg/L)	NH4 (mg/L)	NO3 (mg/L)	NO2 (mg/L)	TKN (mg/L)	TN (mg/L)	TP (µg/L)
16-Jul-18	1	44	0	0.14	0	0.59	0.73	23
	Meta	40	0	0.06	0	0.90	0.96	30
	6	54	0.43	0.06	0	1.31	1.37	200

Date	Depth (m)	Alk (mg/L)	NH4 (mg/L)	NO3 (mg/L)	NO2 (mg/L)	TKN (mg/L)	TN (mg/L)	TP (µg/L)
30-Jul-18	1	43	0	0	0	0.37	0.37	27
	Meta	42	0	0	0	0.28	0.28	27
	6	70	1	0	0	1.38	1.38	150

Date	Depth (m)	Alk (mg/L)	NH4 (mg/L)	NO3 (mg/L)	NO2 (mg/L)	TKN (mg/L)	TN (mg/L)	TP (µg/L)
16-Aug-18	1	42	0	0	0	0.42	0.42	23
	Meta	50	0.23	0	0	0.65	0.65	46
	6	64	1.13	0	0	1.51	1.51	100

Date	Depth (m)	Alk (mg/L)	NH4 (mg/L)	NO3 (mg/L)	NO2 (mg/L)	TKN (mg/L)	TN (mg/L)	TP (µg/L)
24-Sep-18	1	42	0	0	0	0.40	0.40	39
	Meta	42	0	0	0	0.43	0.43	41
	6	41	0	0	0	0.41	0.41	34

Date	Depth (m)	Alk (mg/L)	NH4 (mg/L)	NO3 (mg/L)	NO2 (mg/L)	TKN (mg/L)	TN (mg/L)	TP (µg/L)
22-Oct-18	1	44	0	0	0	0.59	0.59	29
	Meta	45	0	0	0	0.57	0.57	27
	6	46	0	0	0	0.59	0.59	29

North Bay Site 2019

Date	Depth (m)	Alk (mg/L)	NH4 (mg/L)	NO3 (mg/L)	NO2 (mg/L)	TKN (mg/L)	TN (mg/L)	TP (µg/L)
22-Apr-19	1	36	0	0	0	0	0.00	10
	META	36	0	0.17	0	0	0.17	15
	6	36	0	0.16	0	0	0.16	12

Date	Depth (m)	Alk (mg/L)	NH4 (mg/L)	NO3 (mg/L)	NO2 (mg/L)	TKN (mg/L)	TN (mg/L)	TP (µg/L)
21-May-19	1	38	0	0.24	0	0	0.24	6
	META	38	0	0.21	0	0	0.21	8
	6	38	0	0.24	0	0	0.24	7

Date	Depth (m)	Alk (mg/L)	NH4 (mg/L)	NO3 (mg/L)	NO2 (mg/L)	TKN (mg/L)	TN (mg/L)	TP (µg/L)
18-Jun-19	1	40	0	0	0	0	0.00	18
	META	46	0	0.62	0	0	0.62	18
	6	44	0.14	0.16	0	0	0.16	25

Date	Depth (m)	Alk (mg/L)	NH4 (mg/L)	NO3 (mg/L)	NO2 (mg/L)	TKN (mg/L)	TN (mg/L)	TP (µg/L)
15-Jul-19	1	38	0	0.19	0	0	0.19	12
	META	40	0.12	0.14	0	0	0.14	18
	6	42	0.16	0.11	0	0	0.11	39

Date	Depth (m)	Alk (mg/L)	NH4 (mg/L)	NO3 (mg/L)	NO2 (mg/L)	TKN (mg/L)	TN (mg/L)	TP (µg/L)
26-Aug-19	1	42	0	0.103	0	0	0.10	11
	META						0.00	0
	6						0.00	0

Date	Depth (m)	Alk (mg/L)	NH4 (mg/L)	NO3 (mg/L)	NO2 (mg/L)	TKN (mg/L)	TN (mg/L)	TP (µg/L)
9-Sep-19	1	42	0	0.642	0	0	0.64	48
	META	42	0	0.525	0	0	0.53	43
	6	50	0	0.572	0	0	0.57	48

Date	Depth (m)	Alk (mg/L)	NH4 (mg/L)	NO3 (mg/L)	NO2 (mg/L)	TKN (mg/L)	TN (mg/L)	TP (µg/L)
7-Oct-19	1							0
	META							0
	6							0

Center Lake Site 2019

Date	Depth (m)	Alk (mg/L)	NH4 (mg/L)	NO3 (mg/L)	NO2 (mg/L)	TKN (mg/L)	TN (mg/L)	TP (µg/L)
22-Apr-19	1	34	0	0	0	0	0.00	11
	META	34	0	0.12	0	0	0.12	10
	6	38	0	0.29	0	0	0.29	19

Date	Depth (m)	Alk (mg/L)	NH4 (mg/L)	NO3 (mg/L)	NO2 (mg/L)	TKN (mg/L)	TN (mg/L)	TP (µg/L)
21-May-19	1	36	0	0.2	0	0	0.20	8
	META	36	0	0.27	0	0	0.27	7
	6	36	0	0.25	0	0	0.25	9

Date	Depth (m)	Alk (mg/L)	NH4 (mg/L)	NO3 (mg/L)	NO2 (mg/L)	TKN (mg/L)	TN (mg/L)	TP (µg/L)
18-Jun-19	1	38	0.12	0.13	0	0	0.13	16
	META						0.00	0
	6	38	0.26	0.36	0	0	0.36	53

Date	Depth (m)	Alk (mg/L)	NH4 (mg/L)	NO3 (mg/L)	NO2 (mg/L)	TKN (mg/L)	TN (mg/L)	TP (µg/L)
15-Jul-19	1	40	0	0.15	0	0	0.15	11
	META	38	0	0.21	0	0	0.21	19
	6	50	0.32	0.34	0	0	0.34	176

Date	Depth (m)	Alk (mg/L)	NH4 (mg/L)	NO3 (mg/L)	NO2 (mg/L)	TKN (mg/L)	TN (mg/L)	TP (µg/L)
26-Aug-19	1	42	0	0.128	0	0	0.13	3
	META						0.00	0
	6						0.00	0

Date	Depth (m)	Alk (mg/L)	NH4 (mg/L)	NO3 (mg/L)	NO2 (mg/L)	TKN (mg/L)	TN (mg/L)	TP (µg/L)
9-Sep-19	1	42	0	0.629	0	0	0.63	45
	META	42	0.02	0.501	0	0	0.50	45
	6	42	0	0.573	0	0	0.57	55

Date	Depth (m)	Alk (mg/L)	NH4 (mg/L)	NO3 (mg/L)	NO2 (mg/L)	TKN (mg/L)	TN (mg/L)	TP (µg/L)
7-Oct-19	1							0
	META							0
	6							0